EXPERIMENTAL INVESTIGATIONS OF INPUT SHAPING TECHNIQUES FOR DOUBLE PENDULUM TYPE OVERHEAD CRANE (DPTOC) SYSTEM

MOHD NOR AZLAN BIN ZOHARI

UNIVERSITY MALAYSIA PAHANG

UNIVERSITI MALAYSIA PAHANG ◆

BORANG PENGESAHAN STATUS TESIS

JUDUL: **EXPERIMENTAL INVESTIGATIONS OF INPUT SHAPING TECHNIQUES FOR DOUBLE PENDULUM TYPE OVERHEAD CRANE (DPTOC) SYSTEM**

SESI PENGAJIAN: **2010/2011**

Saya **MOHD NOR AZLAN BIN ZOHARI (880816-11-5643)**
(HURUF BESAR)

mengaku membenarkan tesis (Sarjana Muda/~~Sarjana~~ /~~Doktor Falsafah~~)* ini disimpan di Perpustakaan dengan syarat-syarat kegunaan seperti berikut:

1. Tesis adalah hakmilik Universiti Malaysia Pahang (UMP).
2. Perpustakaan dibenarkan membuat salinan untuk tujuan pengajian sahaja.
3. Perpustakaan dibenarkan membuat salinan tesis ini sebagai bahan pertukaran antara institusi pengajian tinggi.
4. **Sila tandakan (√)

☐	**SULIT**	(Mengandungi maklumat yang berdarjah keselamatan atau kepentingan Malaysia seperti yang termaktub di dalam AKTA RAHSIA RASMI 1972)
☐	**TERHAD**	(Mengandungi maklumat TERHAD yang telah ditentukan oleh organisasi/badan di mana penyelidikan dijalankan)
√	**TIDAK TERHAD**	

Disahkan oleh:

_____ (TANDATANGAN PENULIS)

_____ (TANDATANGAN PENYELIA)

Alamat Tetap:

LOT 7121 KG GONG KEKABU
PDG MENGKUANG BKT PAYUNG
21400 MARANG TERENGGANU

MOHD ASHRAF BIN AHMAD
(Nama Penyelia)

Tarikh: **30 NOVEMBER 2010**

Tarikh: : **30 NOVEMBER 2010**

CATATAN:
- * Potong yang tidak berkenaan.
- ** Jika tesis ini SULIT atau TERHAD, sila lampirkan surat daripada pihak berkuasa/organisasi berkenaan dengan menyatakan sekali tempoh tesis ini perlu dikelaskan sebagai atau TERHAD.
- ♦ Tesis dimaksudkan sebagai tesis bagi Ijazah doktor Falsafah dan Sarjana secara Penyelidikan, atau disertasi bagi pengajian secara kerja kursus dan penyelidikan, atau Laporan Projek Sarjana Muda (PSM).

EXPERIMENTAL INVESTIGATIONS OF INPUT SHAPING TECHNIQUES FOR DOUBLE PENDULUM TYPE OVERHEAD CRANE (DPTOC) SYSTEM

MOHD NOR AZLAN BIN ZOHARI

This thesis is submitted as partial fulfillment of the requirements for the award of the Bachelor of Electrical Engineering (Electronics)

Faculty of Electrical & Electronics Engineering
Universiti Malaysia Pahang

NOVEMBER, 2010

"All the trademark and copyrights use herein are property of their respective owner. References of information from other sources are quoted accordingly; otherwise the information presented in this report is solely work of the author."

Signature : _____

Author : MOHD NOR AZLAN BIN ZOHARI

Date : 30 NOVEMBER 2010

Specially dedicated to

My beloved parents

"I hereby acknowledge that the scope and quality of this thesis is qualified for the award of the Bachelor Degree of Electrical Engineering
(Electrical & Electronics)"

Signature : _____

Name : MOHD ASHRAF BIN AHMAD

Date : 30 NOVEMBER 2010

ACKNOWLEDGMENT

Alhamdulillah, the highest thanks to God because with His Willingness I can complete the final year project in time.

I would like to express my gratitude to my dedicated supervisor, Sir Mohd.Ashraf Ahmad for guiding this project with clarity and that priceless gift of getting things done by sharing his valuable ideas as well as her knowledge.

The great cooperation, kindheartedness and readiness to share worth experiences that have been shown by them will be always appreciated and treasured by me. Once again, thank you very much.

ABSTRACT

These project present experimental investigations of input shaping techniques for double pendulum type overhead crane (DPTOC) system. An unshaped bang-bang input force is used to determine the characteristic parameters of the system for design and evaluation of the input shaping control techniques. The positive input shapers with the derivative effects respectively are designed based on the properties of the system. Experimental of the response DPTOC system to shaped input is presented in time and frequency domain. The performance of this project is examined in terms of sway angle reduction and time response specification. Finally comparative assessment of the proposed techniques is presented.

ABSTRAK

Projek ini membentangkan tentang penyelidikan eksperimen teknik pembentukan input positif untuk pendulum berganda jenis ‘‘overhead’’ kren ‘‘DPTOC’’ sistem. Daya input ‘‘bang-bang’’ yang tidak terbentuk digunakan untuk menentukan parameter karakteristik dari system, untuk dibina dan dinilai dari masukan untuk membentuk teknik kawalan. Pembentukan input positif dengan kesan bentukan direka berdasarkan sifat-sifat sistem. Keputusan simulasi tindakbalas sistem ‘‘DPTOC’’ terhadap pembentukan input dibentangkan dalam masa dan domain frekuensi. Prestasi projek ini diperiksa dari segi pengurangan ayunan sudut dan spesifikasi masa tindakbalas. Akhirnya, penilaian perbandingan dari teknik yang dicadangkan dibentangkan.

TABLE OF CONTENTS

CHAPTER	TITLE	PAGE
	TITLE	i
	DECLARATION	ii
	DEDICATION	iii
	ACKNOWLEDGMENT	v
	ABSTRACT	vi
	ABSTRAK	vii
	TABLE OF CONTENTS	viii
	LIST OF TABLES	xii
	LIST OF FIGURES	xiii
	LIST OF SYMBOLS	xix
	LIST OF ABBREVIATIONS	xx
1	**INTRODUCTION**	
	1.1 Introduction	1
	1.2 Problem Statement	3
	1.3 Project Objective	4
	1.4 Project Scopes	4
	1.5 Thesis Outline	5

2 LITERATURE REVIEW

2.1 Introduction 6

2.2 Anti-sway techniques 7

2.2.1 Input Shaping Technique 8

2.2.2 Other techniques 9

3 METHDOLOGY

3.1 Introduction 11

3.2 Work Methodology 12

3.2.1 Modeling of a double pendulum type overhead crane (DPTOC) 12

3.2.2 Dynamic modeling of the double pendulum type overhead crane 14

3.3 Determination of natural frequency 15

3.4 Design of the input shaping using MATLAB 16

3.4.1 Design equation of input shaping 16

3.5 Develop positive input shaping 19

3.5.1 The bang-bang torque of input shaping design in Simulation 21

3.5.2 The bang-bang torque of input shaping design in experimental 23

3.6 Simulation Studies 25

3.7 Experimental Studies 26

3.8 Verification of Control Model Design 30

3.9 Data Collection and Analysis Controller Design 31

4 RESULT AND DISCUSSION

4.1 Introduction 32

4.2 Simulation result using MATLAB software 33

4.2.1 Result simulation of uncontrolled double pendulum type overhead crane 33

4.2.2 Result simulation of positive zero sway (PZS) shaper 36

4.2.3 Result simulation of positive zero sway derivative (PZSD) shaper 39

4.2.4 Result simulation of positive zero sway derivative-derivative (PZSDD) shaper 42

4.3 Comparative assessment of input shaping techniques in simulation resuit 45

4.3.1 Comparison of power spectral density in simulation Result 46

4.3.2 Comparison of sway angle in simulation results 47

4.3.3 Comparison of trolley position in simulation results 49

4.4 Simulation result analysis 50

4.4.1 Simulation result analysis of input shaping 50

4.5 Experimental result using CEMTools software 54

4.5.1 Result experimental of uncontrolled double pendulum type overhead crane 54

4.5.2 Result experimental of positive zero sway (PZS) shaper 57

4.5.3 Result experimental of Positive zero sway derivative (PZSD) shaper 60

4.5.4 Result experimental of positive zero sway derivative-derivative (PZSDD) shaper 63

4.6 Comparative assessment of input shaping techniques in experimental result 66

4.6.1 Comparison of power spectral density in experimental result 67

4.6.2 Comparison of sway angle in experimental result 68

4.6.3 Comparison of trolley position in experimental result 70

4.7 Experimental result analysis 71

4.7.1 Experimental result analysis of input shaping 71

5 CONCLUSION

5.0 Conclusion 75

5.1 Limitation of the Project 76

5.2 Future work Recommendation 76

REFERENCE 77

APPENDIX 80

LIST OF TABLES

TABLE NO	TITLE	PAGE
4.1	Level of sway reduction of the hoisting angle of the pendulum and specification of trolley position response in simulation results	51
4.2	Level of sway reduction of the hoisting angle of the pendulum and specification of trolley position response in experimental results	72

LIST OF FIGURES

FIGURE NO.	TITLE	PAGE
1.1	Double beam overhead crane (EOT) crane	2
1.2	Overhead cranes	3
3.1	Work Methodology	12
3.2	Double pendulum type overhead crane model	13
3.3	Illustration of input shaping technique	16
3.4	Zero Sway	19
3.5	Zero Sway Derivative	20
3.6	Zero Sway Derivative Derivatives	20
3.7	Bang -bang input of positive zero sway (PZS) response in simulation	21
3.8	Bang-bang input of positive zero sway derivatives (PZSD) in simulation	22
3.9	Bang-bang input of positive zero sway derivative -derivative (PZSDD) in simulation	22
3.10	Bang-bang input of positive zero sway (PZS) response	23
3.11	Bang-bang input of positive zero sway derivative (PZSD) response	24

3.12	Bang-bang input of positive zero sway derivative-derivative (PZSDD) response	24
3.13	Simulink model of double pendulum type overhead crane	25
3.14	Interfacing connection between CEMTools and Real Gain Swing-Up Inverted Pendulum	26
3.15	A SIMTool Model Design without controller	27
3.16	Parameter Setting for Step 1	28
3.17	Parameter Setting for Step 2	28
3.18	Parameter Setting for Step 3	29
3.19	Parameter setting for Step 4	29
3.20	Configuration of workspace	30
3.21	A SIMTool Model Design with controller	31
4.1	Response of the power spectral density hook swing angle	34
4.2	Response of the power spectral density load swing angle	34
4.3	Response of the hook swing angle	35
4.4	Response of the load swing angle	35
4.5	Response of the trolley position	36
4.6	Response of the power spectral density hook swing angle with PZS shaper	37
4.7	Response of the power spectral density load swing angle with PZS shaper	37

4.8	Response of the hook swing angle with PZS shaper	38
4.9	Response of the load swing angle with PZS shaper	38
4.10	Response of the trolley position with PZS shaper	39
4.11	Response of the power spectral density hook swing angle with PZSD shaper	40
4.12	Response of the power spectral density load swing angle with PZSD shaper	40
4.13	Response of the hook swing angle with PZSD shaper	41
4.14	Response of the load swing angle with PZSD shaper	41
4.15	Response of the trolley position with PZSD shaper	42
4.16	Response of the power spectral density hook sway angle with PZSDD shaper	43
4.17	Response of the power spectral density load sway angle with PZSDD shaper	43
4.18	Response of the hook swing angle with PZSDD shaper	44
4.19	Response of the load swing angle with PZSDD shaper	44
4.20	Response of the trolley position with PZSDD	45
4.21	Power spectral density at hook swing angle in simulation result	46
4.22	Power spectral density at load swing angle in simulation result	47
4.23	Response of the hook swing angle in simulation results	48

4.24	Response of the load swing angle in simulation result	48
4.25	Response of the trolley position in simulation result	49
4.26	Level of sway reduction for hook swing angle in simulation	52
4.27	Level of sway reduction for load swing angle in simulation	52
4.28	Time response specifications in simulation	53
4.29	Power Spectra Density at hook sway angle without controller	55
4.30	Power Spectra Density at load sway angle without controller	55
4.31	Hook sway angle without controller	56
4.32	Load sway angle without controller	56
4.33	Position of the cart without controller	57
4.34	Power Spectra Density of hook sway angle with PZS input shaper	58
4.35	Power spectral density of load sway angle with PZS input shaper	58
4.36	Hook swing angle with PZS input shaper	59
4.37	Load swing angle with PZS input shaper	59
4.38	Position of cart with PZS input shaper	60

4.39	Power spectral density at hook sway angle with PZSD input shaper	61
4.40	Power spectral density at load sway angle with PZSD input shaper	61
4.41	Hook swing angle with PZSD input shaper	62
4.42	Load swing angle with PZSD input shaper	62
4.43	Position of cart with PZSD input shaper	63
4.44	Power spectral density at hook sway angle with PZSDD input shaper	64
4.45	Power spectral density at load sway angle with PZSDD input shaper	64
4.46	Hook swing angle with PZSDD input shaper	65
4.47	Load swing angle with PZSDD input shaper	65
4.48	Position of the cart with PZSDD input shaper	66
4.49	Power spectral density of the hook swing angle in experimental result	67
4.50	Power spectral density of the load swing angle in experimental result	68
4.51	Response of the hook swing angle in experimental result	69
4.52	Response of the load swing angle in experimental result	69
4.53	Response of the trolley position in experimental result	70
4.54	Level of sway reduction for hook swing angle in experimental result	73

4.55	Level of sway reduction for load swing angle in experimental result	73
4.56	Time response specifications in experimental result	74

LIST OF SYMBOLS

m	mass of trolley (kg)
m_1	mass of the Hook (kg)
m_2	mass of the Payload (kg)
x	Trolley Position (m)
F	Force apply to the trolley (N)
θ_1	hook swing angle (rad)
θ_2	payload swing angle (rad)
l_1	length of the pendulum at hook (m)
l_2	length of the pendulum at load (m)
g	gravity acceleration (m/s^2)
$\boldsymbol{g}$	gravity effect
$\boldsymbol{q}$	state vector
$\boldsymbol{\tau}$	control vector
ω_n	natural frequency
ζ	damping ratio
A	amplitude of the impulse
t_0	time location of the impulse

LIST OF ABBREVIATIONS

PZS	Positive Zero Sway
PZSD	Positive Zero Sway Derivative
PZSDD	Positive Zero Sway Derivative Derivative
DPTOC	Double Pendulums Type Overhead Crane

CHAPTER 1

INTRODUCTION

1.1 Introduction

Overhead crane is important machinery that has been used at construction or industrial site to transfer the material. In order to make work easier, overhead cranes have been used to transfer the material that are usually heavy, large and hazardous which cannot be handling by worker. In handling the crane, safety is the most important aspect to consider while operating crane. It also has a problem when carrying the heavy load, the overhead crane tents to be unbalance causing its cart to sway excessively.

There are many cases and incident regarding on the crane's accident. For example, in April 1993, the crane becomes unbalanced during two separated incidents at DOE sites in United State of America, which is in Hanford Sites and Bryan Mound Site. For the first accidents happened in 28th April 1993, where a crane becomes unbalanced while the boom was being lowered and two day later in 30th April 1993, which crane loading the load, the weight of the load caused the crane to tip forward. Relate to this accident, effective controller need to be applied into the crane system to meet safety requirement and smooth operation.

Input shaping is a feed forward control technique for improving the settling time and positioning accuracy, while minimizing residual vibrations of computer controlled machines. Input shaping is a strategy for a generation of time-optimal shaped commands using only a simple model, which consist of the estimate of natural frequency and damping ratio so, input shaping is a simple method to reduce the sway of double pendulum type overhead crane (DPTOC) system. It offers several clear advantages over conventional approaches for trajectory generation [1].

i) Designing an input shaping does not require an analytical model of the system; it can be generated from simple, empirical measurements of the actual physical system [1].

ii) Input shaping does not affect the stability of the closed loop system in any way. It simply modifies the command signal to the system so that all moves, regardless of length, are vibration free [1].

So in this project the positive input shaping algorithm will be used to reduce the sway of double pendulum type overhead crane system. The positive input shaping is implemented by convolving a positive sequence of impulse, an input shaper with a desired system command to produce a shaped input. Figure 1.1 and 1.2 show examples of overhead cranes using in industry.

Figure 1.1: Double beam overhead crane (EOT crane)

Figure 1.2: Overhead cranes

The requirement of precise sway control of overhead crane implies that residual sway of the payload should be zero or near zero. As the performance requirements imposed by the industry become more severe, the need to understand how to model and control the overhead crane becomes an issue of concern. Thus, it becomes necessary to anticipate and control such sway in order to obtain robust and fast response of the overhead crane.

1.2 Problem statement

When carrying heavy loads, the overhead crane tends to be unbalance causing its cart to sway excessively. This can cause accidents. The accidents which caused by cranes have been recorded [1] and this prove that gantry crane can be hazardous. To solve this problem, input shaping technique is introduced.

1.3 Project Objective

The objectives of this project:

i) To develop positive input shaping technique for anti sway control of double pendulum type overhead crane system.

ii) To determined the amplitude and time locations of the impulse in order to reduce the natural frequencies and damping ratio of the system.

iii) To investigate the effects of the difference derivative order of the positive input shaper in terms of level sway reduction and time response specifications.

1.4 Project Scopes

The scopes of this project:

i) Modeling of overhead crane.
Modeling is needed to present a real system that will be focused in order to do the analysis. Further work involves obtaining the dynamic characteristic and to predict the problem that will occur before the control of the system is implemented.

ii) Design the positive input shaping controller.
Positive input shaping is developed based on positive zero sway (PZS), positive zero sway derivative (PZSD) and positive zero sway derivative-derivative (PZSDD). Each positive input shaping contains difference value of impulse.

iii) Simulation studies using MATLAB software.
For simulation studies, MATLAB 7.6 is used for input shaping design before it is used for experimental studies.

iv) Experimental studies using CEMTool and MATLAB 7.6 software.
To carry out this project after simulation studies is done; this software will be used to interface the design program with its experimental hardware.

1.5 Thesis Outline

This section will give an outlines of the structure of the thesis. This thesis will consist of five chapters including this chapter. The following is an explanation for each chapter:

Chapter 2 discusses the previous work that been done around the world about the crane, in term of modeling, the crane. Literature that been done will cover, for instance, modeling, control algorithm design and others.

Chapter 3 explains on methodology of this project. In this chapter, each step in the work methodology flow chart starting from modelling of the gantry crane was explained.

.

Chapter 4 consists of experimental results and results analysis. Comparison between each negative input shaping derivative order was done.

Lastly, Chapter 5 summarizes the overall conclusion for this thesis and a few suggestion and recommendation for future development.

CHAPTER 2

LITERATURE REVIEW

2.1 Introduction

An overhead crane has been used to lift and move the payload from one location to another place that are usually heavy, large and hazardous which cannot be handling by worker. In operating the overhead crane, when the load moves, the crane must be controlled so that the load reaches the location needed with less or without swinging.

In operating the overhead crane, the oscillation that occurs is seemly like a pendulum motion which is at certain level, the operating must be stopped until the swing or oscillation reduced [2]. This happen when the cart in which carries the load will produce a sway which cause the cart and the load to oscillate. One of the incidents occurred in 28th April 1993, where a crane becomes unbalanced while the boom was being lowered [2].

Due to this problem, to prevent the accidents, the controller of positive input shaping technique will be implemented. The timeliness and effectiveness of this manipulation system are important contributors to industrial production. Beyond the basic pendulum mode, crane also has additional dynamic effects such as motor time constants, velocity limits and nonlinear payload dynamics that make them well suited for both introductory and advance study [3].

Today most existing crane control systems are designed to maximize speed, in an attempt to minimize system sway and achieve good positional accuracy in minimum duration. High stiffness can be achieved by using short rope or heavy carrier head. As a result, such cranes are usually heavy with respect to it payload. This limits the speed of operation of transportation, increases size of driving motor and energy consumption [4, 5].

2.2 Anti-sway techniques

The vibration or sway is a significant problem in dynamical systems that are required to perform precise motion in presence of structural flexibility. Step motors, robotic arms, flexible manipulators and crane systems are some examples for this category. In reducing the excessive sway of an overhead crane, many researches and paper work had been done in proposing the techniques to overcome the problem. These are some techniques which had been done over the years which include input shaping, filtering technique, and feedback control technique.

2.2.1 Input Shaping Technique

Feed-forward control schemes are mainly develop for sway suppression and involve developing the control input through consideration of the physical and swaying properties of the system so that system sways at response modes are reduced [4]. The earliest incarnation of this self canceling command generations was developed by smith [4, 5, and 6]. His posicast control method involved breaking a command of certain magnitude into two smaller magnitude commands, one of which is delayed one-half period of vibration.

Unfortunately, his technique was extremely sensitive to modeling errors [6]. Singer and Seering developed reference commands that were robust enough to be effective on a range of systems [5, 7]. This new robust technique is named as input shaping.

Input shaping is implemented by convolving a sequence of impulses, an input shaper, with a desired system command to produce a shaped input that produces self canceling command signal [4, 8, 9, and 10]. Input shaping is easier to derive and implement than time-optimal control schemes and does not require the feedback mechanisms of closed loop and adaptive controllers [9, 10].

Input shaper is designed by generating a set of constraint equations which limit the residual vibration, maintain actuator limitations, and ensure some level of robustness to modeling errors [11]. Input shaping is a form of Finite Impulse Response (FIR) filtering that places zeros near the locations of the original system's flexible poles. The impulse amplitudes are equivalent to the filter coefficients. The impulse amplitudes and time locations are determined by satisfying a set of constraint equations [8, 9, and 10].

According to Sirri Sunay Gurleyuk, Ozgur Bahadir, Yunus Turkkan and Hakan Usenti which had proposed in their paper Three-Step (TS) input shaping technique state that Zero Vibration (ZV), Zero Vibration and Derivative (ZVD) and Extra Insensitive (EI) are the most common shaper types. Improving the robustness respect to modeling errors requires more impulses [5].

The requirement of positive amplitudes for the input shapers has been used in most input shaping schemes. The requirement of positive amplitude for the impulses is to avoid the problem of large amplitude impulses [4]. The shapers containing negative impulses have tendency to excite unmodeled high modes and they are slightly less robust as compared to the positive shapers besides, negative input shapers require more actuator effort than the positive shapers due to high changes in the set-point command at each new impulse time location [4].

In this project, by related the advantage and disadvantage of the positive input shaping technique and negative input shaping technique, this experimental will use positive input shaping technique as the controller of double pendulum type overhead crane (DPTOC) system.

2.2.2 Other Techniques

In the paper entitled Experimental Investigations of Low pass Filter Techniques for Sway Control of a Gantry Crane System by M.A. Ahmad, F.R. Misran, M.S. Ramli, and R.M.T. Raja Ismail it presents investigations into the development of IIR low-pass filter techniques in anti-swaying control of a gantry crane system. According this paper, filtering techniques is developed on the basic of extracting input energy around natural frequencies of the system.

The filters are thus used for pre-processing the input signal so that no energy is fed into the system at the natural frequencies. In this manner, the flexural modes of the system are not excited, leading to a sway-free motion. This can be realized by employing either low-pass (LPF) or band-stop (BSF) filters [12].

In the former, the filter is designed with cut-off frequency lower than the first natural frequency of the system. There are various filter types such as Butterworth, Chebyshev and Elliptic that can be designed and employed [12].

By implementation of IIR low-pass filter techniques show that the low pass filter techniques with higher number of order provide higher level of sway reduction. However, in term of speed of the response, the low number of filter order result is in a higher speed of tracking response [12].

Various of the anti-sway techniques in controlling the cranes system based on open loop system were proposed. For example, input shaping and IIR filtering technique that used to reduce the oscillation of the cranes system. However open loop strategy is sensitive to the system parameters (e.g. rope length) and could not compensate for wind disturbances. On the other hand, feedback control which is well known to be less sensitive to disturbance and parameter variations is also adopted for controlling the cranes system [13].

In the paper entitled Anti-sway Control of a Gantry Crane System based on Feedback Loop Approaches by M.A. Ahmad, R.M.T Raja Ismail, A.N.K. Nasir and M.S. Ramli presents investigations of anti-sway angle control approach in order to eliminate the effect of disturbances applied to the gantry crane system. A simulation environment is developed within Simulink and Matlab for evaluation of the control strategies [13].

To demonstrate the effectiveness of the proposed control strategy, the disturbances effect is applied at the hoisting rope of the gantry crane. This is then extended to develop a feedback control strategy for sway angle reduction and disturbances rejection [13]. Two feedback control strategies which are Delayed feedback signal and sliding mode controller are developed in this simulation work [13]. Performances of each controller are examined in terms of sway angle suppression and disturbance rejection [13].

CHAPTER 3

METHODOLOGY

3.1 Introduction

This section described the methods used to reduce sway angle of double pendulum type overhead crane system by using positive input shaping technique. The methods explained in this section are very important procedures in order to ensure the flow of research move smoothly as planned. The methodology of this research is divided into four major sections:

i. Modeling of a double pendulum type overhead crane.
ii. Design and develop positive input shaping.
iii. Simulation and experimental of double pendulum type overhead crane by using MATLAB 7.6 and CEMTOOL software.
iv. Data collection and analysis controller design.

3.2 Work Methodology

In term of work methodology, it can be summarized in Figure 3.1

.

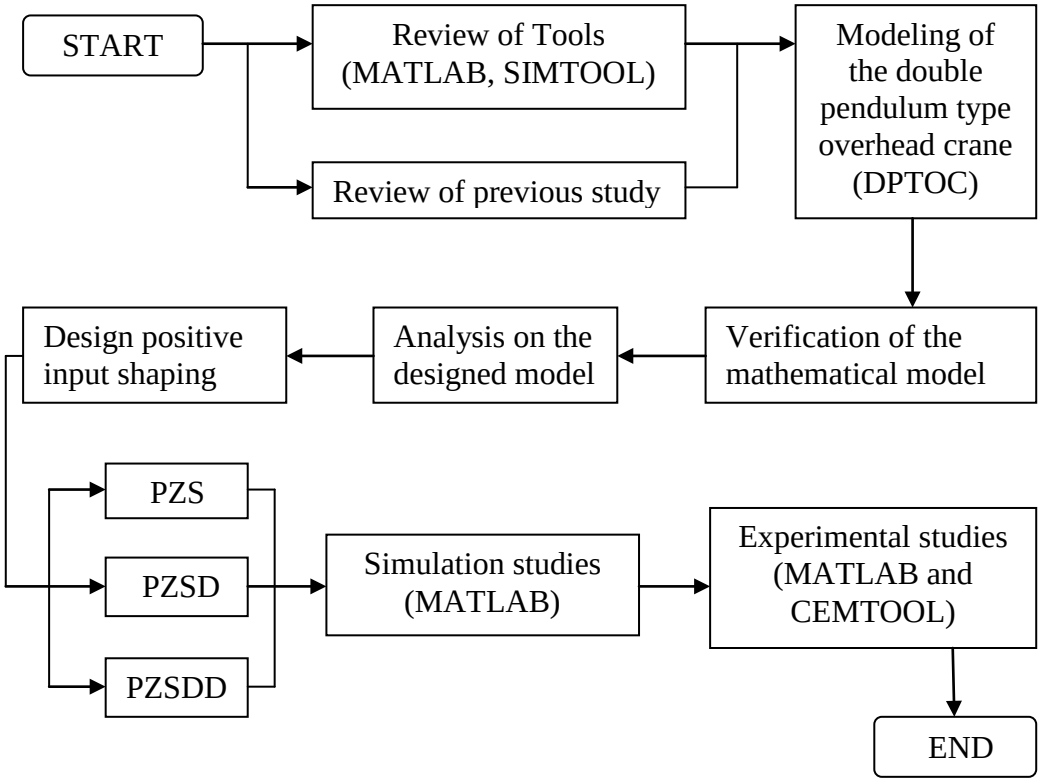

Figure 3.1: Work Methodology

3.2.1 Modeling of a double pendulum type overhead crane (DPTOC) system

In this experimental, modeling of a double pendulum type overhead crane is the first steps require representing a real system in order to do the design analysis. This involves obtaining the dynamic characteristic of the system and with dynamic analysis, it can predict the problem that will occur before the system is built.

The DPTOC system with its hook and load considered in this work is show in Figure 3.2, where x is the trolley position, m is the trolley mass, m_1 and m_2 are the hook and load mass respectively. θ_1 is the hook swing angle, θ_2 is the load swing angle, l_1 and l_2 are the cable length of the hook and load respectively and F is the trolley drive force. In this simulation the hook and load can be considered as point masses.

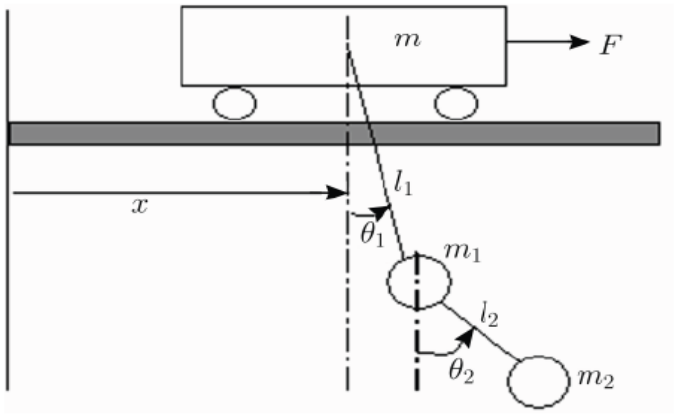

Figure 3.2: Double pendulum type overhead crane model

the characteristic parameter of modeling double pendulum type overhead crane (DPTOC) system:

x = Trolley Position
F = Force apply to the trolley
m = mass of trolley
m_1 = mass of the Hook
m_2 = mass of the Payload
θ_1 = hook swing angle
θ_2 = payload swing angle
l_1 and l_2 = length of the pendulum

3.2.2 Dynamic modeling of the double pendulum type overhead crane

This section provides a brief description on the modeling of the DPTOC system, as a basic of a simulation enviroment for development and assessment of the feed forward control technique. The Euler-Lagrange formulation is considered in characterizing the dynamic behavior of the crane system incorporate payload. By using Lagrange's equations, the dynamic model of the DPTOC system is assumed to have the following form [4] :

$$M(q)\ddot{q} + C(q,\dot{q})\dot{q} + G(q) = \bar{\tau} \tag{3.1}$$

where the matrices $M(q) \in \Re^{3\times3}$,$C(q,\dot{q}) \in \Re^{3\times3}$ and $G(q) \in \Re^{5}$ represent the inertia , Centrifugal-Coriolis terms and gravity. Respectively define as:

$$M(q) = \begin{bmatrix} m + m_1 + m_2 & (m_1+m_2)l_1 cos\theta_1 & m_2 l_2 cos\theta_2 \\ (m_1+m_2)l_1 cos\theta_1 & (m_1+m_2)l_1^2 & m_2 l_1 l_2 cos(\theta_1-\theta_2) \\ m_2 l_2 cos\theta_2 & m_2 l_1 l_2 cos(\theta_1-\theta_2) & m_2 l_1^2 \end{bmatrix} \tag{3.2}$$

$$C(q,\dot{q}) = \begin{bmatrix} 0 & -(m_1+m_2)l_1\dot{\theta}_1 sin\theta_1 & -m_2 l_2 \dot{\theta}_2 sin\theta_2 \\ 0 & 0 & m_2 l_1 l_2 \dot{\theta}_1 \sin(\theta_1-\theta_2) \\ 0 & -m_2 l_1 l_2 \dot{\theta}_1 \sin(\theta_1-\theta_2) & 0 \end{bmatrix} \tag{3.3}$$

$$G(q) = [0 \quad (m_1+m_2)g l_1 sin\theta_1 \quad m_2 g l_2 sin\theta_2]^T \tag{3.4}$$

where $\boldsymbol{g}$ are the gravity effect, the state vector $\boldsymbol{q}$ and the control vector $\boldsymbol{\tau}$ are defined as:

$$q = [x \quad \theta_1 \quad \theta_2]^T \tag{3.4}$$

$$\bar{\tau} = [F \quad O \quad 0]^T \tag{3.5}$$

after rearranging equation (3.1) and multiplying both sides by M^{-1}, one obtains:

$$\ddot{q} = M^{-1}[-C\dot{q} - G + \bar{\tau}] \quad (3.6)$$

where M^{-1} is guaranteed to exist due to det(M) > 0. In this study the values of the parameters are defined as m=5 kg, m_1=2 kg, m_2=5 kg, l_1=2 m, l_2=1m and g = 9.8 m-s^{-2} [4].

3.3 Determination of natural frequency

The natural frequency is the oscillation frequency of the system with all the damping is removed. An ideal pendulum will oscillate at its natural frequency once it is released from an unstable position. In this project, natural frequency for the experimental studies was obtained from the response of power spectral density of uncontrolled gantry crane system. The value obtained then will be multiply with 2π to get the exact value of the natural frequency, ω_n.

To evaluate the performance of the positive input shaping technique, the level of sway reduction at the natural frequency were calculated to get its attenuation. This is done by comparing the PSD responses of positive input shaping of each derivative order with the PSD response of uncontrolled.

3.4 Design of the input shaping using MATLAB

Positive input shaping was generated through convolution of impulses function with bang-bang input. Each of the positive input shaping contains different values of impulses. An unshaped bang-bang force input is used to determine the characteristic parameters of the system for design and evaluation of the input shaping control technique. Each of the input shaping positive zero sway (PZS), positive zero sway derivatives (PZSD) and positive zero sway derivative –derivative (PZSDD) of bang-bang input was generated through its own coding by using MATLAB software. Figure 3.3 show illustration of input shaping technique.

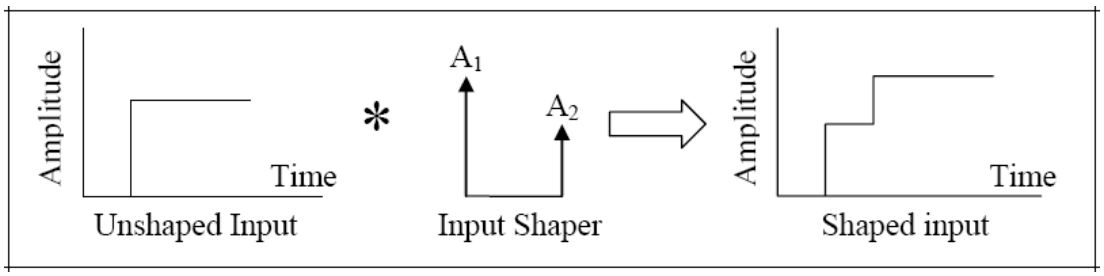

Figure 3.3: Illustration of input shaping technique

3.4.1 Design equation of input shaping

Design objectives are to determine the amplitude and time locations of the impulses, so that the shaped command reduces the detrimental effects of system flexibility [14]. Generally, an input shaping of any order can be modeled as a superposition of second order systems each with a transfer function [14].

$$G(s) = \frac{\omega^2}{s^2+2\zeta\omega s+\omega^2}$$

where ω is the natural frequency of the sway double pendulum type overhead crane and ζ is the damping ratio of the system [14].

thus, the response of the system in time domain can be obtained as

$$y(t) = \frac{A\omega}{\sqrt{1-\zeta^2}} e^{-\zeta\omega(t-t_0)} \sin[\omega\sqrt{1-\zeta^2}(t-t_0)]$$

where A and t_0 are the amplitude and the time location of the impulse respectively. The response to a sequence of impulse can be obtained by superposition of the impulse response [14]. Thus, for N impulses, with $\omega_d = \omega\sqrt{1-\zeta^2}$, the impulse response can be expressed as

$$y(t) = Msin(\omega_d t + \beta)$$

where

$$M = \sqrt{(\sum_{i=1}^{n} B_i cos\phi_i)^2 + (\sum_{i=1}^{n} B_i sin\phi_i)^2} \ , \ B = \frac{A_i\omega}{\sqrt{1-\zeta}} e^{-\zeta\omega(t-t_0)} , \phi_i = \omega_d t_{\ i}$$

A_i and $t_{\ i}$ are the amplitude and time locations of the impulses [14].

The residual signal mode vibration amplitude of the impulse response is obtained at the time of the last impulse t_N as

$$V = \sqrt{V_1^2 + V_2^2} \tag{3.7}$$

where

$$V_1 = \sum_{i=1}^{N} \frac{A_i\omega_n}{\sqrt{1-\zeta^2}} e^{-\zeta\omega_n(t_N-t_i)} \cos(\omega_d t_i) \ ; \ V_2 = \sum_{i=1}^{N} \frac{A_i\omega_n}{\sqrt{1-\zeta^2}} e^{-\zeta\omega_n(t_N-t_i)} \sin(\omega_d t_i)$$

to achieve zero sway after the last impulse, it is required that both V_1 and V_2 in Equation (4.0) are independently zero. In order to ensure that the shaped command input produces the same rigid body motion as the unshaped reference command, it is required that the sum of amplitudes of the impulses is unity [14].

this yield the unity amplitude summation constraint as

$$\sum_{i=1}^{N} A_i = 1$$

In order to avoid response delay, time optimality constraint is utilized. The first impulse is selected at time t_1=0 and the last impulse must be at minimum, i.e.min(t_N) [14]. The robustness of the input shaper to errors in natural frequencies of the system can be increased by taking the derivatives of V_1 and V_2 to zero [14].

Setting the derivatives to zero is equivalent to producing small changes in vibration corresponding to the frequency changes [14]. The level of robustness can further be increased by increasing the order of derivatives V_1 and V_2 and set them to zero [14]. Thus, the robustness constraints can obtain as

$$\frac{d^i V_1}{d\omega_n^i} = 0 \; ; \; \frac{d^i V_2}{d\omega_n^i} = 0$$

simplifying $\frac{d^2 V_i}{d\omega_n^2}$, yields

$$\frac{d^2 V_1}{d\omega_n^2} = \sum_{i=1}^{N} A_i t_i^2 e^{-\zeta\omega_n(t_N - t_i)} \sin(\omega_d t_i) \; ;$$

$$\frac{d^2 V_2}{d\omega_n^2} = \sum_{i=1}^{N} A_i t_i^2 e^{-\xi\omega_n(t_N - t_i)} cos(\omega_d t_i) \qquad (3.8)$$

The input shaper, i.e. four-impulse sequence is obtained by setting Equation (3.7) and (3.8) to zero and solving with the other constraint equations. Hence, a four-impulse sequence can be obtained with the parameters as

$$t_1 = 0, t_2 = \frac{\pi}{\omega_d} \; , t_3 = \frac{2\pi}{\omega_d} \; , t_4 = \frac{3\pi}{\omega_d}$$
$$A_1 = \frac{1}{1+3K+3K^2+K^3}, A_2 = \frac{3K}{1+3K+3K^2+K^3} \qquad (3.9)$$
$$A_3 = \frac{3K^2}{1+3K+3K^2+K^3}, A_4 = \frac{K^3}{1+3K+3K^2+K^3}$$

where

$$K = e^{-\frac{\zeta\pi}{\sqrt{1-\zeta^2}}}, \quad \omega_d = \omega_n\sqrt{1-\zeta^2}$$

where ω_n and ζ representing the natural frequency and damping ratio respectively. For the impulses, t_j and A_j are the time location and amplitude of impulses j respectively.

3.5 Develop positive input shaping

For this project, positive input shaping controller of anti sway control is developed for the system. Based on research that has been reviewed, input shaping technique can reduce the sway of a system significantly. The positive input shaping control scheme will divide into three types which are positive zero sway (PZS), positive zero sway derivative (PZSD) and positive zero sway derivative-derivative (PZSDD) and each of the positive input shaping contains different values of impulses.

Zero sway (ZS) shaper consists of two impulses response as shown in Figure 3.4. ZS shaper does not take robustness constraint into account. It only considers zero residual sway, unity amplitude summation and time optimality constraints.

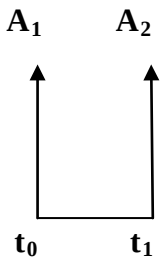

Figure 3.4: Zero Sway

Zero Sway-Derivative (ZSD) shaper consists of 3 impulses response as shown in Figure 3.5. The constraints equations considered in designing of ZSD shaper are zero residual sway, unity amplitude summation, time optimality constraints and first order robustness constraint equation.

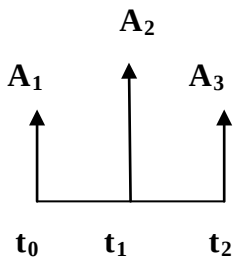

Figure 3.5: Zero Sway Derivatives

Zero Sway-Derivative-Derivative (ZSDD) shaper consists of four impulses response as shown in figure 3.6. The constraints equations considered in designing of ZSDD shaper are zero residual sway, unity amplitude summation, time optimality constraints and second order robustness constraint equation.

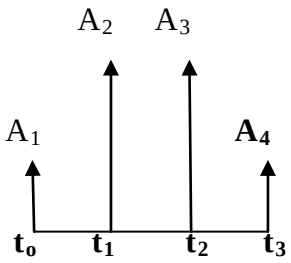

Figure 3.6: Zero Sway Derivative Derivatives

3.5.1 The bang-bang torque of input shaping design in simulation

The bang-bang input of positive input shaping were generated through convolution of it impulses. The Figures 3.7, 3.8 and 3.9 show the bang-bang input of positive zero sway (PZS) shaper, positive zero sway derivative (PZSD) shaper and positive zero sway derivative-derivative (PZSDD) shaper in simulation.

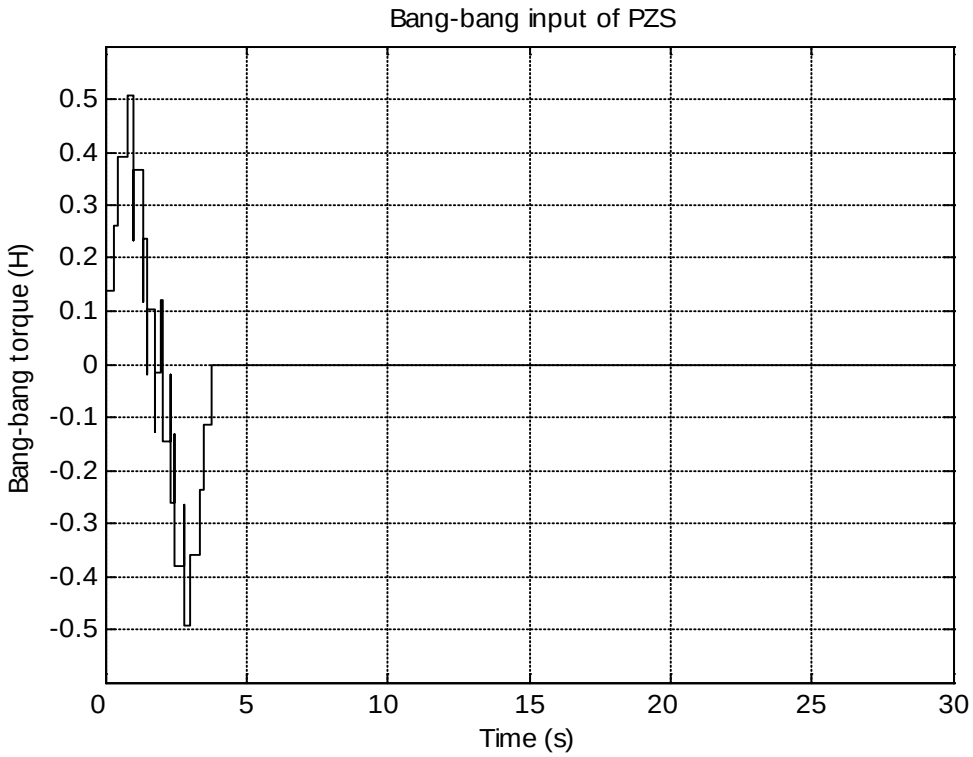

Figure 3.7: Bang -bang input of positive zero sway (PZS) response in simulation

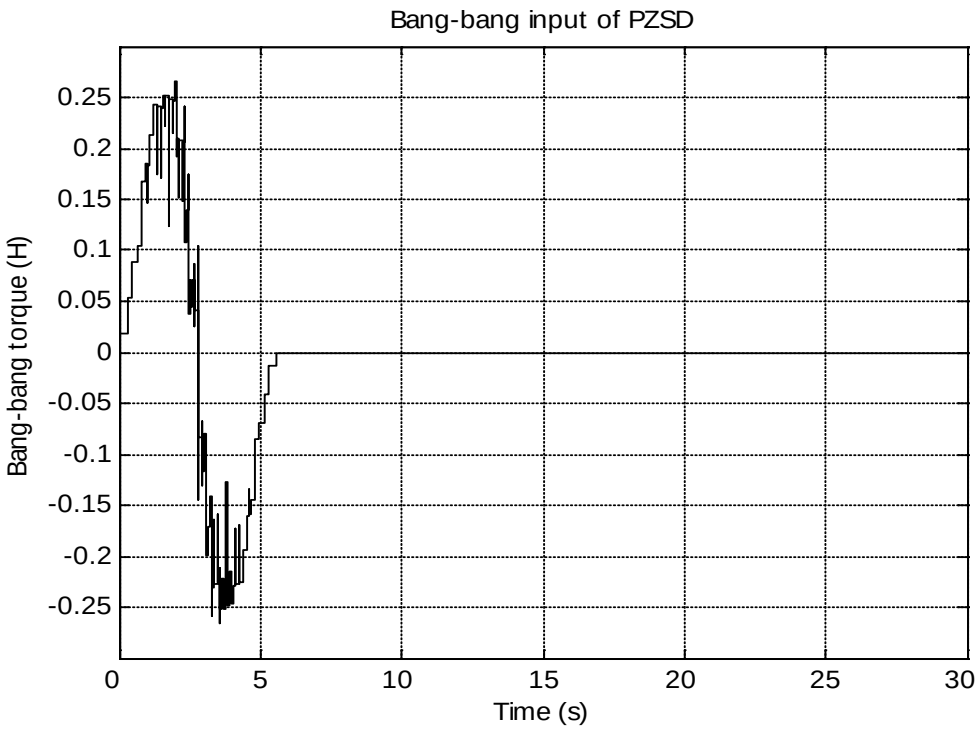

Figure 3.8: Bang-bang input of positive zero sway derivatives (PZSD) in simulation

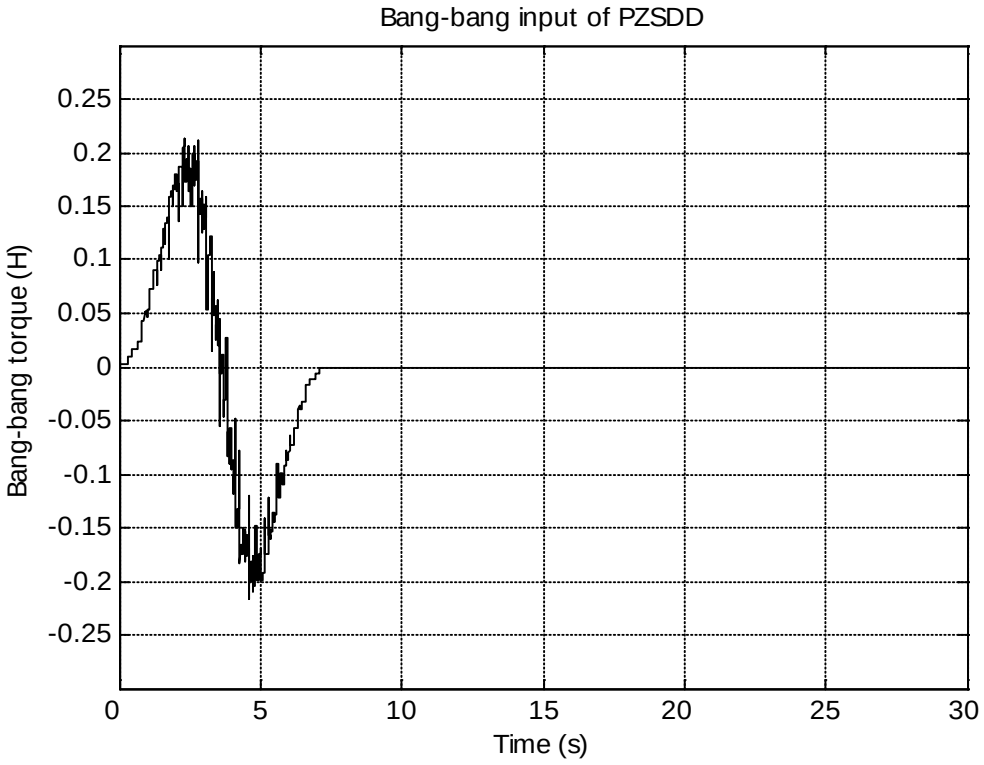

Figure 3.9: Bang-bang input of positive zero sway derivative-derivative (PZSDD) in simulation

3.5.2 The bang-bang torque of input shaping design in experimental

The bang-bang input of positive input shaping were generated through convolution of it impulses. The Figures 3.10, 3.11 and 3.12 show the bang-bang input of positive zero sway (PZS) shaper, positive zero sway derivative (PZSD) shaper and positive zero sway derivative-derivative (PZSDD) shaper in experimental.

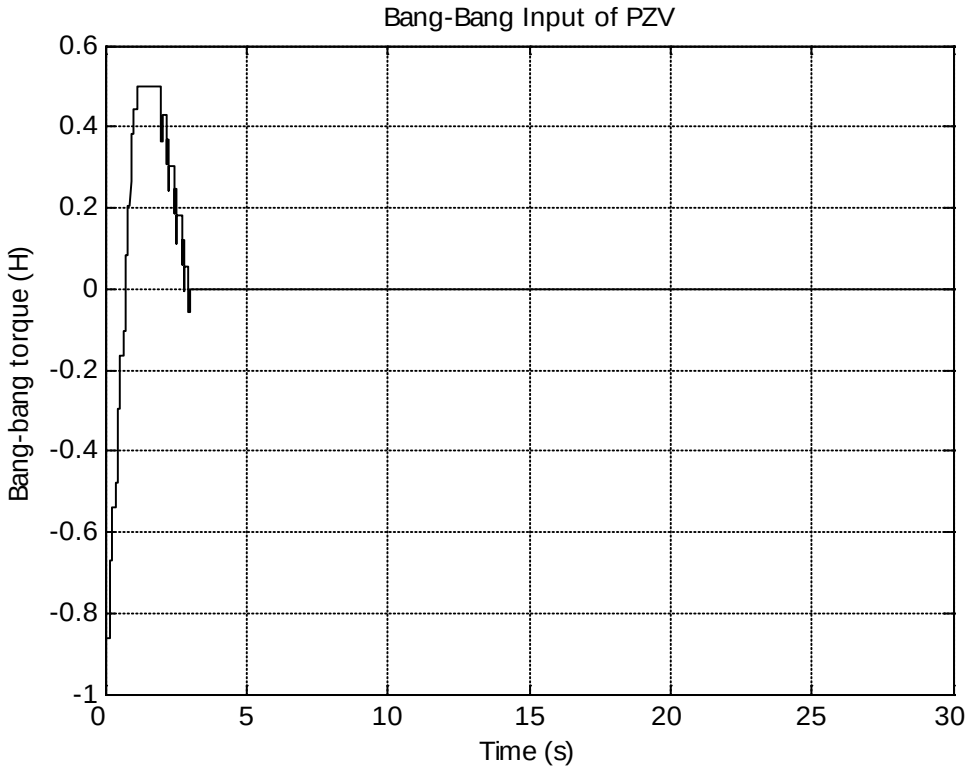

Figure 3.10: bang-bang input of positive zero sway (PZS) response

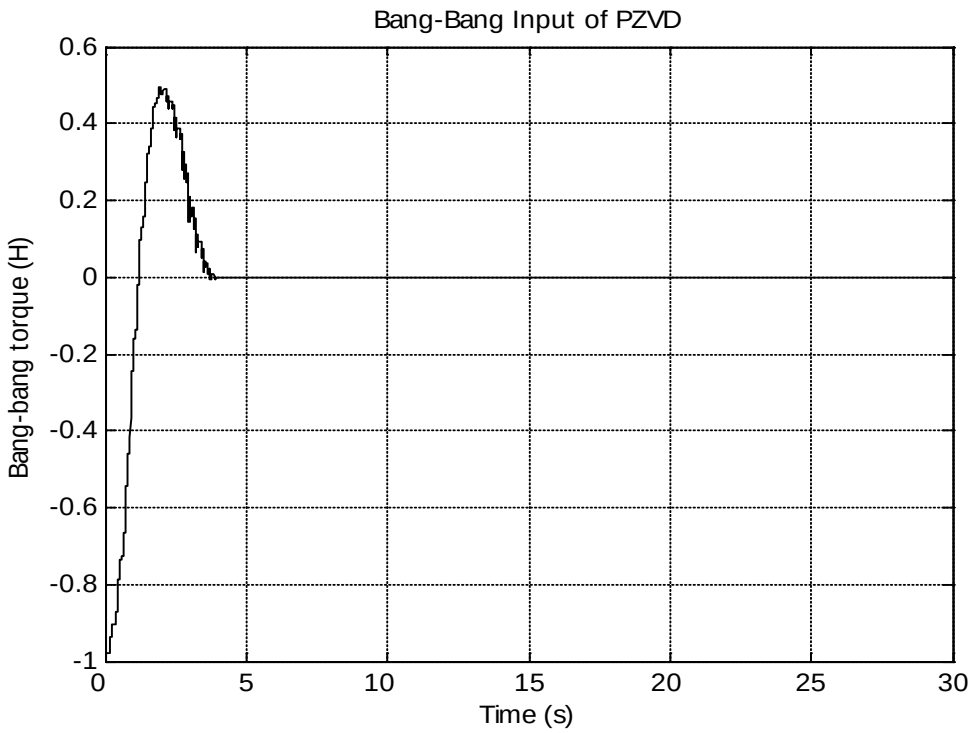

Figure 3.11: bang-bang input of positive zero sway derivative (PZSD) response

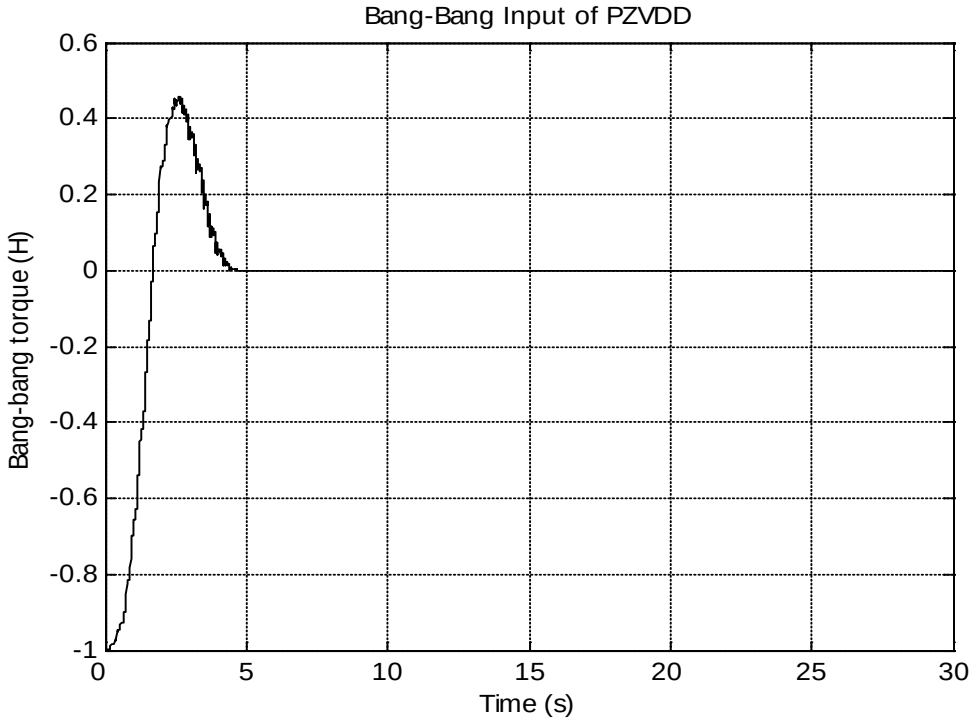

Figure 3.12: bang-bang input of positive zero sway derivative-derivative (PZSDD) response

3.6 Simulation Studies

The output signal that generated from simulation will give preliminary result of angle sway, position and velocity for positive zero sway (PZS), positive zero sway derivatives (PZSD) and positive zero sway derivative-derivative (PZSDD). Figure 3.13 show the simulink model of double pendulum type overhead crane with different derivative order of input shaping technique.

The output signal then use as reference for the experimental of reducing sway angle of double pendulum type overhead crane system. Simulation result of the response of the double pendulum type overhead crane (DPTOC) system to the shaped input is presented in time and frequency domains.

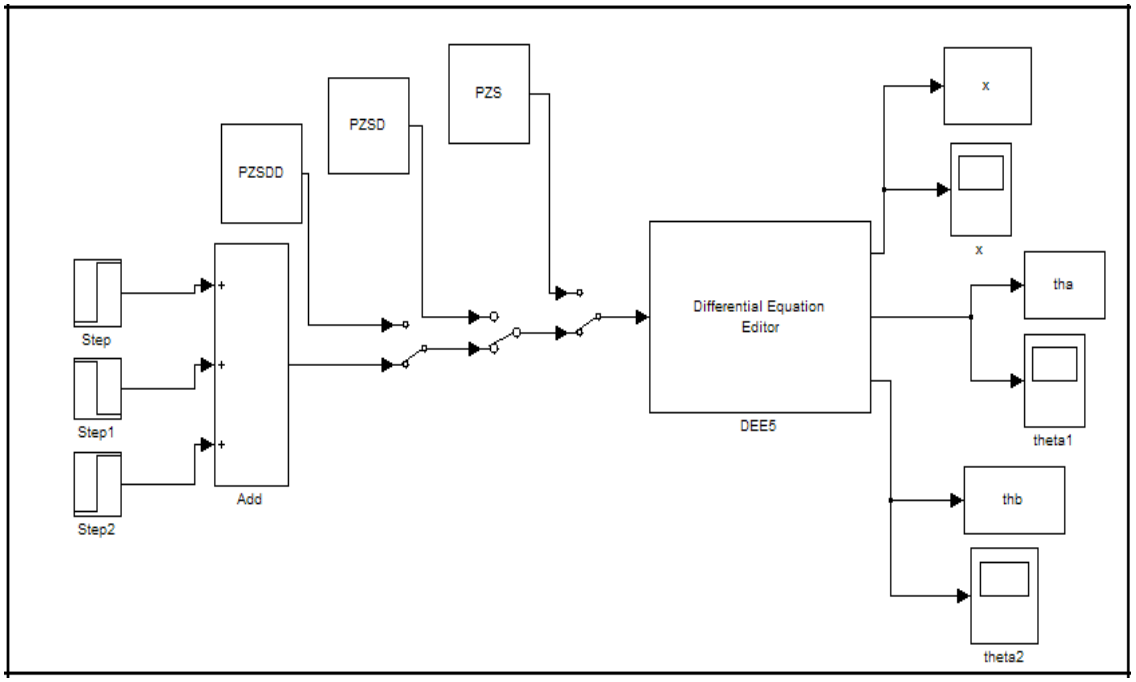

Figure 3.13: Simulink model of double pendulum type overhead crane

3.7 Experimental Studies

The experiments will be conducted by using CEMTools software, MATLAB software, Swing up inverted pendulum system and I/O board hardware to achieve the same output as the simulation studies. The unshaped bang-bang torque input is designed in SIMTools to determined characteristic parameter of the system for the design and evaluation of the positive input shaping technique. The experimental is continued to find the natural frequency ω_n by taking the highest amplitude in the power spectral density PSD response and the multiply it with 2π to get the natural frequency that will be used in coding in CEMTools.

Performances of the shapers are examined in terms of swing angle reduction and time response specifications. Finally, a comparative assessment of the control techniques is presented and discussed. As shown in Figure 3.14 the experimental study was developed by using CEMTools interface with Real Gain Swing-Up Inverted Pendulum and the block diagram for SIMtool Model Design without controller is shown in Figure 3.15.

Figure 3.14: Interfacing connection between CEMTools and Real Gain Swing-Up Inverted Pendulum

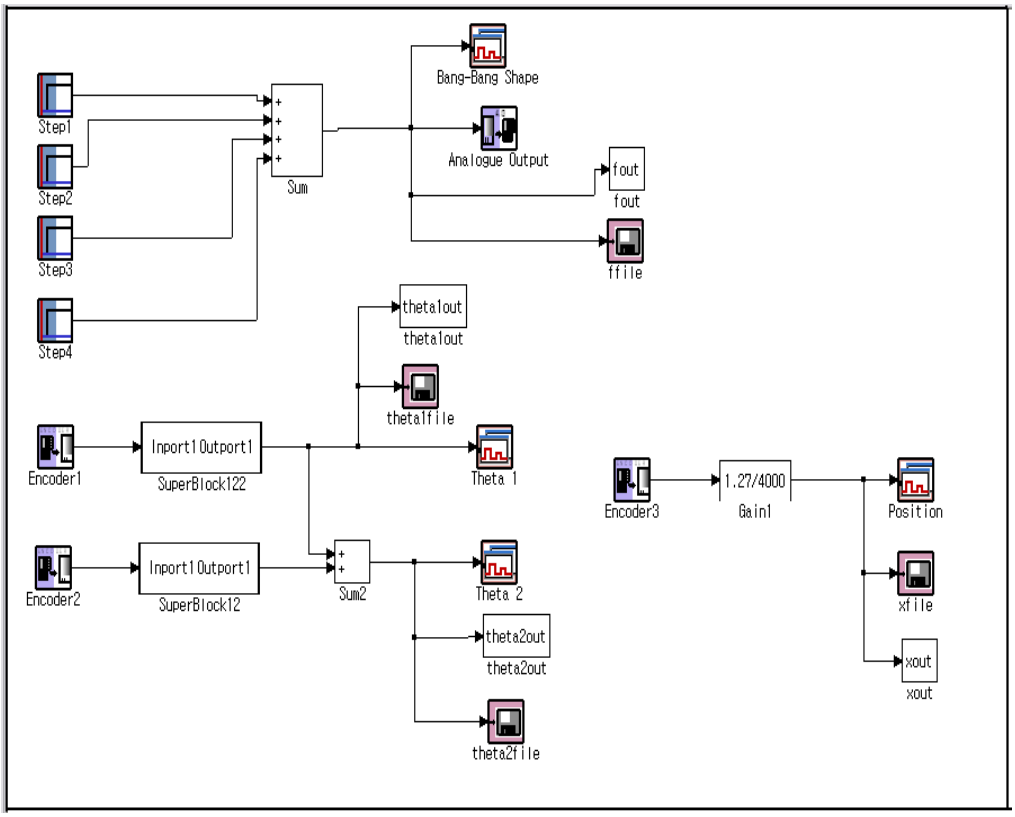

Figure 3.15: A SIMTool Model Design without controller

the configurations for parameter settings of unshaped bang-bang torque input are shown in Figures 3.16 - 3.19.

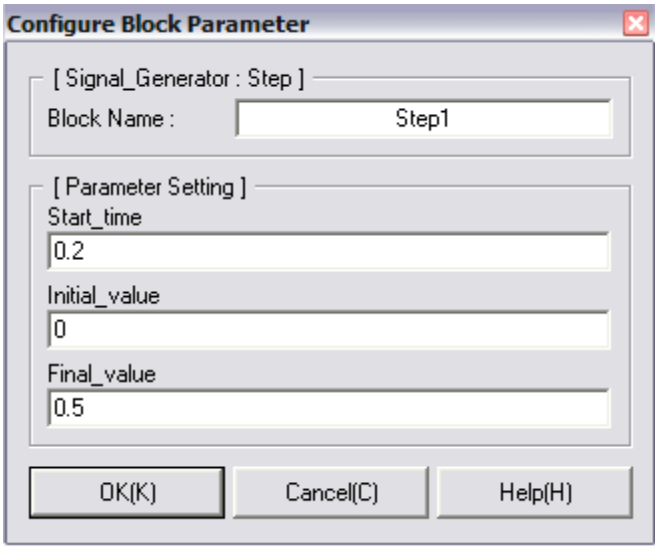

Figure 3.16: Parameter Setting for Step 1

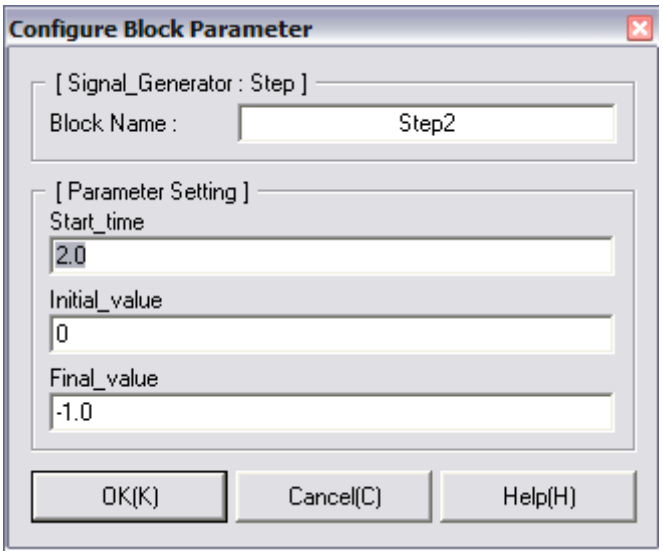

Figure 3.17: Parameter Setting for Step 2

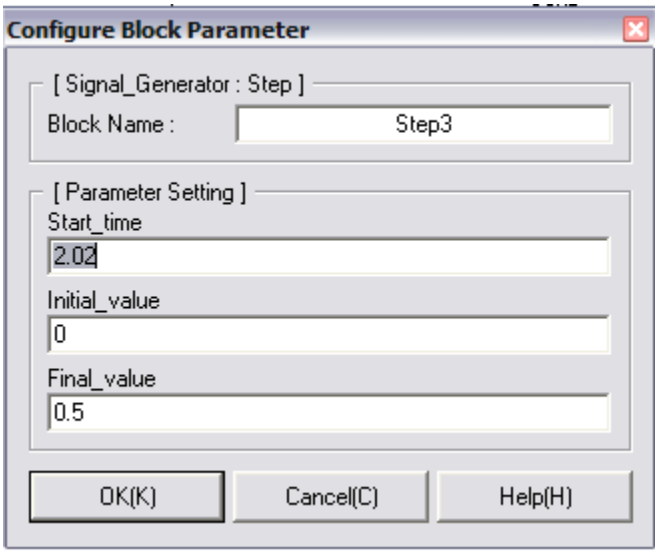

Figure 3.18: Parameter Setting for Step 3

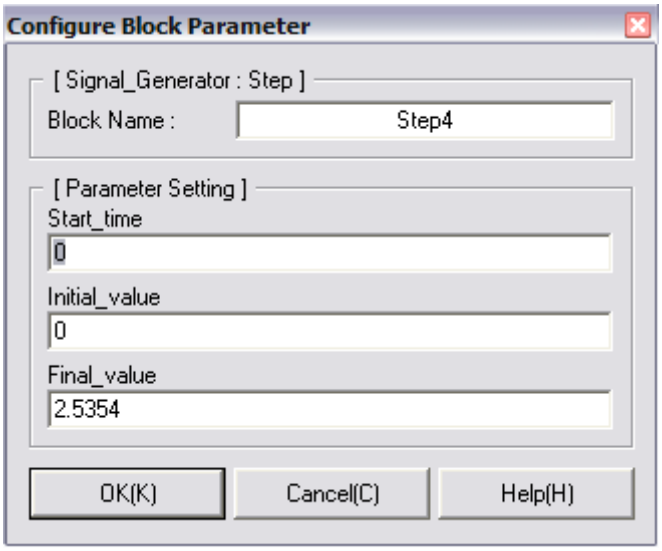

Figure 3.19: Parameter setting for step 4

3.8 Verification of Control Model Design

The coding for positive input shaping in M-file mode is converted to CEM mode. The coding is run in CEM mode and the variable is stored in workspace in SIMTool. The variable stored in workspace is depending on the derivatives of input shaping

After the coding has been run in CEMTools, the result will be stored in workspace under the name of 'ans'. Using 'ans' from the workspace, SIMTool model was started to obtain the graph result for sway angle and position for double pendulum type overhead crane. The configurations of workspace in SIMTool model is shown in Figure 3.20:

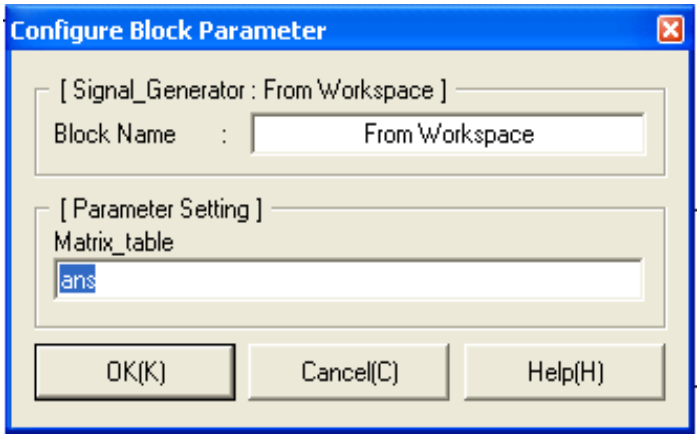

Figure 3.20: Configuration of workspace

3.9 Data Collection and Analysis Controller Design

Figure 3.21 show a complete design model based on the positive input shaping technique. The different derivatives of the positive input shaping are used to evaluate the performance of the system. The experiment result for the responses of double pendulum type overhead crane will be analyzed and compared between PZS, PZSD and PZSDD shaper to decide which is more efficient to reduce a sway angle of the pendulum.

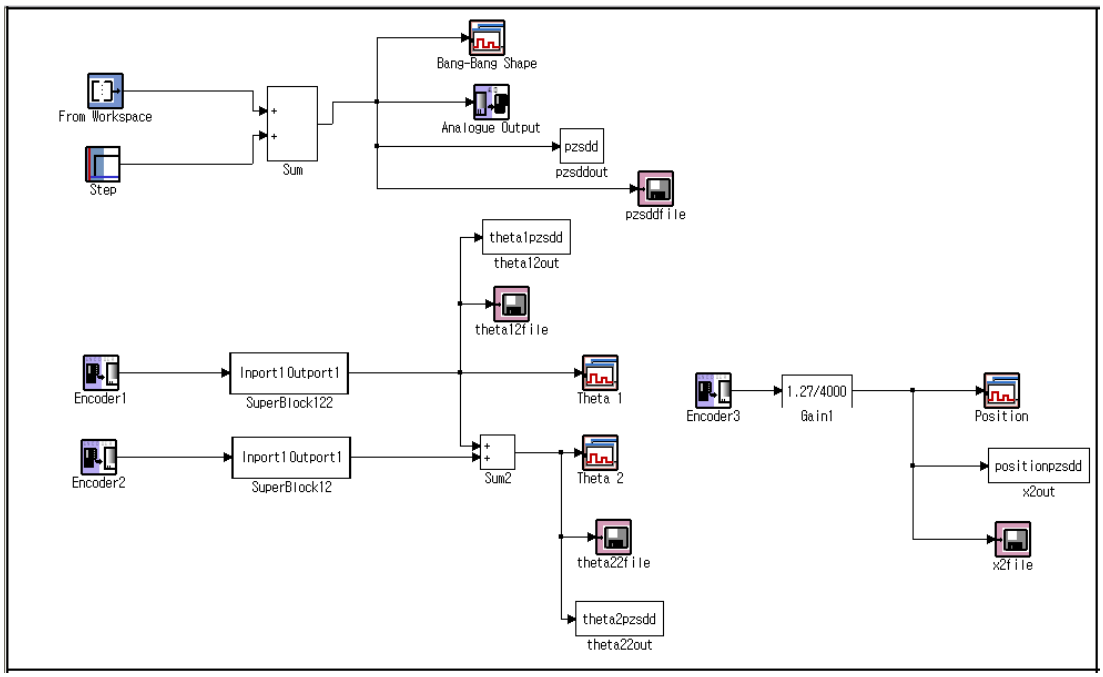

Figure 3.21: A SIMTool Model Design with controller

CHAPTER 4

RESULTS AND ANALYSIS

4.1 Introduction

This chapter will discuss all the result which are simulation and experimental results. Each of the results were presented and analyzed. The simulation studies were done using MATLAB 7.6 and experimental studies were done using CEMTools with Real Gain Swing-Up Inverted Pendulum. The results and analysis will divide into four major sections:

i. Simulation result using Matlab software
ii. Experimental result using CEMTools software
iii. Comparative assessment of input shaping techniques
iv. Result analysis

4.2 Simulation result using MATLAB software

Simulation results were obtained by using MATLAB software. After executing the positive input shaping coding in MATLAB software, all the variable were stored in workspace will be used in DPTOC model design to simulink the result. Simulation results of the response of the DPTOC system to the shaper input are presented in time and frequency domains. Performances of the shapers are examined in terms of swing angles reduction and time response specifications. Finally a comparative assessment of the control techniques is presented and discussed.

4.2.1 Results simulation of uncontrolled double pendulum type overhead crane

Figures 4.1- 4.5 show the power spectra density, swing angle of hook and load response and its trolley position of overhead crane system without input shaping controller. The results were used to evaluate the performance of the positive input shaping technique by comparing the results of uncontrolled overhead crane with controlled overhead crane.

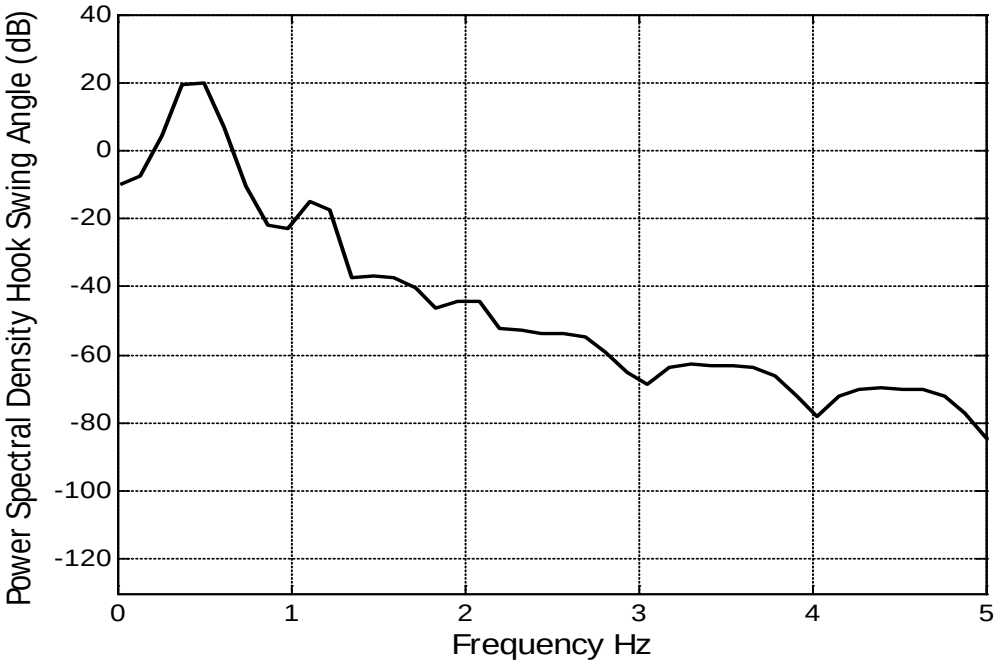

Figure 4.1: Response of the power spectral density hook swing angle

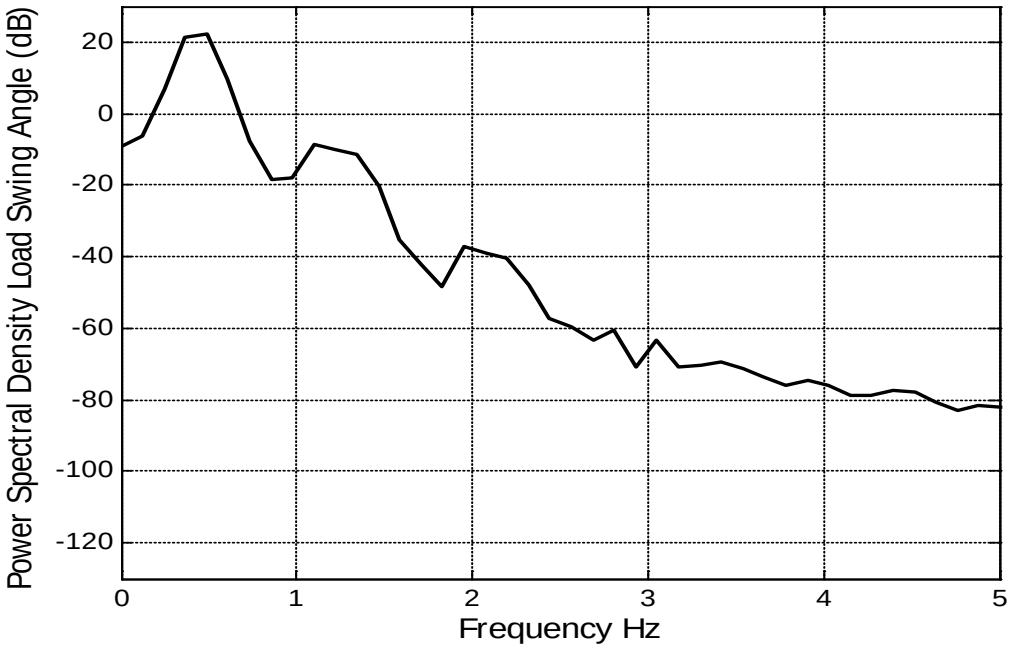

Figure 4.2: Response of the power spectral density load swing angle

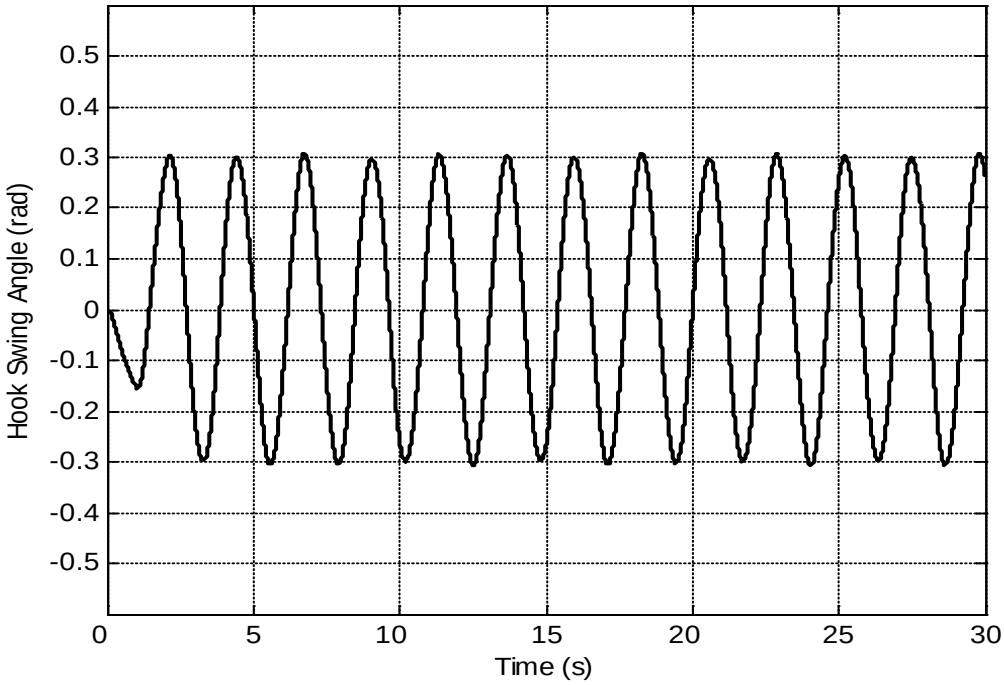

Figure 4.3: Response of the hook swing angle

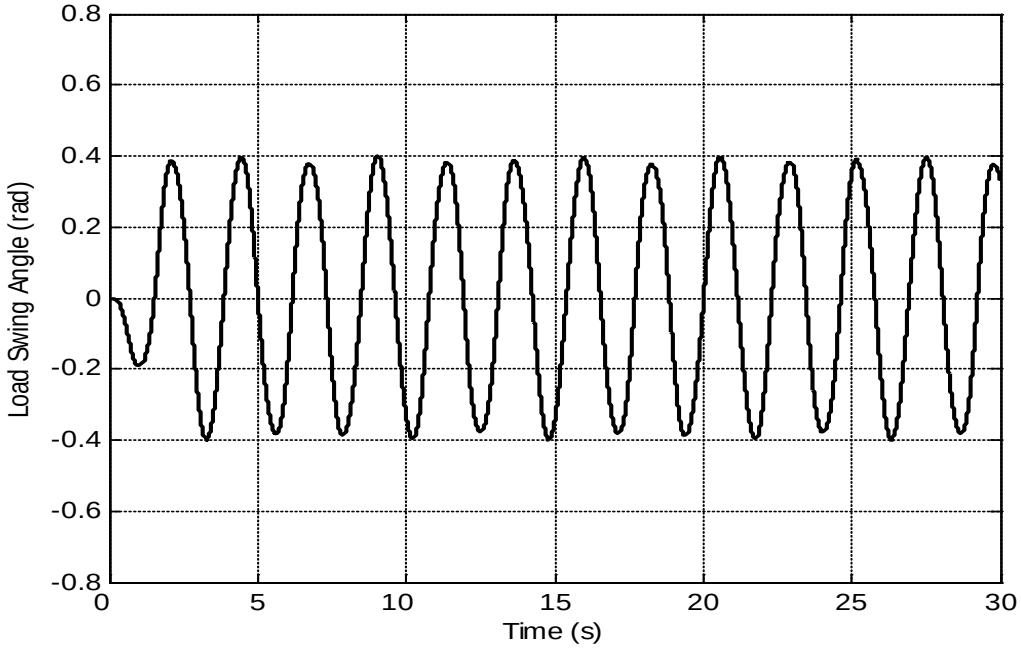

Figure 4.4: Response of the load swing angle

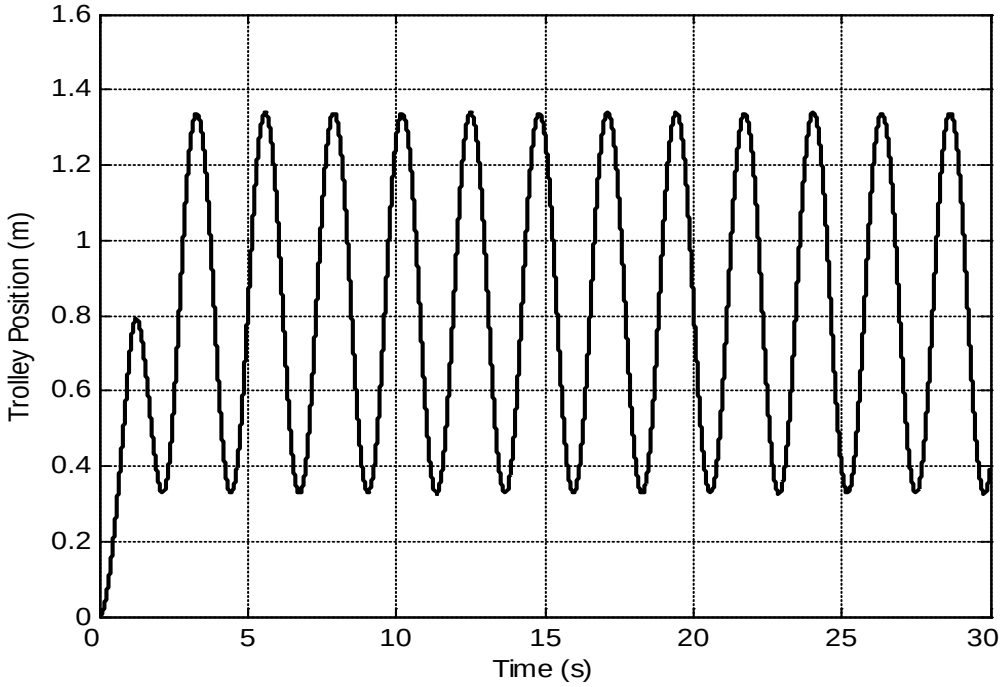

Figure 4.5: Response of the trolley position

4.2.2 Result simulation of positive zero sway (PZS) shaper

Figures 4.6 - 4.10 show the power spectra density, swing angle of hook and load response and its trolley position of overhead crane system after positive zero sway (PZS) shaper being applied to the system.

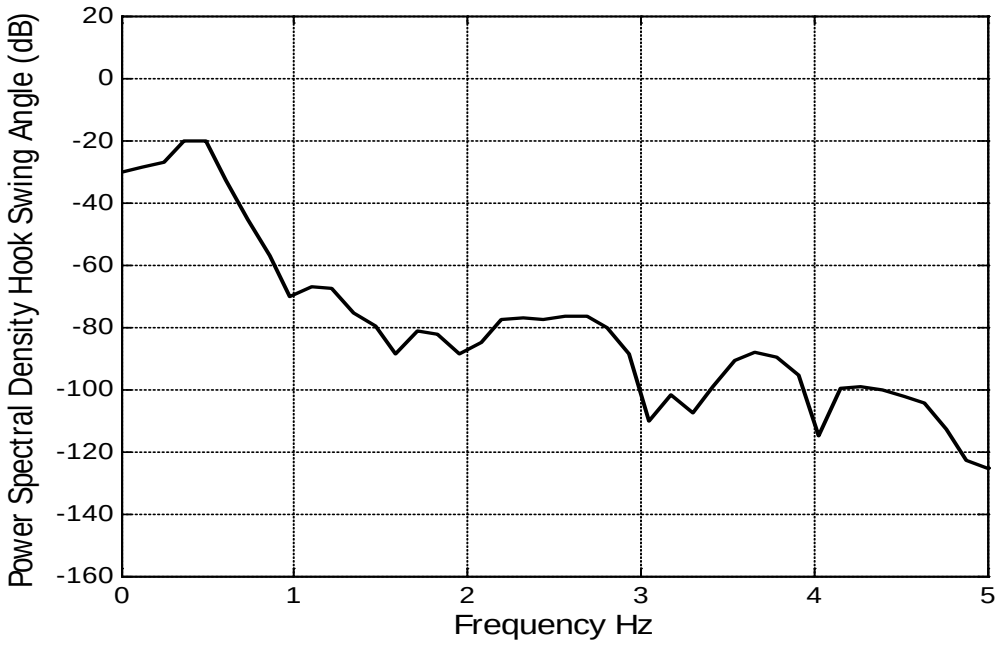

Figure 4.6: Response of the power spectral density hook swing angle with PZS shaper

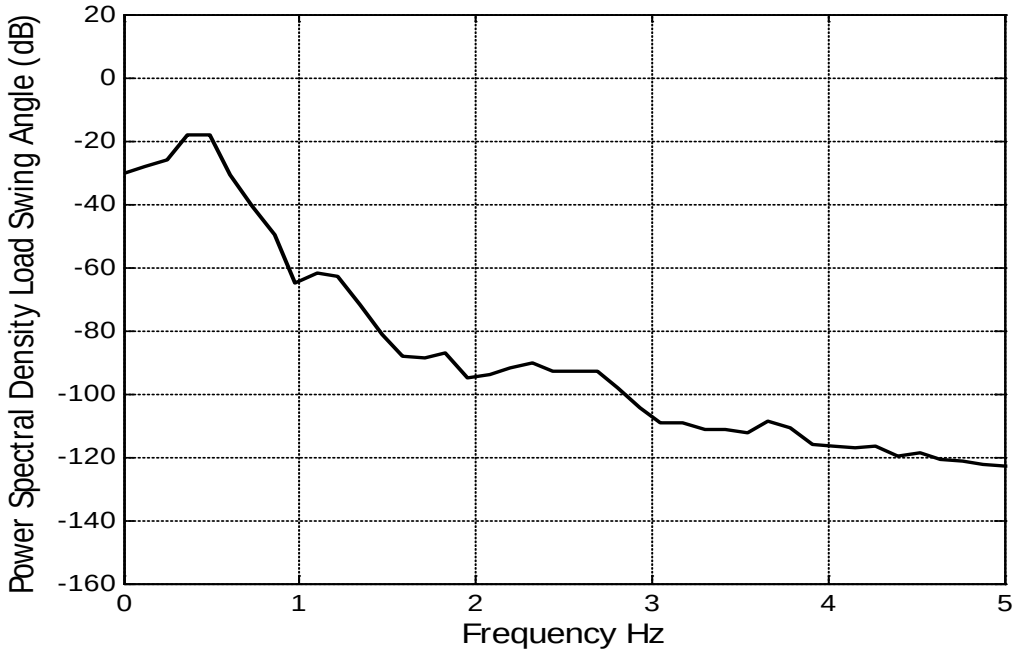

Figure 4.7: Response of the power spectral density load swing angle with PZS shaper

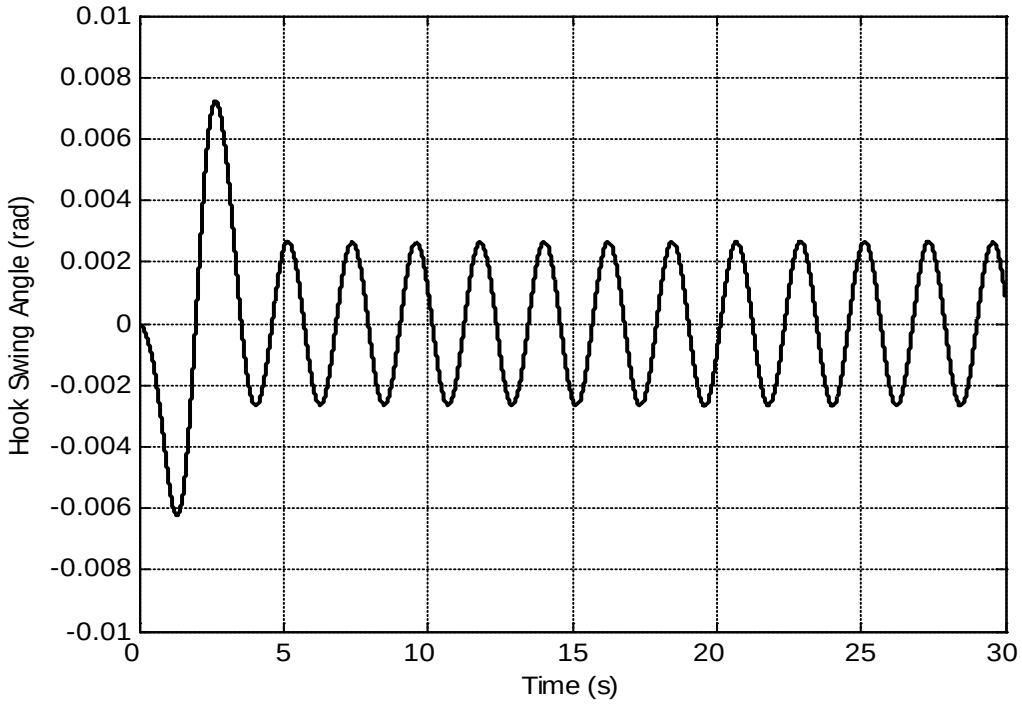

Figure 4.8: Response of the hook swing angle with PZS shaper

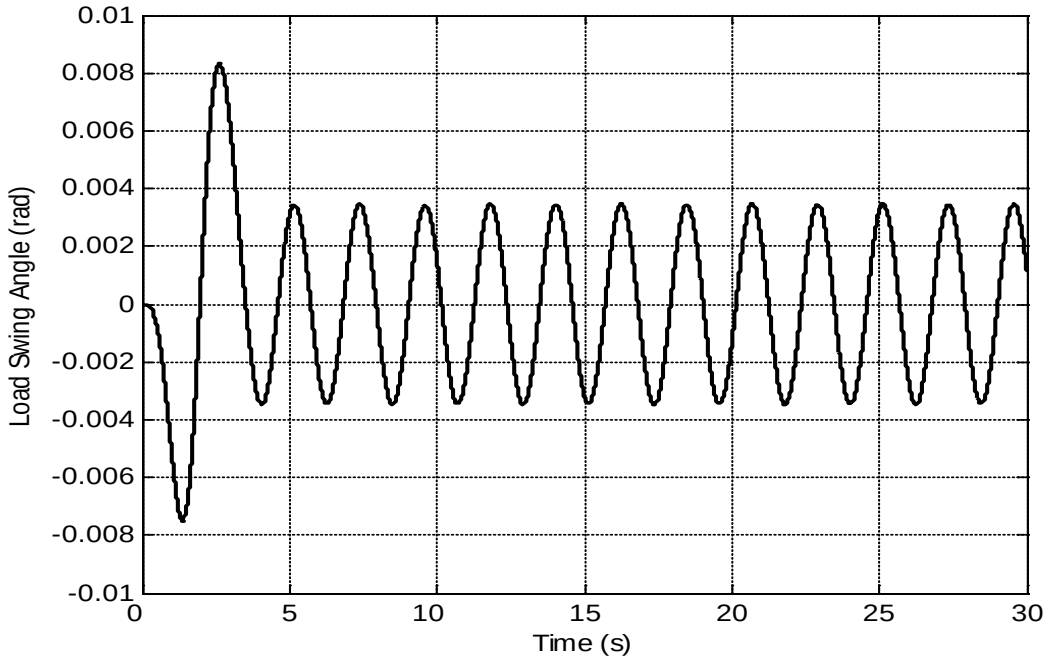

Figure 4.9: Response of the load swing angle with PZS shaper

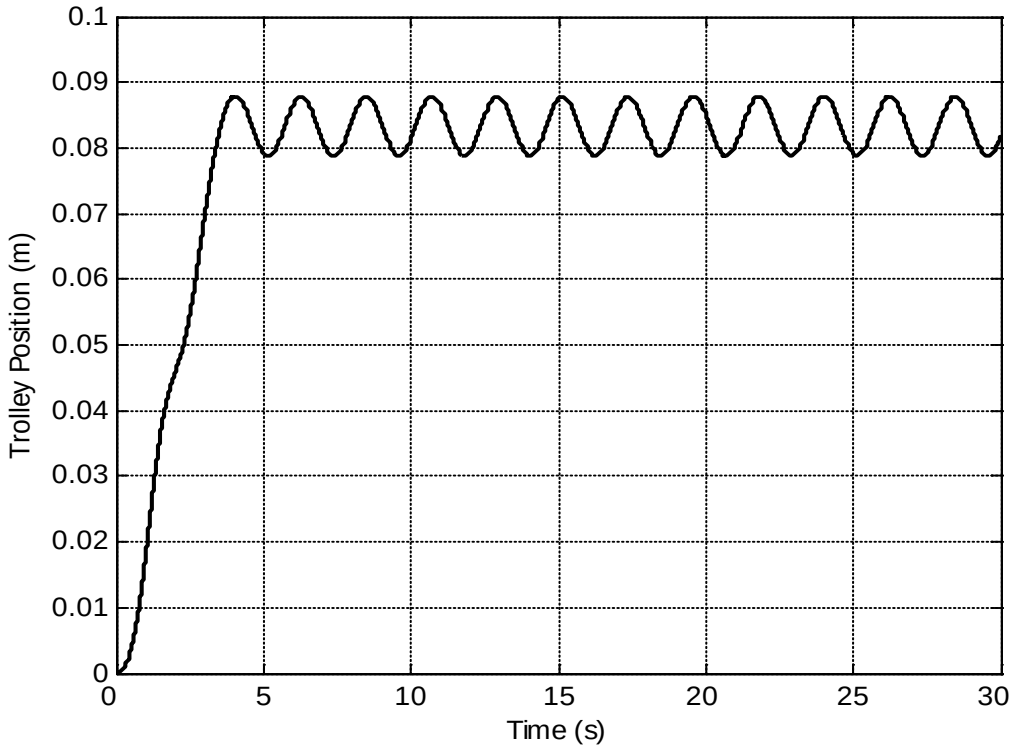

Figure 4.10: Response of the trolley position with PZS shaper

4.2.3 Result simulation of positive zero sway derivative (PZSD) shaper.

Figures 4.11 - 4.15 show the power spectra density, swing angle of hook and load response and its trolley position of overhead crane system after positive zero sway derivative (PZSD) shaper being applied to the system.

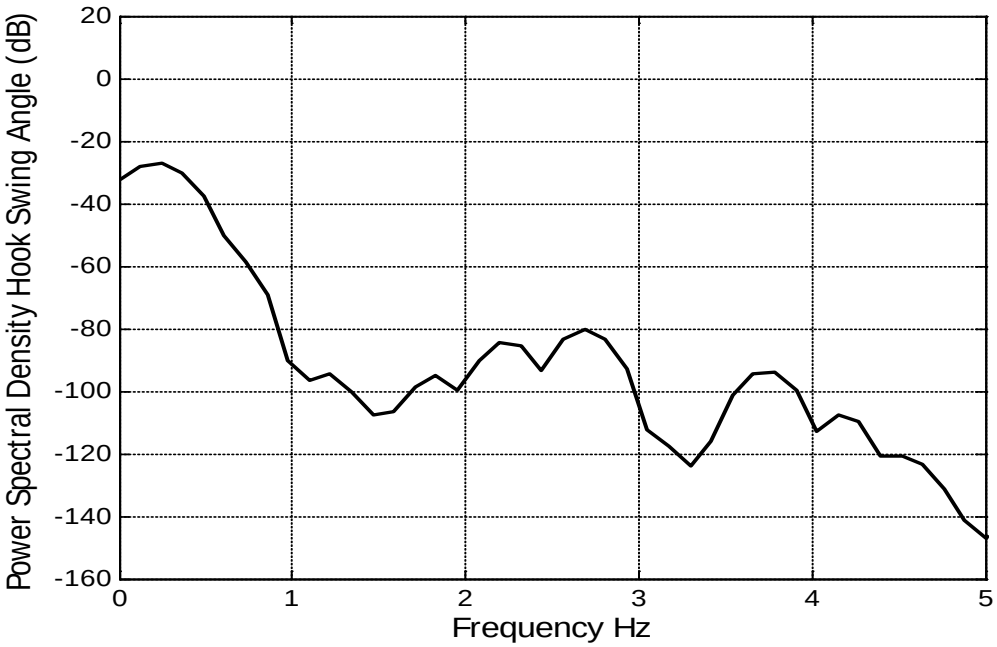

Figures 4.11: Response of the power spectral density hook swing angle with PZSD shaper

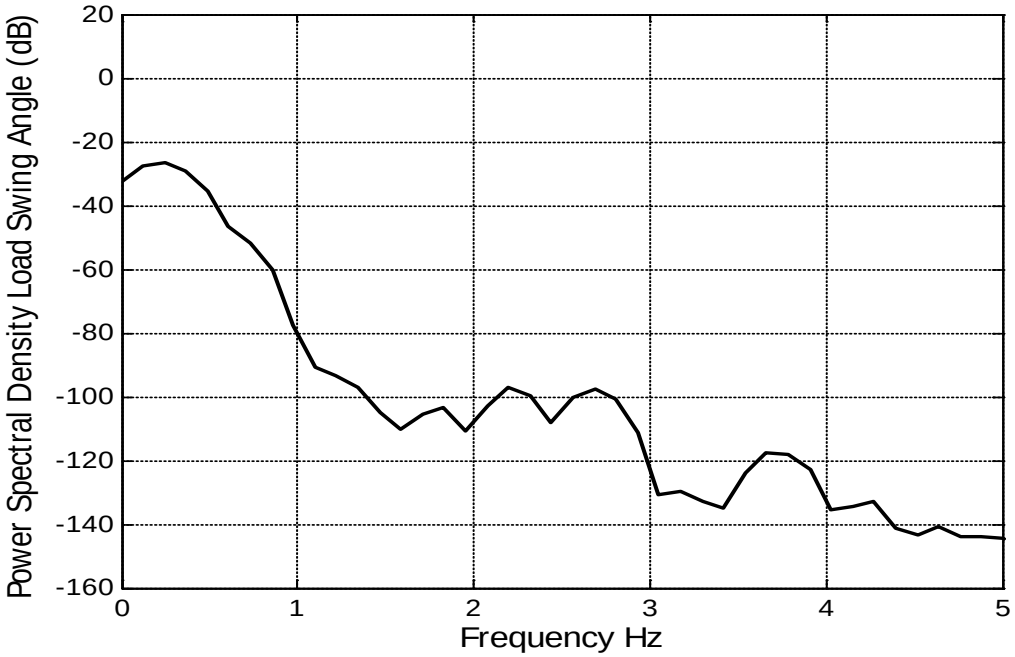

Figures 4.12: Response of the power spectral density load swing angle with PZSD shaper

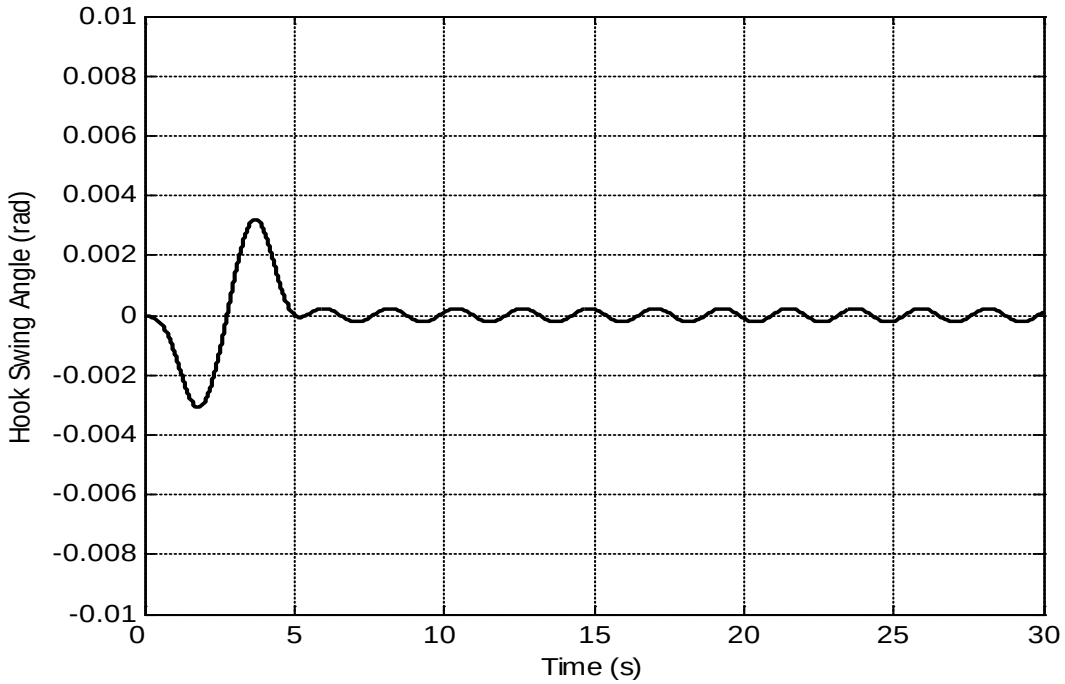

Figure 4.13: Response of the hook swing angle with PZSD shaper

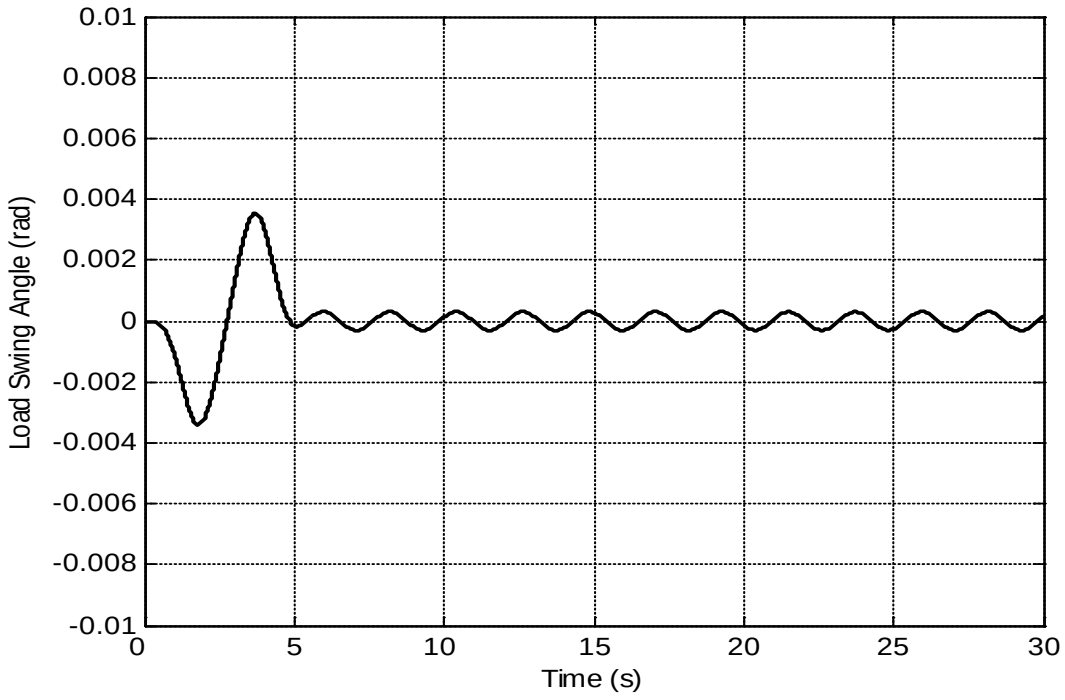

Figure 4.14: Response of the load swing angle with PZSD shaper

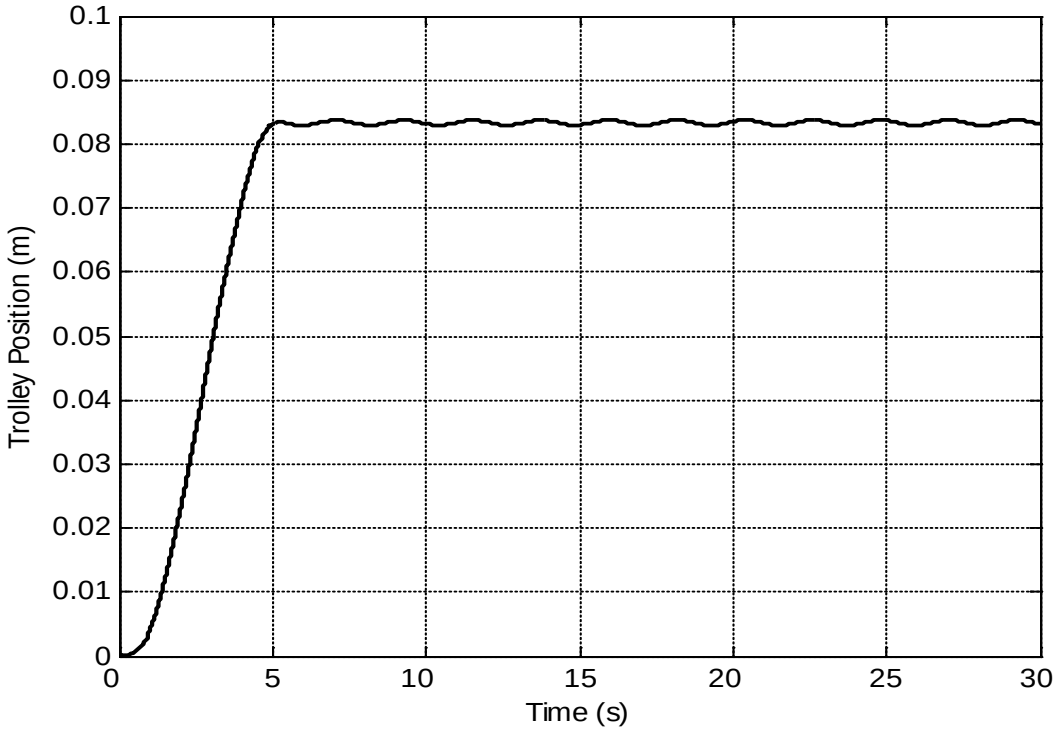

Figure 4.15: Response of the trolley position with PZSD shaper

4.2.4 Simulation result of positive zero sways derivative-derivative (PZSDD) shaper.

Figures 4.16 - 4.20 show the power spectra density, swing angle of hook and load response and its trolley position of overhead crane system after positive zero sway derivative - derivative (PZSDD) shaper being applied to the system.

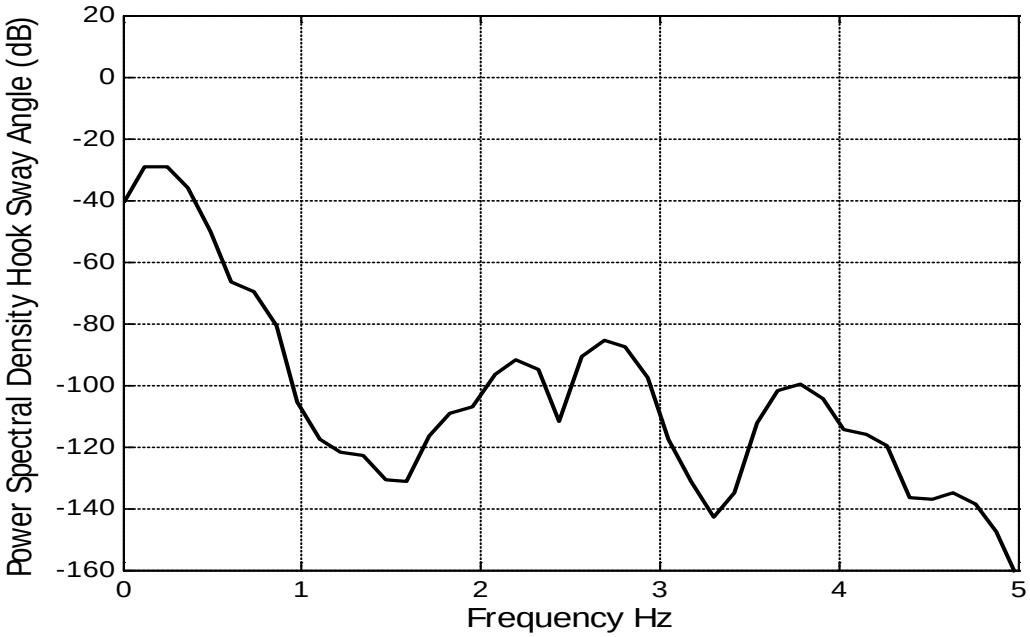

Figure 4.16: Response of the power spectral density hook sway angle with PZSDD shaper

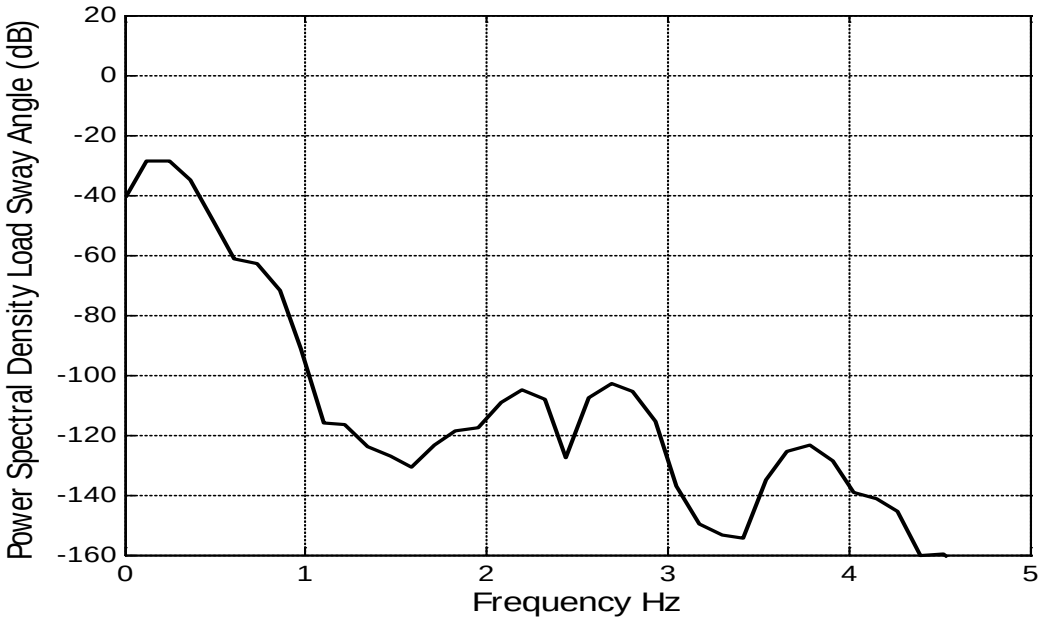

Figure 4.17: Response of the power spectral density load sway angle with PZSDD shaper

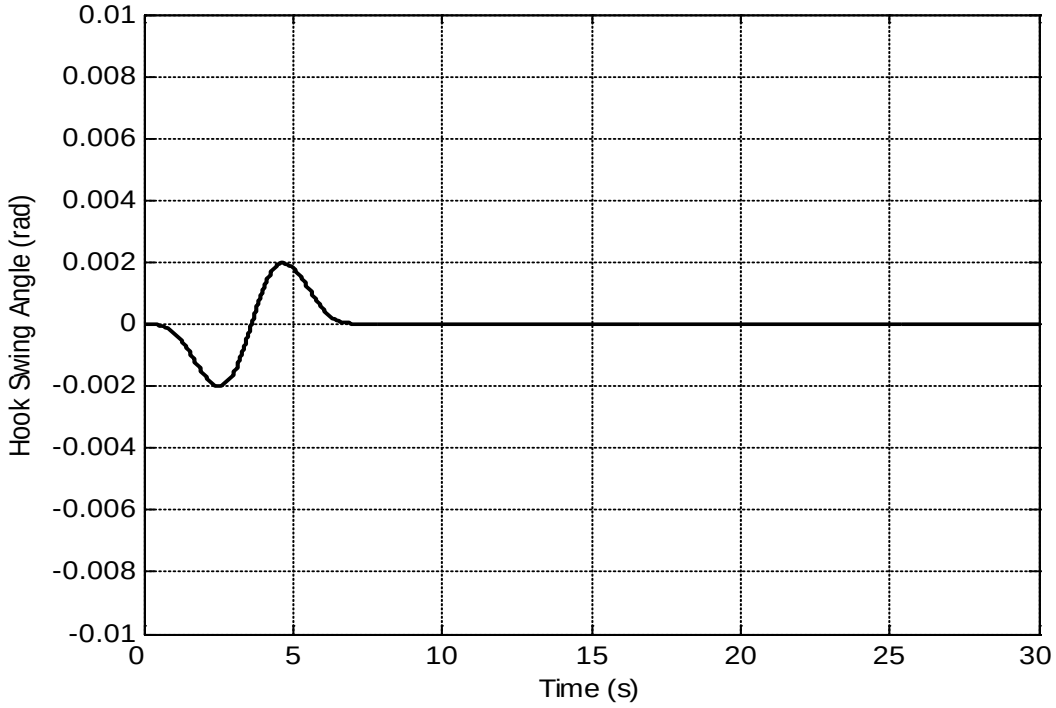

Figure 4.18: Response of the hook swing angle with PZSDD shaper

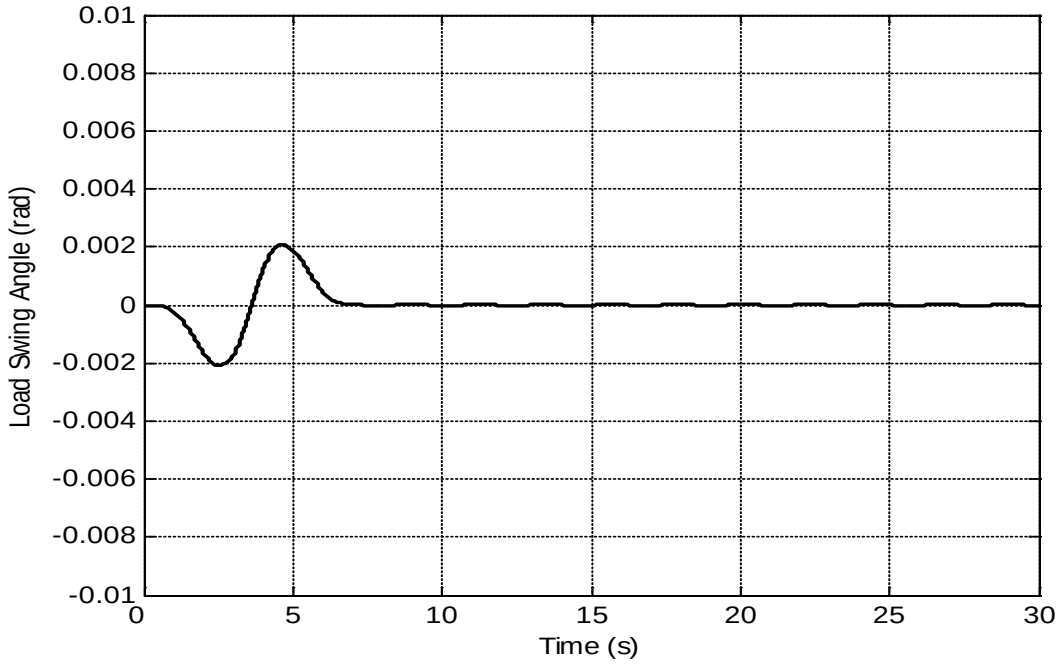

Figure 4.19: Response of the load swing angle with PZSDD shaper

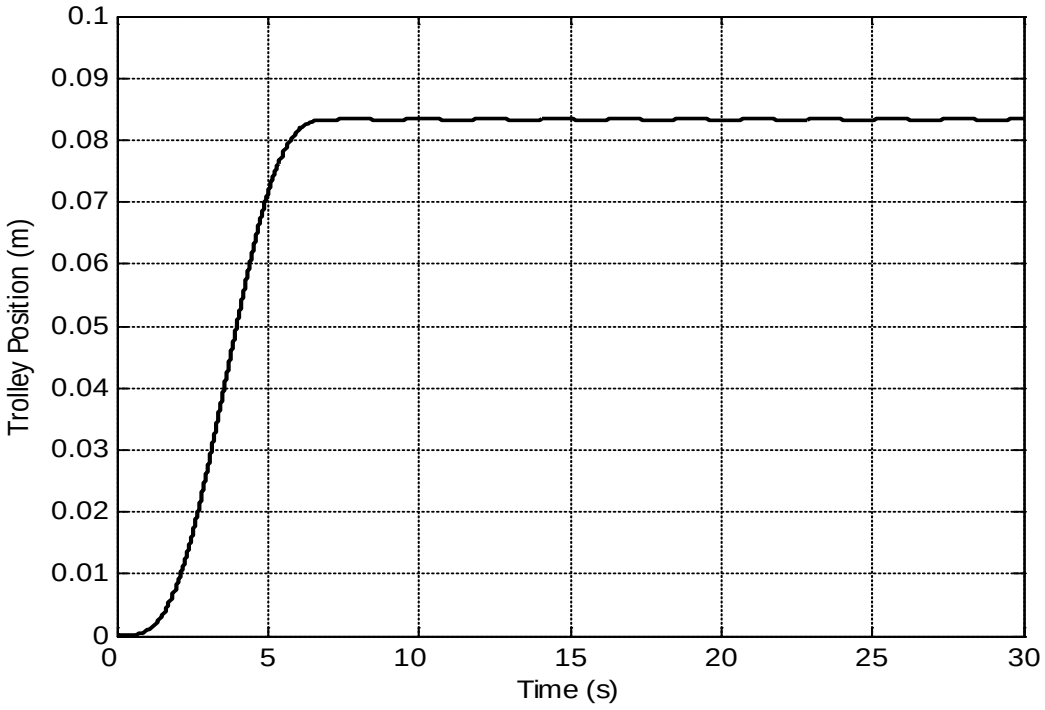

Figure 4.20: Response of the trolley position with PZSDD

4.3 Comparative assessment of input shaping techniques in simulation results

From the simulation result of the PZS, PZSD and PZSDD shaper in term of power spectral density, hook sway angle, load sway angle and trolley position were be compared with each other to show the different effect of the positive input shaper derivative order in terms of level of sway reduction and time response specification. The comparison simulation result of input shaping is shown below.

4.3.1 Comparison of power spectral density in simulation result

Figures 4.21 and 4.22 shows the comparison of power spectral density of hook and load sway angle between positive zero sway (PZS), positive zero sway derivative (PZSD) and positive zero sway derivative-derivative (PZSDD) shaper in simulation result. The first three mode of sway of the system are considered, as these dominate the dynamic of the system. The sway frequencies for both hook and load sway angle were obtained as 0.4883 Hz, 1.099 Hz and 1.587 Hz for the first three modes of sway. The attenuation of level of sway angle data in power spectral density was analyzed of each type of shaper.

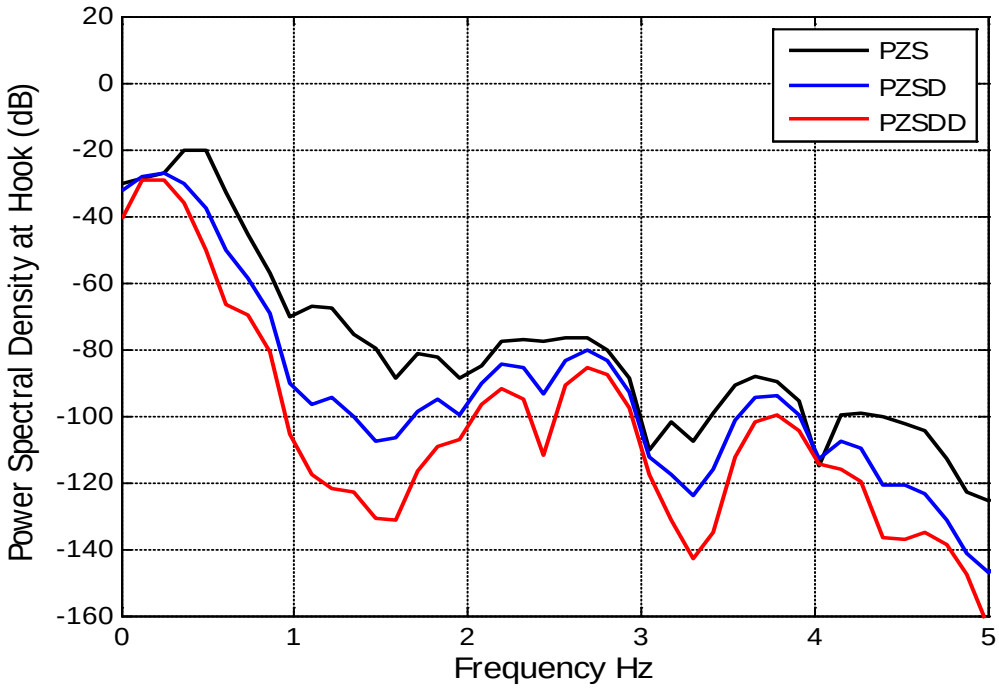

Figure 4.21: Power spectral density at hook swing angle in simulation result

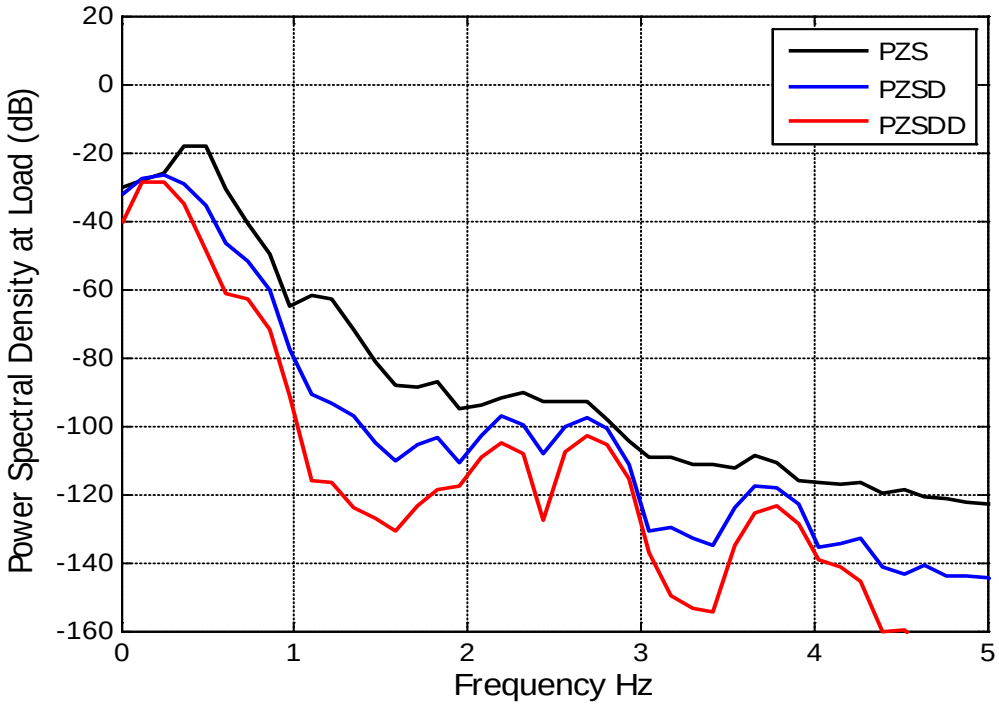

Figure 4.22: Power spectral density at load swing angle in simulation result

4.3.2 Comparison of sway angle in simulation result

Figures 4.23 and 4.24 shows the comparison of the hook and load sway angle response between positive zero sway (PZS), positive zero sway derivative (PZSD) and positive zero sway derivative-derivative (PZSDD) shaper in simulation result. From the comparison, show that the level sway angles were significantly reduced with the increasing of positive input shaping derivative order.

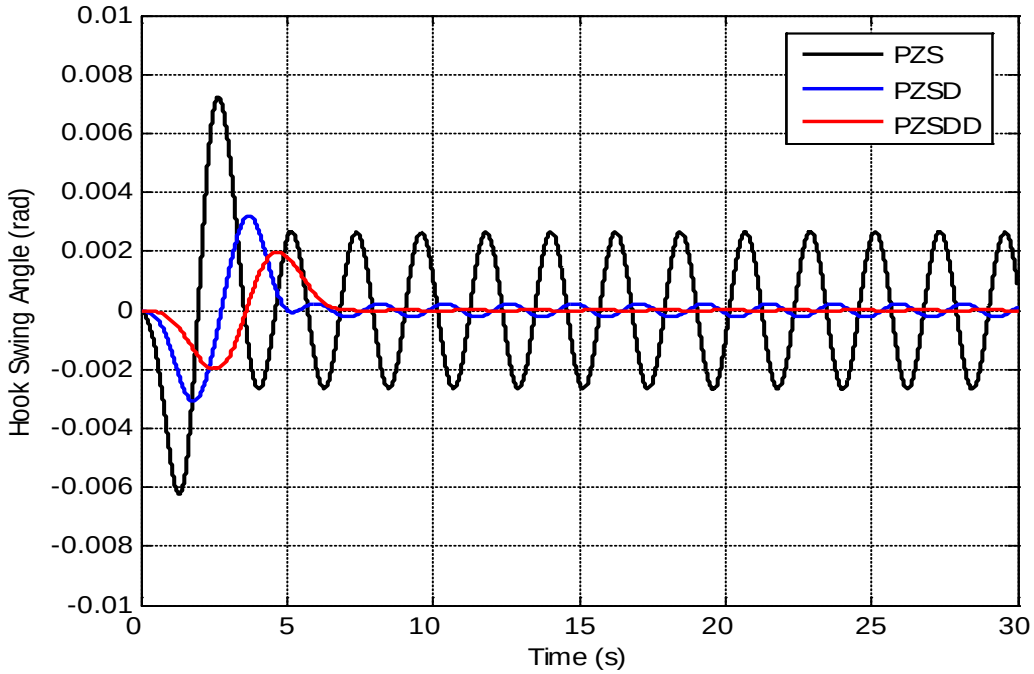

Figure 4.23: Response of the hook swing angle in simulation results

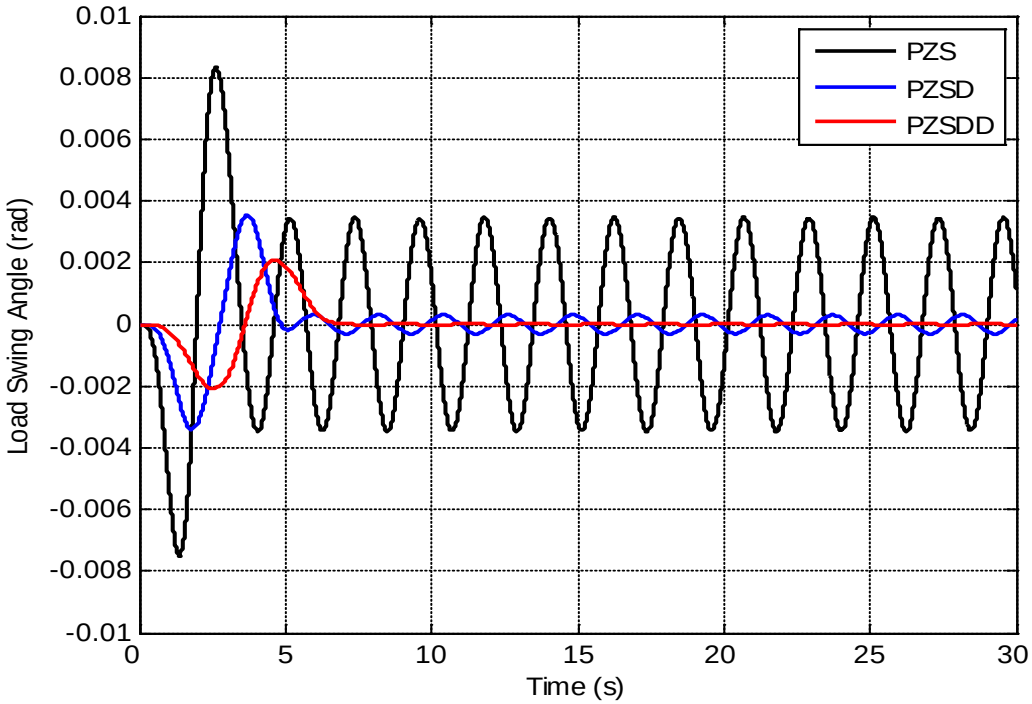

Figure 4.24: Response of the load swing angle in simulation result

4.3.3 Comparison of trolley position in simulation result.

Figure 4.25 shows the comparison of the trolley position response between positive zero sway (PZS), positive zero sway derivative (PZSD) and positive zero sway derivative-derivative (PZSDD) shaper in simulation result. The position of the trolley keeps reducing with higher derivative order of positive input shaping. Therefore, the speed of the system response were reduces with the increasing the number of impulse sequence. The corresponding rise time, settling time and overshoot of the trolley position response were be analyzed.

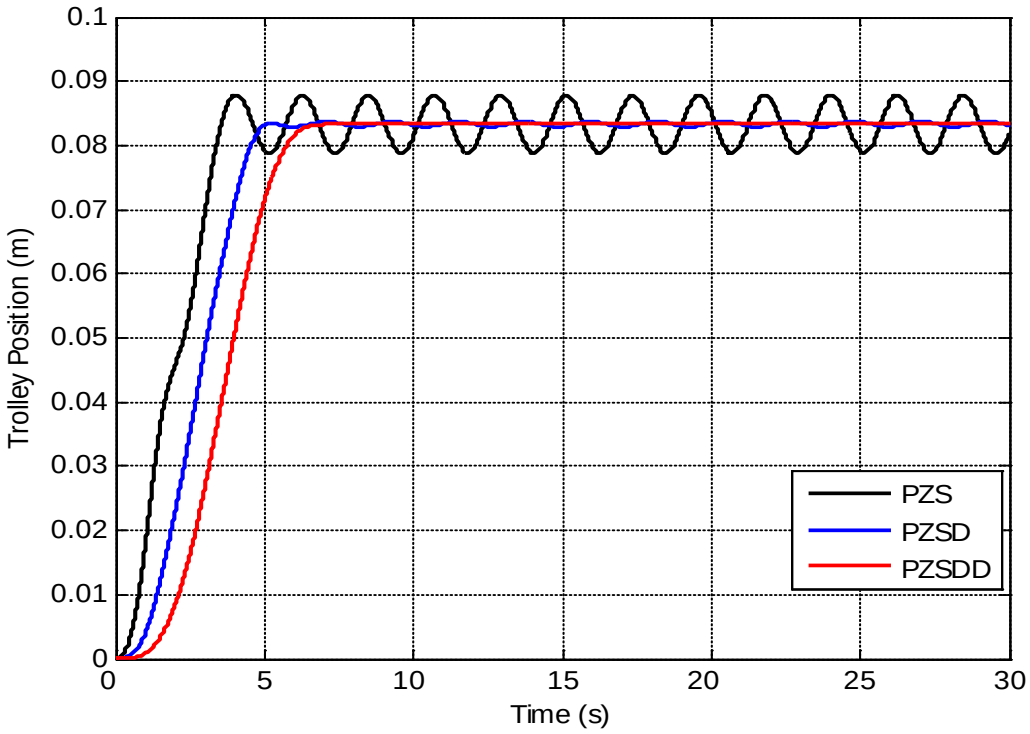

Figure 4.25: Response of the trolley position in simulation result

4.4 Simulation result analysis

The simulation result analysis of this project were done by investigating the effect of each positive input shaper derivative order in terms of attenuation sway of the cable and specification of trolley position response. For the sway suppression schemes, PZS, PZSD and PZSDD are designed based on the sway frequencies and damping ratios of the DPTOC system.

The responses of the DPTOC system to the unshaped input were analyzed in time-domain and frequency domain (spectral density). These simulation results were considered as the system response to the unshaped input and will be used to evaluate as the performance of the input shaping technique.

High level of sway reduction were obtained using positive zero sway derivative-derivative (PZSDD) shaper as compare to the case with using positive zero sway (PZS) and positive zero sway derivative (PZSD) on the double pendulum type overhead crane (DPTOC) system. The corresponding rise time, settling time and overshoot of the trolley position response of each positive input shaper derivative order is depicted in simulation table analysis.

4.4.1 Simulation result analysis of input shaping

Table 4.1 show summaries the levels of sway reduction of the system responses at the first three modes in simulation results. By comparing the result presented in table 4.1, it is noted that the higher performance in the reduction of sway of the system is achieved using positive zero sway derivative-derivative (PZSDD) shaper. This is observed and compared with the positive zero sway (PZS) and positive zero sway derivative (PZSD).

Table 4.1: Level of sway reduction of the hoisting angle of the pendulum and specification of trolley position response in simulation results

Types of shaper	Swing angle	Attenuation (dB) of sway of the cable			Specification of trolley position response		
		Mode 1	Mode 2	Mode 3	Rise time (s)	Settling time (s)	Overshoot (%)
PZS	Hook swing angle, $\theta 1$	40.18	52.35	43.71	2.425	2.985	7.427
	Load swing angle, $\theta 2$	40.42	53.11	53.19			
PZSD	Hook swing angle, $\theta 1$	46.96	81.67	61.16	2.905	4.701	0.677
	Load swing angle, $\theta 2$	48.69	91.81	75.11			
PZSDD	Hook swing angle, $\theta 1$	48.84	102.6	79.05	3.255	6.039	0.003
	Load swing angle, $\theta 2$	50.66	107.6	95.81			

For comparative assessment in simulation, the levels of sway reduction of the hoisting angles of the hook and load sway angle of each positive input shaper derivative order PZS, PZSD and PZSDD shapers are shown with the bar graphs in Figure 4.26 and Figure 4.27, respectively. The result shows that, highest level of sway reduction is achieved in control schemes using the positive zero sway derivative-derivative (PZSDD) shaper, followed by using positive zero sway derivative (PZSD) shaper and lastly using positive zero sway (PZS) shaper for all modes of sway, for both of hook and load swing angles.

Therefore, it can be concluded that the positive zero sway derivative-derivative (PZSDD) shaper provide better performance in sway reduction, followed by using positive zero sway derivative (PZSD) shaper and lastly by using positive zero sway (PZS) shaper in overall.

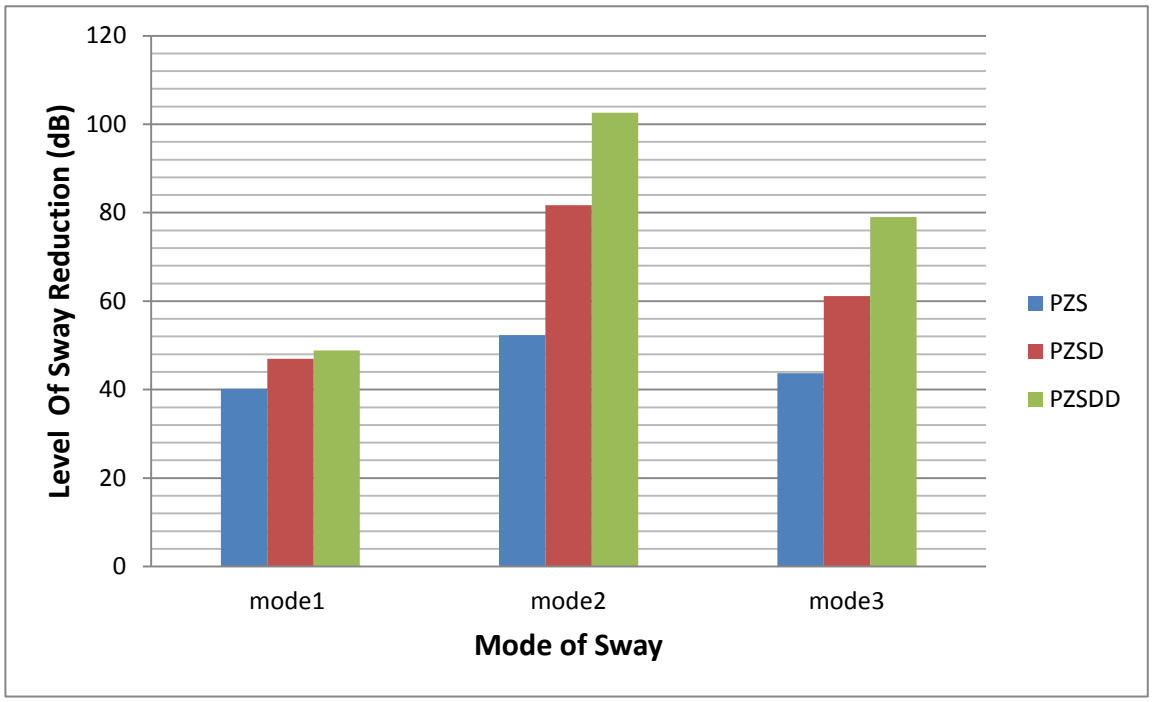

Figure 4.26: Level of sway reduction for hook swing angle in simulation

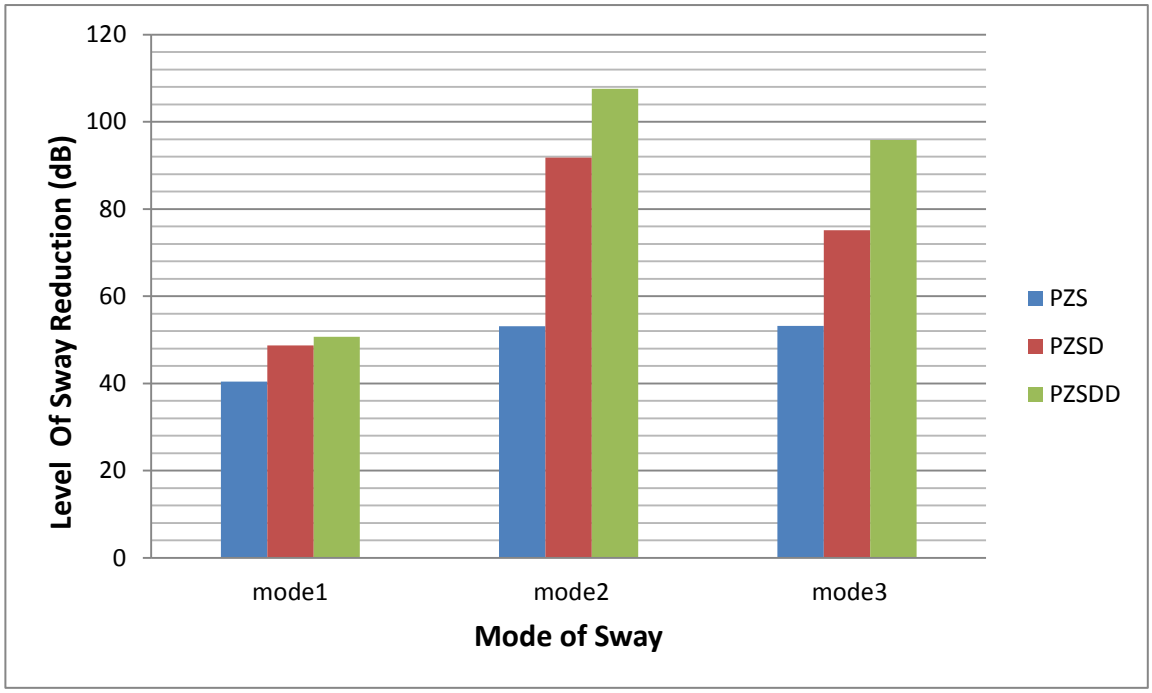

Figure 4.27: Level of sway reduction for load swing angle in simulation

Comparisons of the specifications of the trolley position response of input shaping control schemes of each positive input shaper derivative order in simulation are summarized in Figure 4.28 for the rise times and settling times. It is noted that settling time of the cart position response by using the positive zero sway (PZS) shaper is faster than the case using the positive zero sway derivative-derivative (PZSDD) shaper. It shows that, in term of settling time, the speed of the system response can be improved by using the positive zero sway (PZS) shaper.

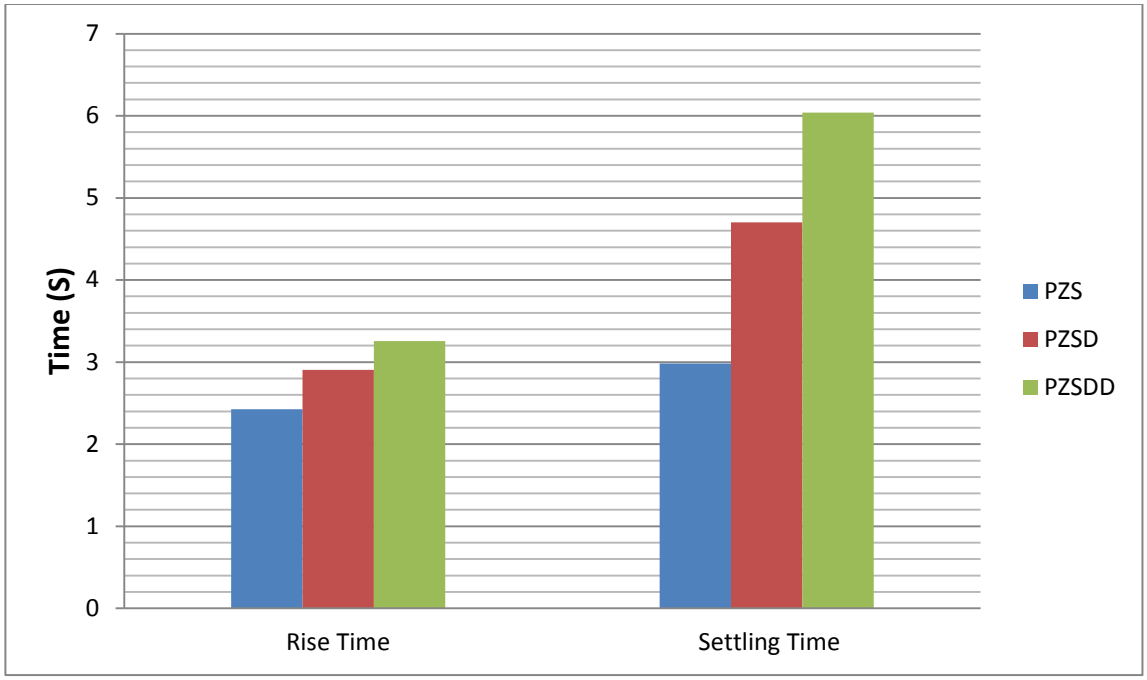

Figure 4.28: Time response specifications in simulation

4.5 Experimental result using CEMTools software

Experimental results were obtained by using both CEMTool and MATLAB software. After executing the positive input shaping coding in CEMTool, all the variables were stored in workspace will be used in SIMTool Model design of the double pendulum type overhead crane system. The experimental results from CEMTool then were being transferred into MATLAB software to get the final result. The experimental responses investigated are examined in terms of swing angles reduction and time response specifications. Finally a comparative assessment of the control techniques is presented and discussed.

4.5.1 Results experimental of uncontrolled double pendulum type overhead crane

Figures 4.29- 4.33 show the power spectra density, swing angle of hook and load response and its trolley position of overhead crane system without input shaping controller. The results were used to evaluate the performance of the positive input shaping technique by comparing the results of uncontrolled overhead crane with controlled overhead crane.

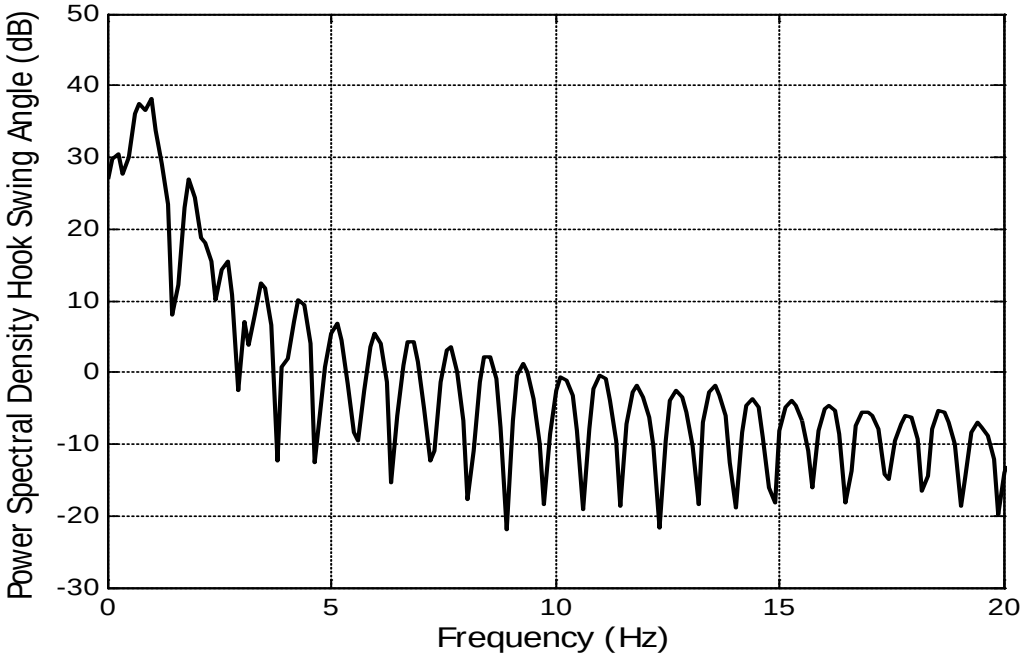

Figure 4.29: Power Spectra Density at hook sway angle without controller

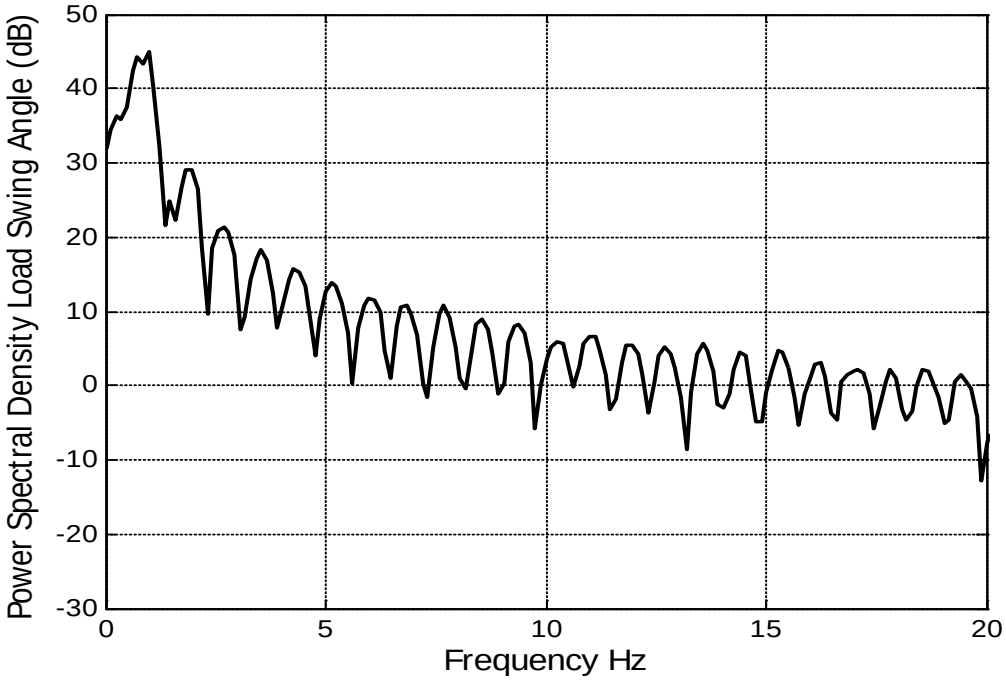

Figure 4.30: Power Spectra Density at load sway angle without controller

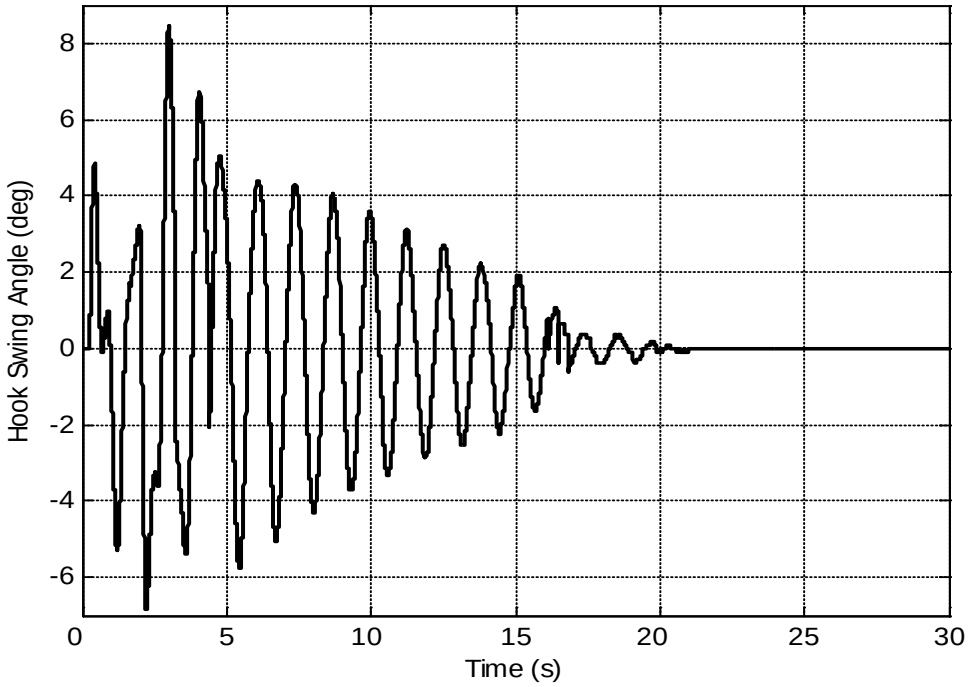

Figure 4.31: Hook sway angle without controller

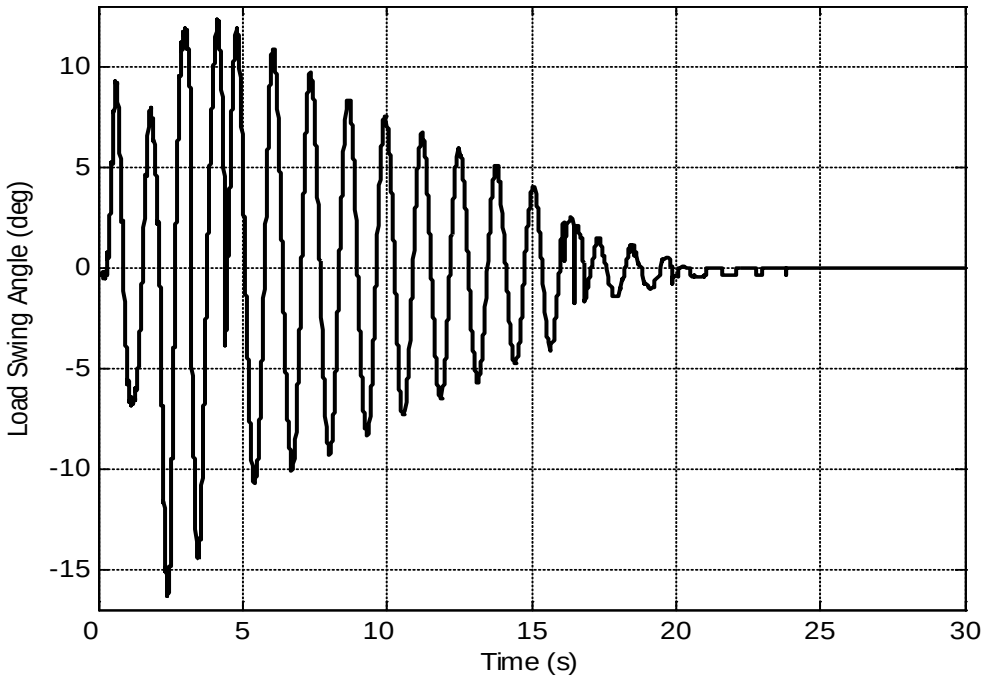

Figure 4.32: Load sway angle without controller

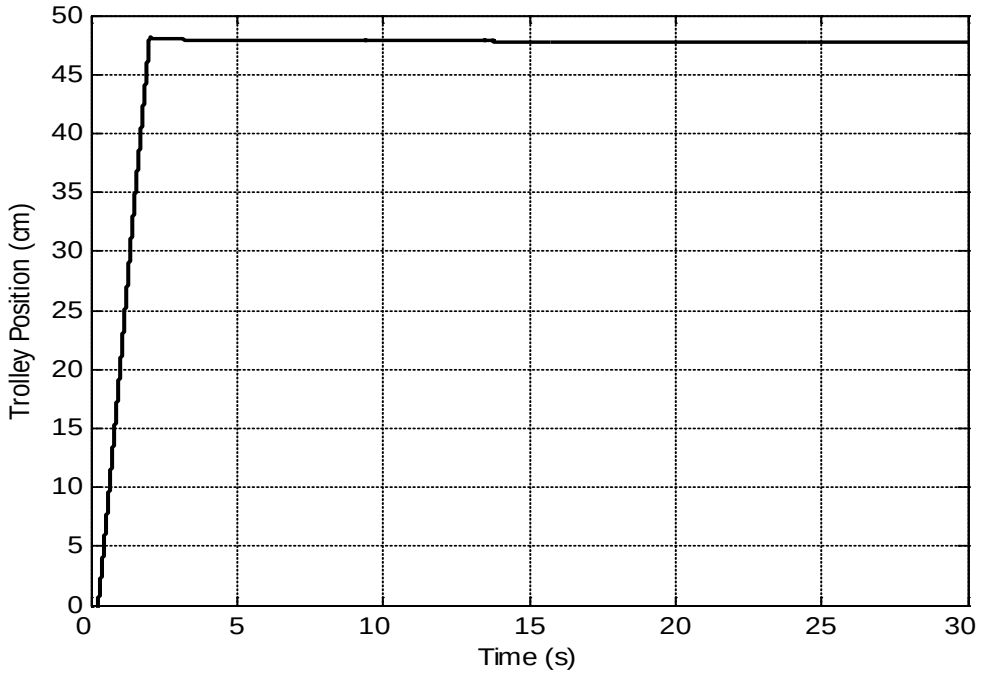

Figure 4.33: Position of the cart without controller

4.5.2 Results experimental of positive zero sway (PZS) shaper

Figures 4.34 - 4.38 show the power spectra density, swing angle of hook and load response and its trolley position of overhead crane system after positive zero sway (PZS) shaper being applied to the system.

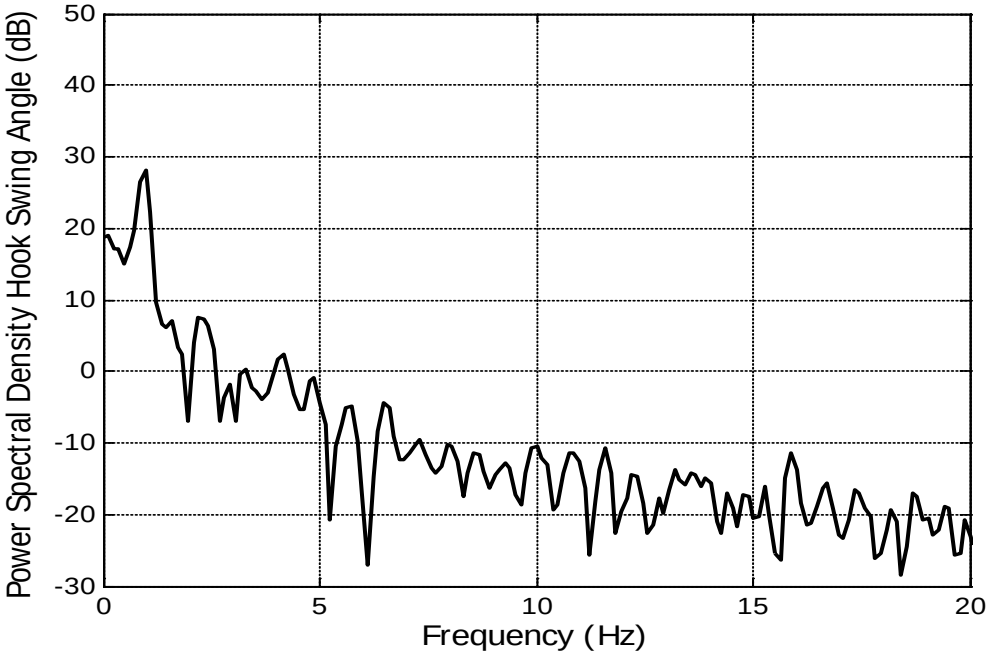

Figure 4.34: Power Spectra Density of hook sway angle with PZS input shaper

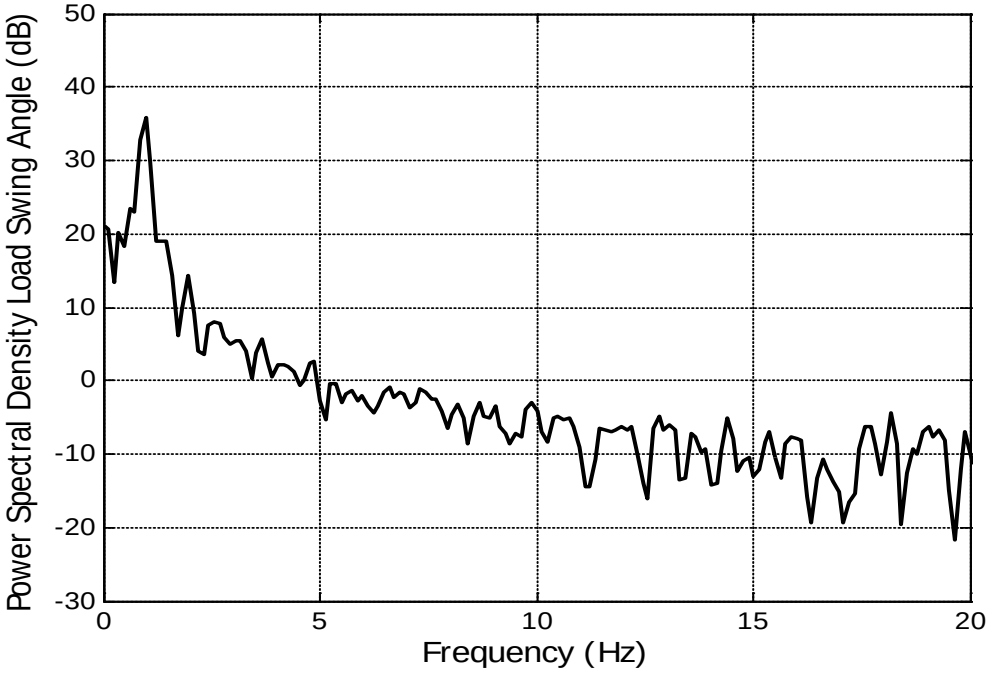

Figure 4.35: Power spectral density of load sway angle with PZS input shaper

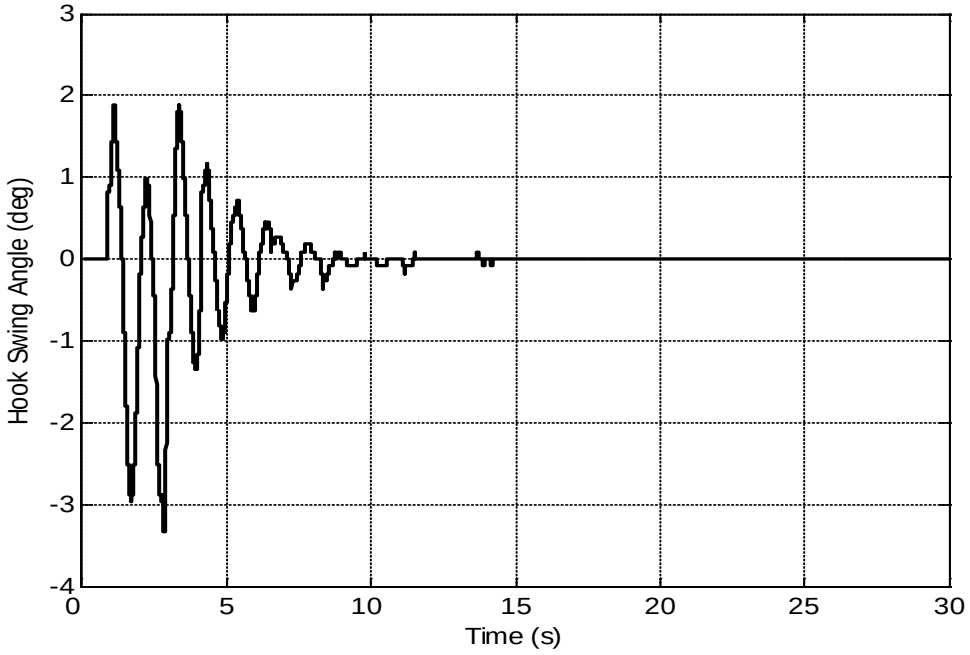

Figure 4.36: Hook swing angle with PZS input shaper

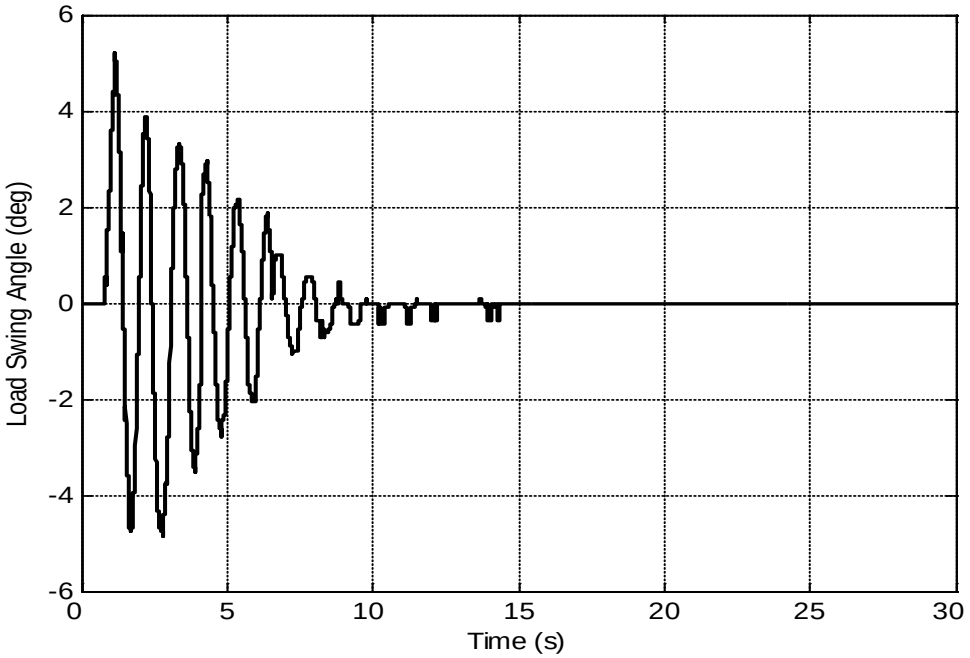

Figure 4.37: Load swing angle with PZS input shaper

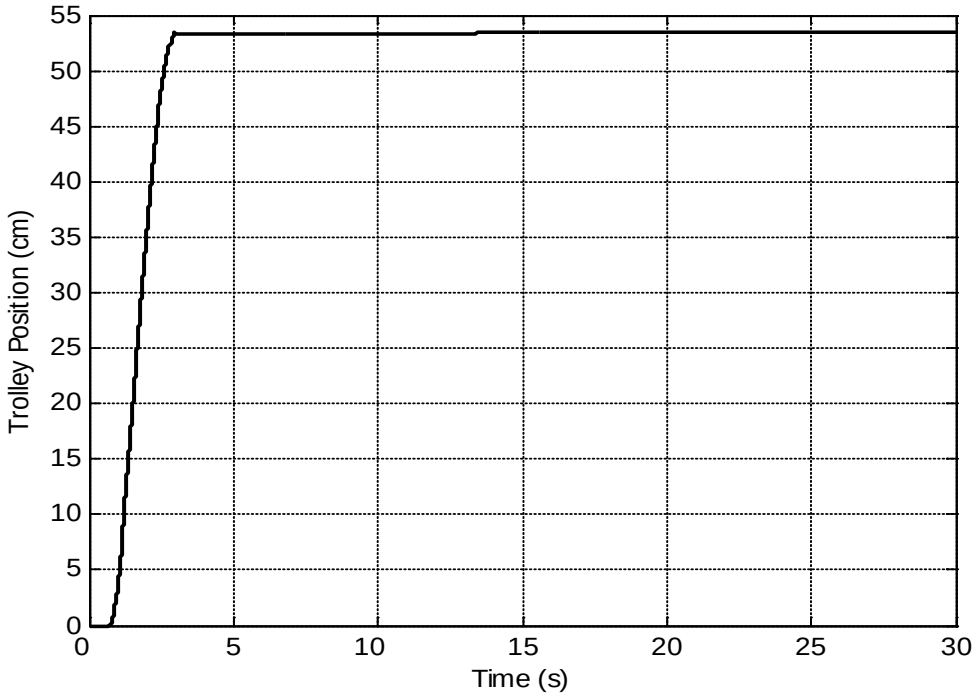

Figure 4.38: Position of cart with PZS input shaper

4.5.3 Result experimental of positive zero sway derivative (PZSD) shaper.

Figures 4.39 - 4.43 show the power spectra density, swing angle of hook and load response and its trolley position of overhead crane system after positive zero sway derivative (PZSD) shaper being applied to the system.

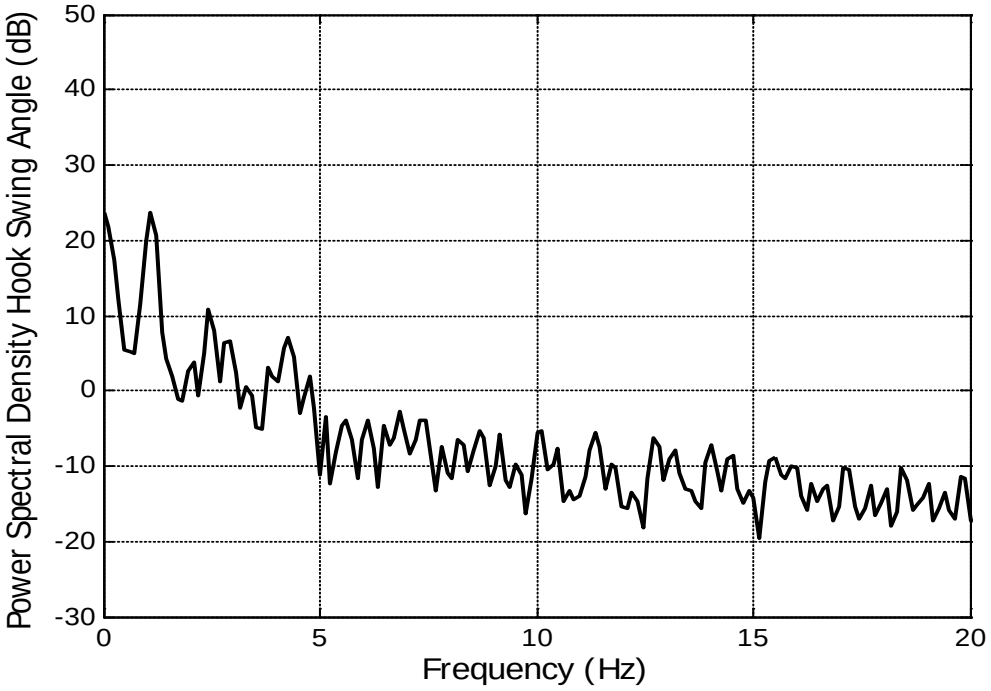

Figure 4.39: Power spectral density at hook sway angle with PZSD input shaper

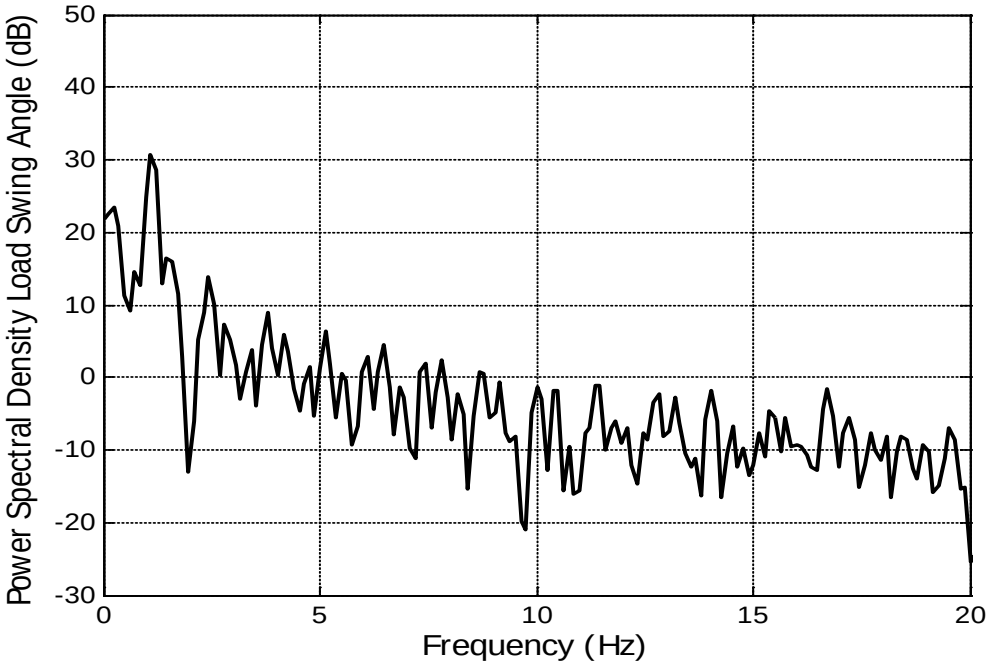

Figure 4.40: Power spectral density at load sway angle with PZSD input shaper

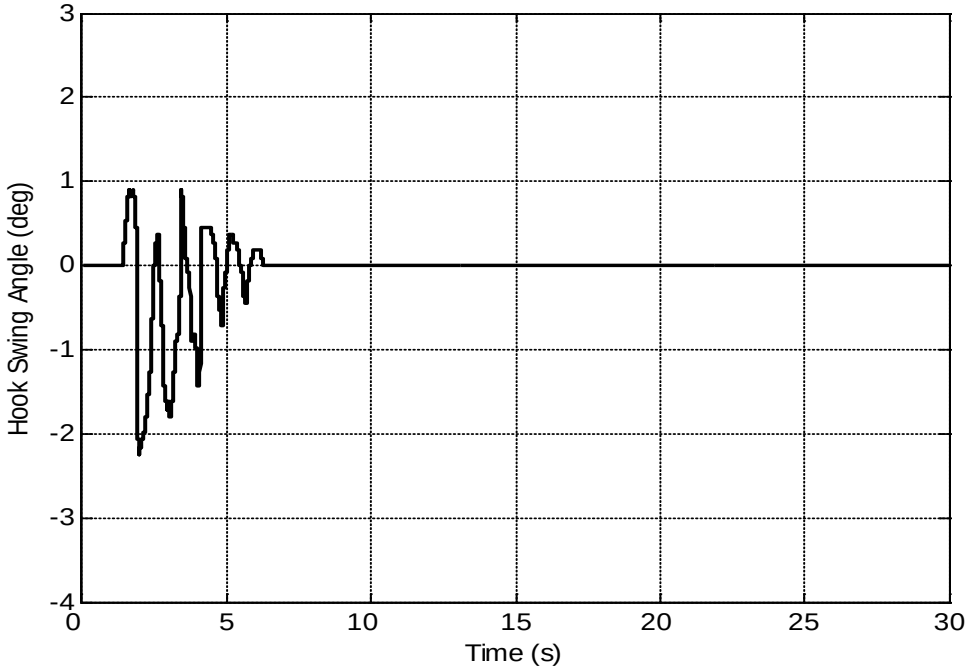

Figure 4.41: Hook swing angle with PZSD input shaper

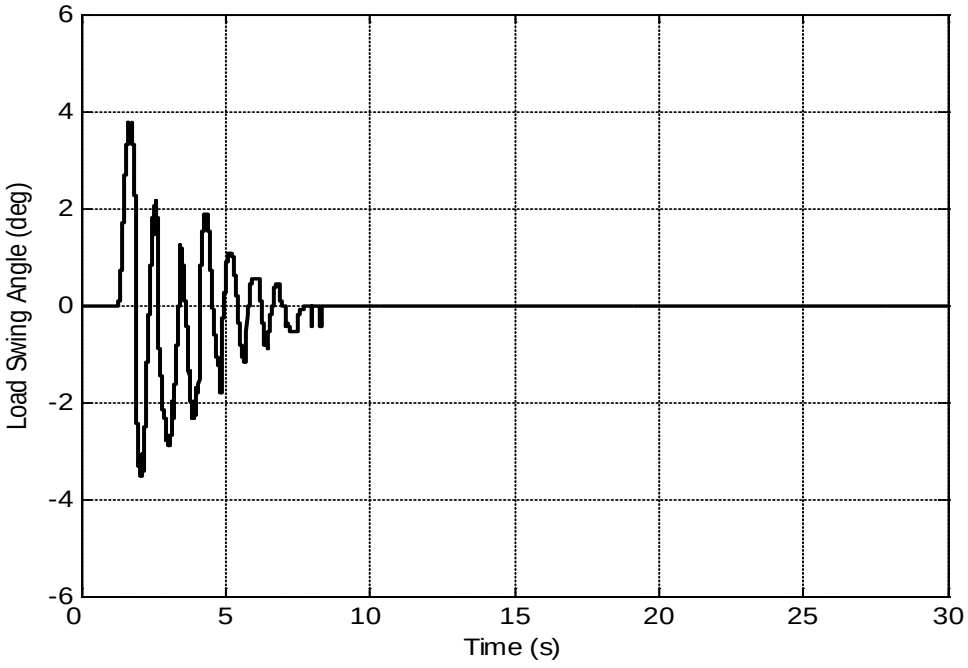

Figure 4.42: Load swing angle with PZSD input shaper

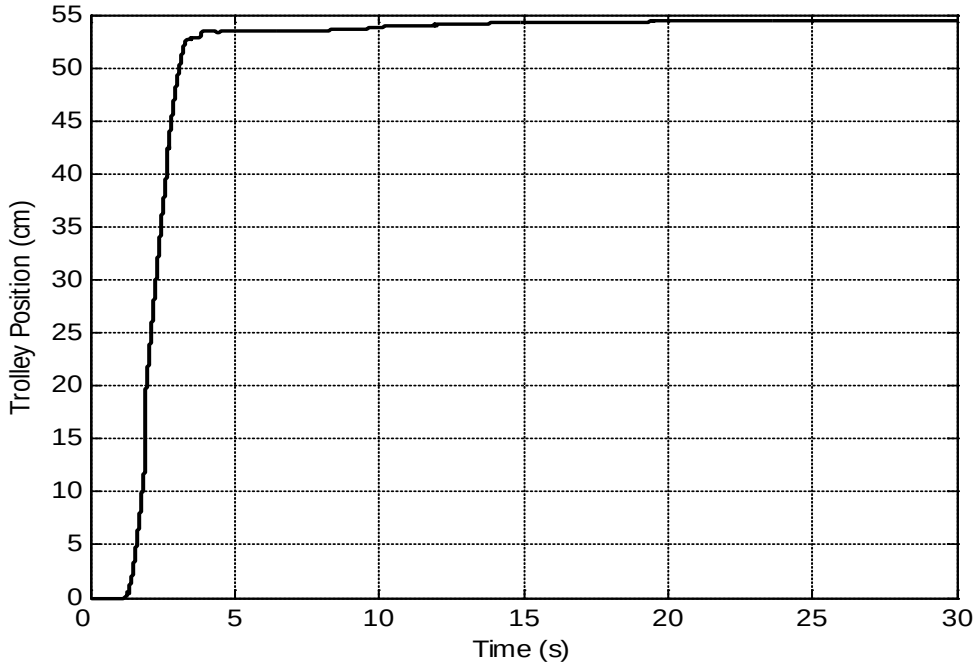

Figure 4.43: Position of cart with PZSD input shaper

4.5.4 Positive zero sway derivative-derivative (PZSDD) shaper.

Figures 4.44 - 4.48 show the power spectra density, swing angle of hook and load response and its trolley position of overhead crane system after positive zero sway derivative - derivative (PZSDD) shaper being applied to the system.

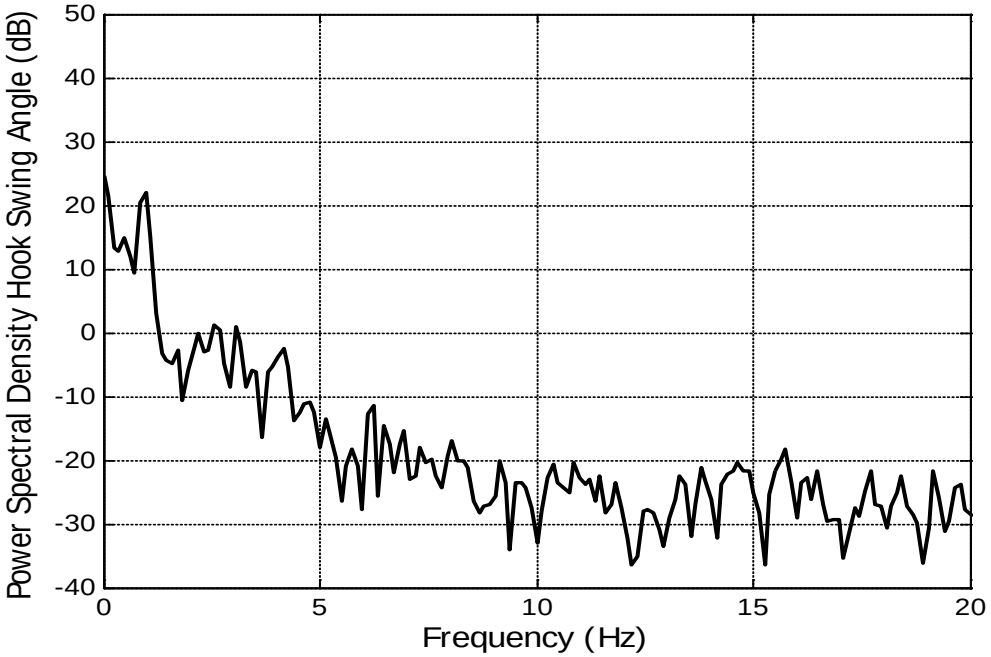

Figure 4.44: Power spectral density at hook sway angle with PZSDD input shaper

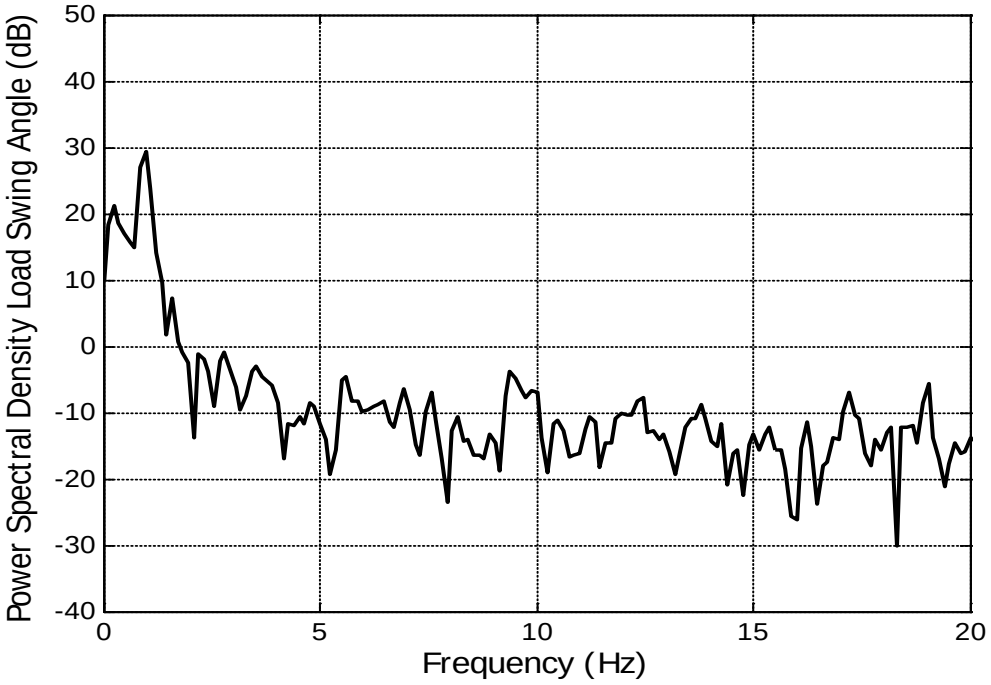

Figure 4.45: Power spectral density at load sway angle with PZSDD input shaper.

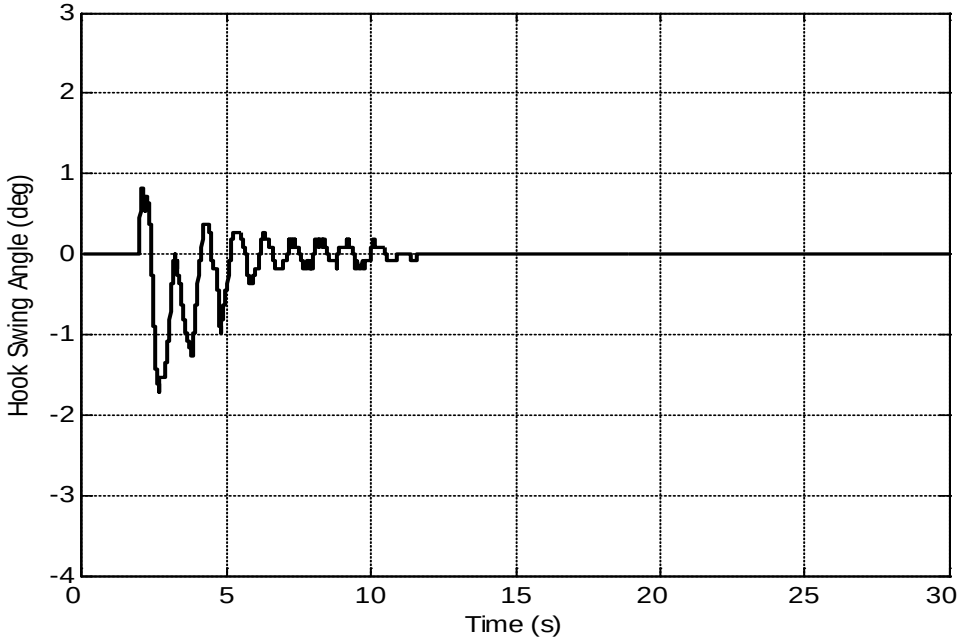

Figure 4.46: Hook swing angle with PZSDD input shaper

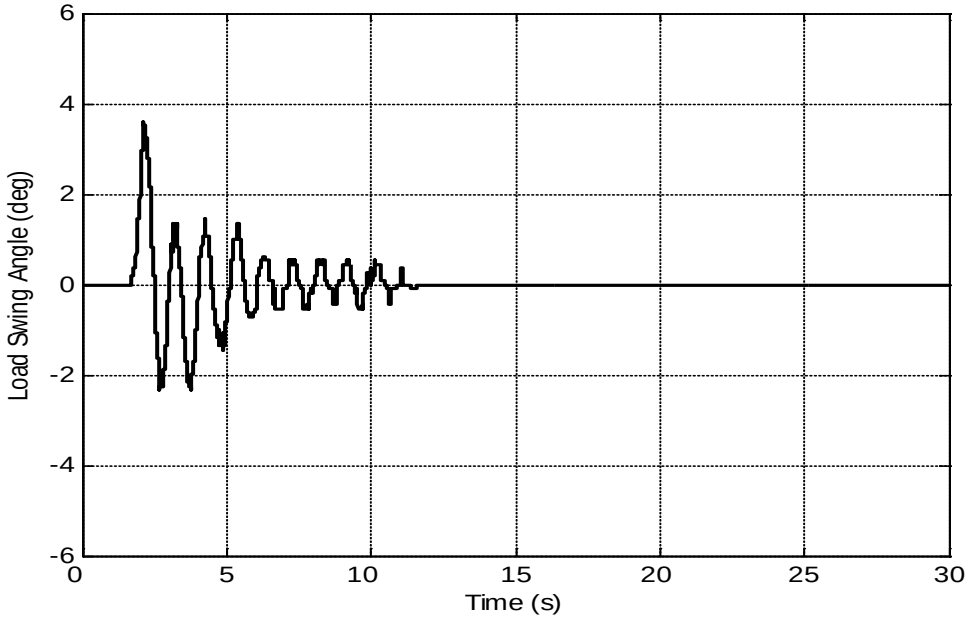

Figure 4.47: Load swing angle with PZSDD input shaper

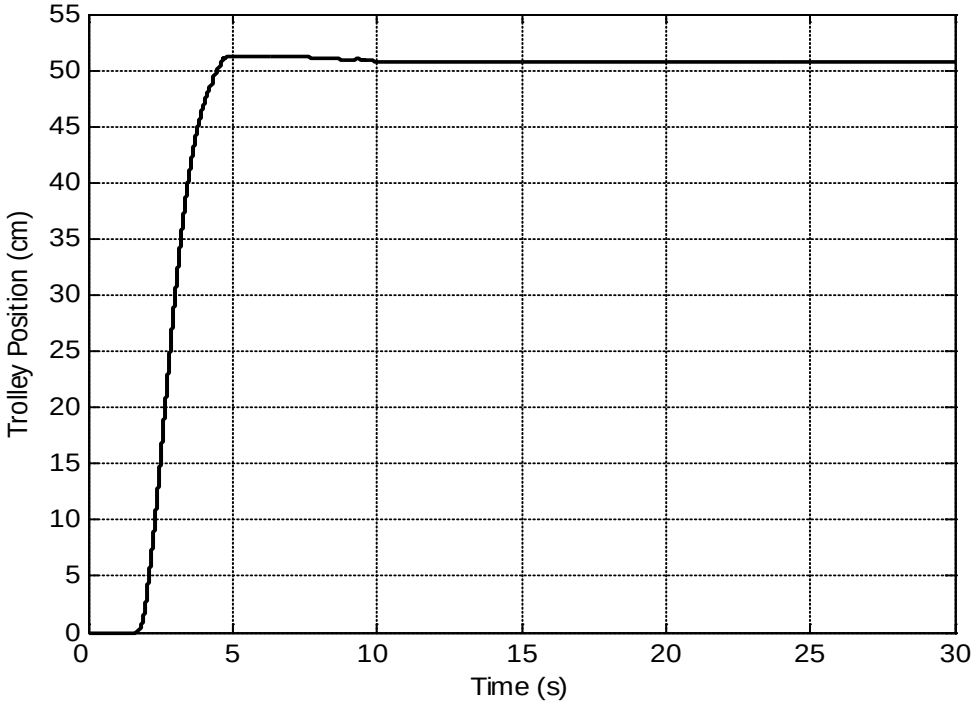

Figure 4.48: Position of the cart with PZSDD input shaper

4.6 Comparative assessment of input shaping techniques in experimental results

From the experimental result of the PZS, PZSD and PZSDD shaper in term of power spectral density, hook sway angle, load sway angle and trolley position will be compared with each other to show the different effect of the positive input shaper derivative order in terms of level of sway reduction and time response specification. The comparison experimental result of input shaping is shown below.

4.6.1 Comparison of power spectral density in experimental result

Figures 4.49 and 4.50 shows the comparison of power spectral density of hook and load sway angle between positive zero sway (PZS), positive zero sway derivative (PZSD) and positive zero sway derivative-derivative (PZSDD) shaper in experimental result. The first three mode of sway of the system are considered, as these dominate the dynamic of the system. The sway frequencies for both hook and load sway angle were obtained as 0.977 Hz, 1.953 Hz and 2.686 Hz for the first three modes of sway. The attenuation of level of sway angle data in power spectral density was analyzed of each type of shaper.

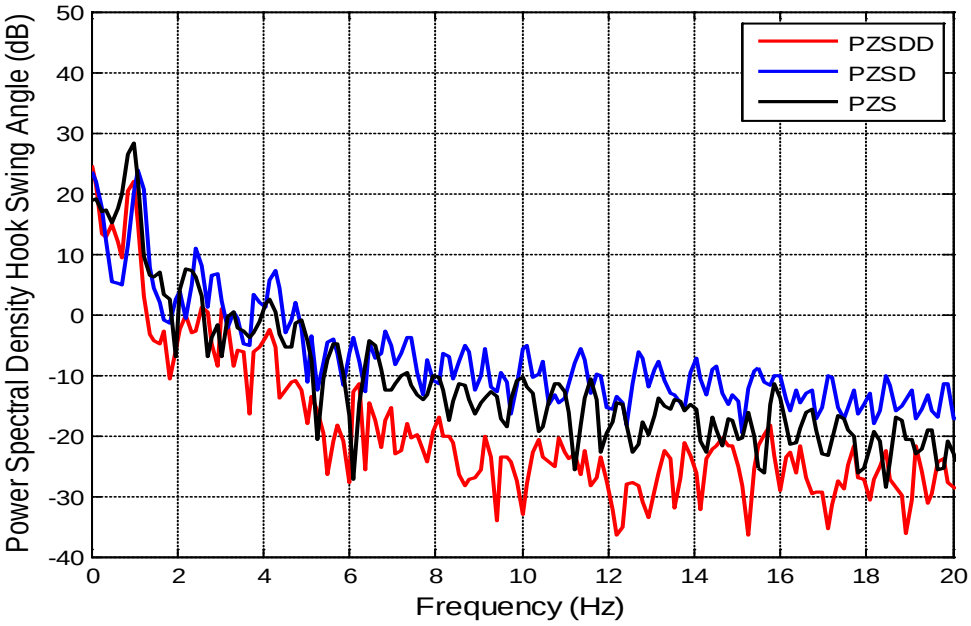

Figure 4.49: Power spectral density of the hook swing angle in experimental result

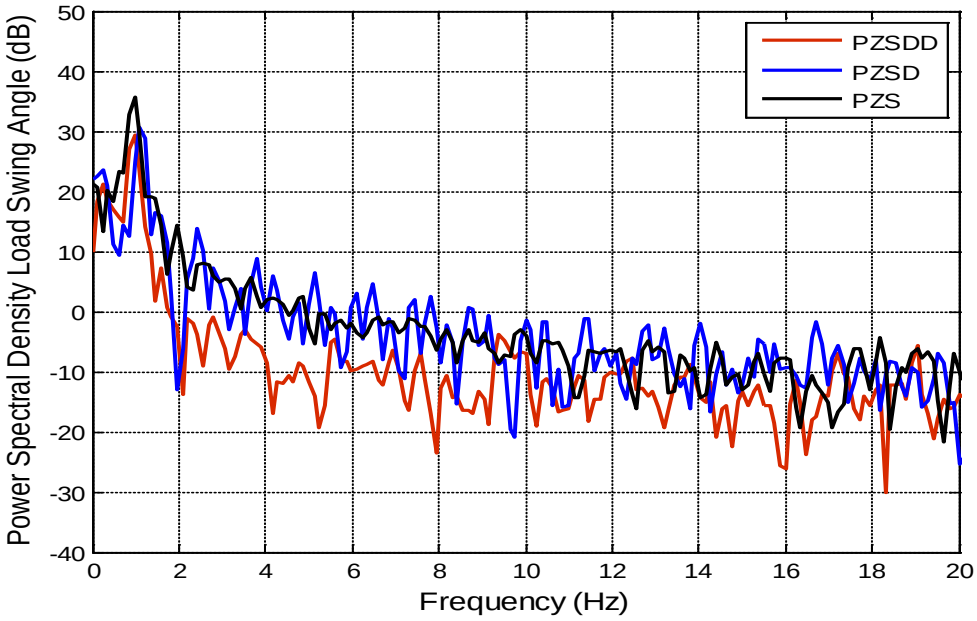

Figure 4.50: Power spectral density of the load swing angle in experimental result

4.6.2 Comparison of Sway Angle in experimental result.

Figures 4.51 and 4.52 show the comparison of the hook and load sway angle response between positive zero sway (PZS), positive zero sway derivative (PZSD) and positive zero sway derivative-derivative (PZSDD) shaper in experimental result. From the comparison show that the level sway angle were significantly reduced with the increasing of positive input shaping derivative order.

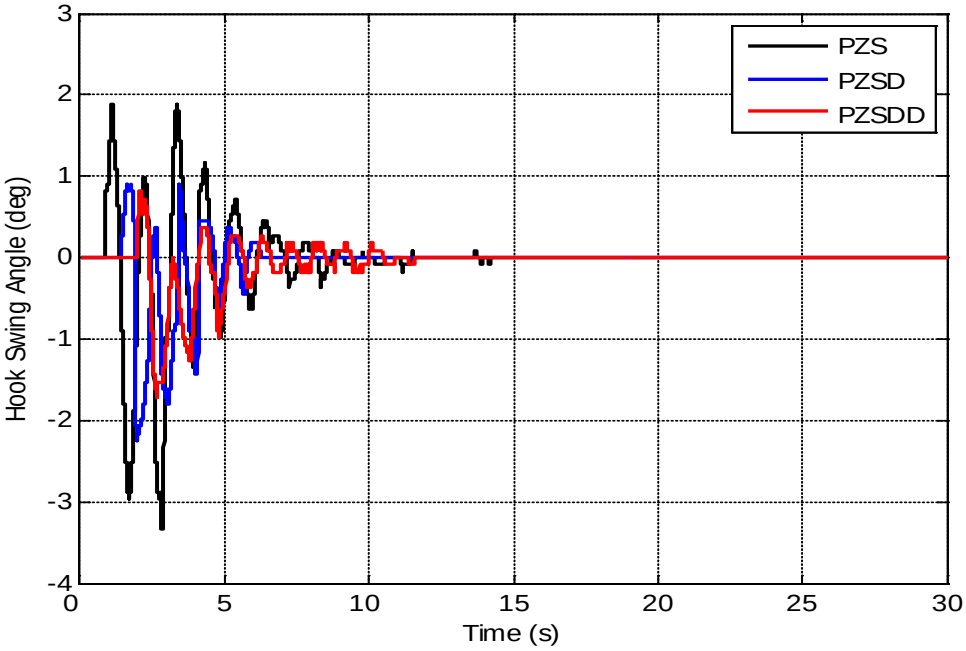

Figure 4.51: Response of the hook swing angle in experimental result

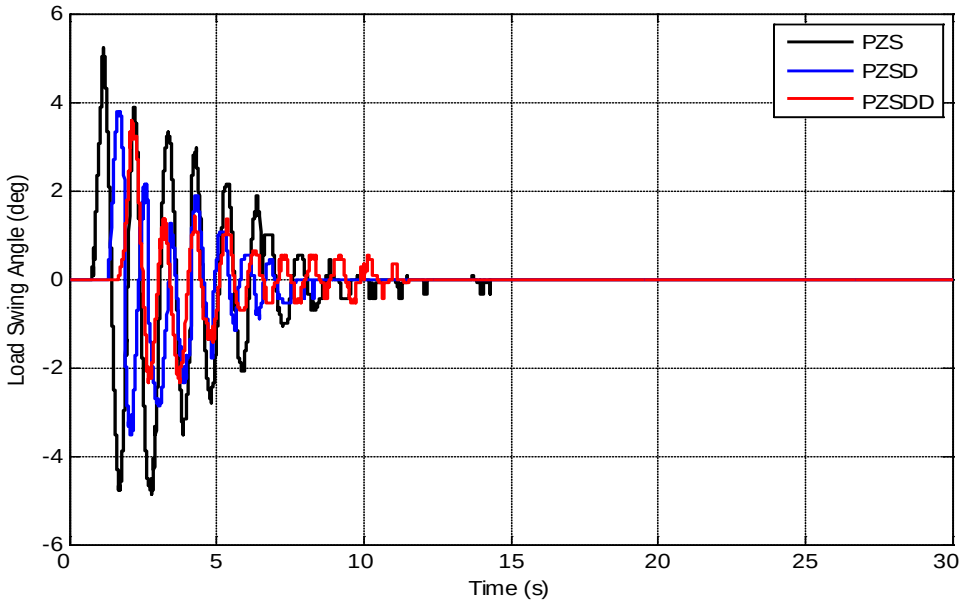

Figure 4.52: Response of the load swing angle in experimental result

4.6.3 Comparison of trolley position in experimental result.

Figure 4.53 shows the comparison of the trolley position response between positive zero sway (PZS), positive zero sway derivative (PZSD) and positive zero sway derivative-derivative (PZSDD) shaper in experimental result. The position of the trolley keeps reducing with higher derivative order of positive input shaping. Therefore, the speed of the system response were reduces with the increasing the number of impulse sequence. The corresponding rise time, settling time and overshoot of the trolley position response were be analyzed.

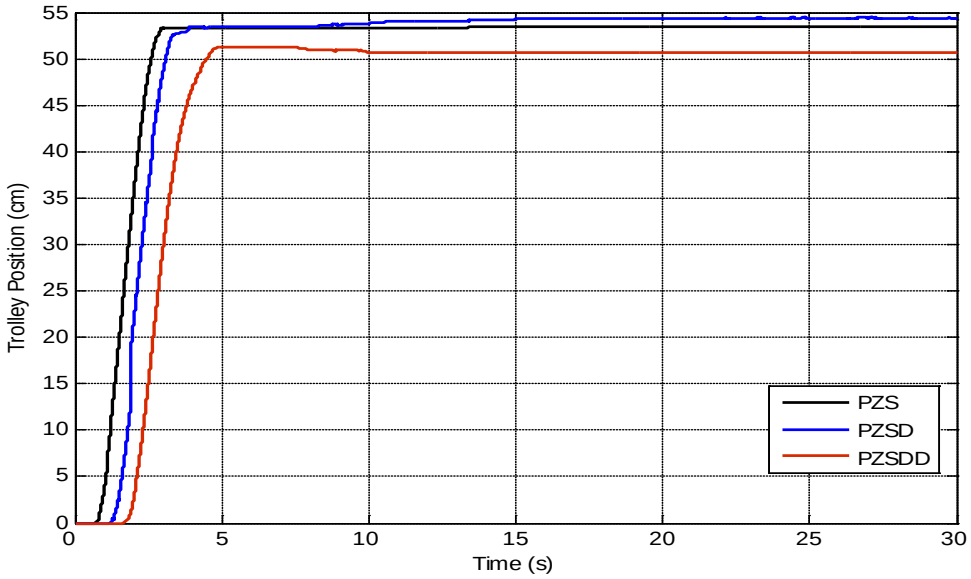

Figure 4.53: Response of the trolley position in experimental result

4.7 Experimental result analysis

The experimental result analysis of this project were done by investigating the effect of each positive input shaper derivative order in terms of attenuation sway of the cable and specification of trolley position response. For the sway suppression schemes, PZS, PZSD and PZSDD are designed based on the sway frequencies and damping ratios of the DPTOC system.

The responses of the DPTOC system to the unshaped input were analyzed in time-domain and frequency domain (spectral density). These experimental results were considered as the system response to the unshaped input and will be used to evaluate as the performance of the input shaping technique.

High level of sway reduction were obtained using positive zero sway derivative-derivative (PZSDD) shaper as compare to the case with using positive zero sway (PZS) and positive zero sway derivative (PZSD) on the double pendulum type overhead crane (DPTOC) system. The corresponding rise time, settling time and overshoot of the trolley position response of each positive input shaper derivative order is depicted in experimental table analysis.

4.7.1 Experimental result analysis of input shaping

Table 4.2 show summaries the levels of sway reduction of the system responses at the first three modes in experimental results. Comparing the result presented in table 4.2, it is noted that the higher performance in the reduction of sway of the system is achieved using positive zero sway derivative-derivative (PZSDD) shaper. This is observed and compared with the positive zero sway (PZS) and positive zero sway derivative (PZSD).

Table 4.2: Level of sway reduction of the hoisting angle of the pendulum and specification of trolley position response in experimental results

Types of shaper	Swing angle	Attenuation (dB) of sway of the cable			Specification of trolley position response		
		Mode 1	Mode 2	Mode 3	Rise time (s)	Settling time (s)	Overshoot (%)
PZS	Hook swing angle, $\theta 1$	09.91	24.38	11.95	1.4114	2.8222	0.0036
	Load swing angle, $\theta 2$	09.30	14.86	13.45			
PZSD	Hook swing angle, $\theta 1$	14.46	28.19	11.95	1.4007	3.8834	0.0257
	Load swing angle, $\theta 2$	15.31	42.01	20.97			
PZSDD	Hook swing angle, $\theta 1$	16.18	37.62	18.38	1.7517	4.3984	1.0986
	Load swing angle, $\theta 2$	15.73	42.86	23.55			

For comparative assessment, the levels of sway reduction of the hoisting angles of the hook and load sway angle of each positive input shaper derivative order PZS, PZSD and PZSDD shapers in experimental result are shown with the bar graphs in Figure 4.54 and Figure 4.55, respectively. The result shows that, highest level of sway reduction is achieved in control schemes using the positive zero sway derivative-derivative (PZSDD) shaper, followed by using positive zero sway derivative (PZSD) shaper and lastly using positive zero sway (PZS) shaper for all modes of sway, for both of hook and load swing angles.

Therefore, it can be concluded that the positive zero sway derivative-derivative (PZSDD) shaper provide better performance in sway reduction, followed by using positive zero sway derivative (PZSD) shaper and lastly by using positive zero sway (PZS) shaper in overall.

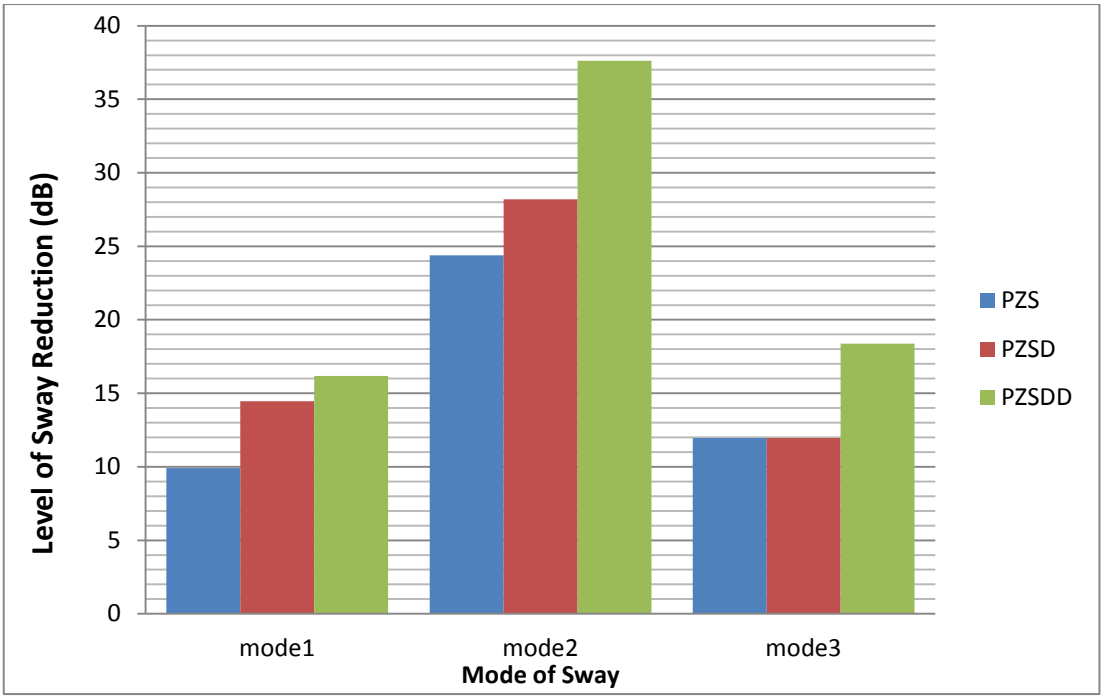

Figure 4.54: Level of sway reduction for hook swing angle in experimental result.

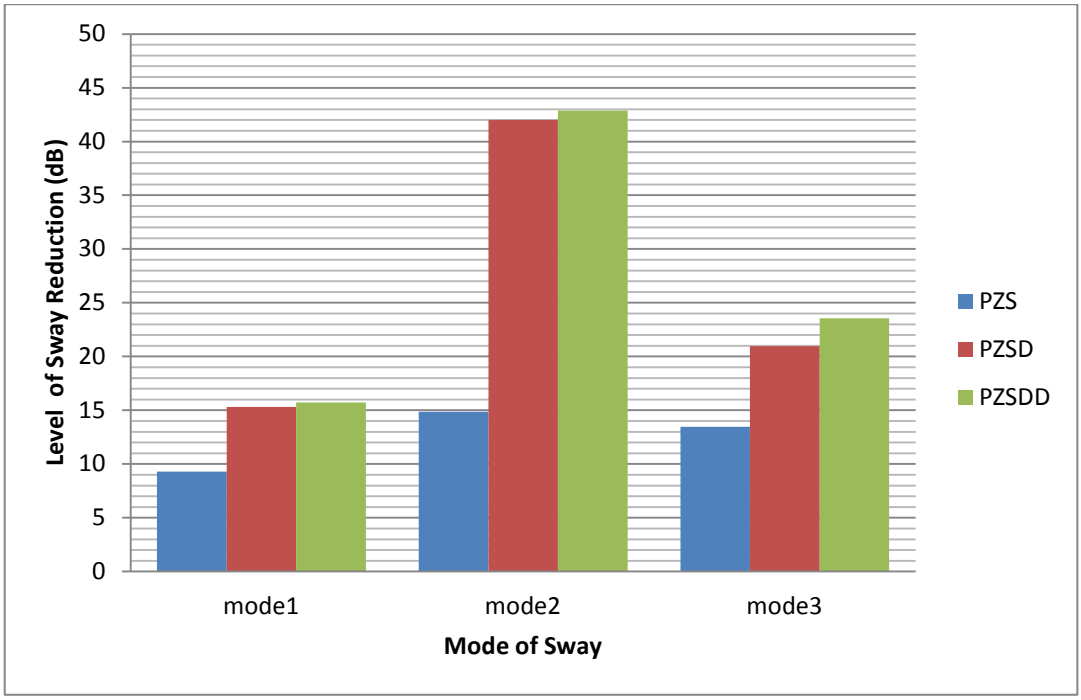

Figure 4.55: Level of sway reduction for load swing angle in experimental result.

Comparisons of the specifications of the trolley position response of input shaping control schemes of each positive input shaper derivative order in experimental result are summarized in Figure 4.56 for the rise times and settling times. It is noted that settling time of the cart position response by using the positive zero sway (PZS) shaper is faster than the case using the positive zero sway derivative-derivative (PZSDD) shaper. It shows that, in term of settling time, the speed of the system response can be improved by using the positive zero sway (PZS) shaper.

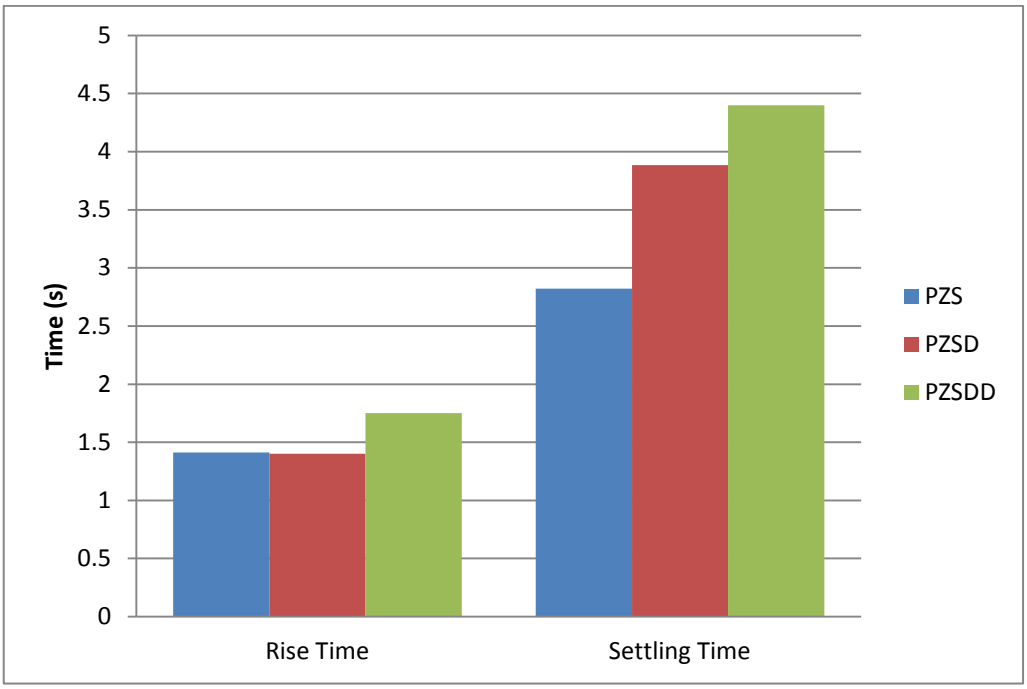

Figure 4.56: Time response specifications in experimental result

CHAPTER 5

CONCLUSION

5.0 Conclusion

The positive input shaping has been successfully developed to control the sway double pendulum type overhead crane system. The objectives set in this project had been successfully fulfilled such that a controller to control the sway of double pendulum type overhead crane system has been developing using positive input shaping technique. Besides, the effects of the difference derivative order of the positive input shaper in terms of level of sway reduction and time response specifications has been studied. The comparison has been made so that the most effective positive input shaper can be determined.

From the experimental results obtained and discussion, some conclusions have been made. A significant reduction in the system sway has been achieved with positive input shaping techniques. Besides, the level of sway-angle reduction improved with the increase in the number of impulses of the shapers which proved PZSDD to be the most effective positive input shaper.

5.1 Limitation of the Project

In this project, the investigation into the positive input shaping control of the double pendulum type overhead crane is done by using MATLAB and CEMTool software. Even though the double pendulum type overhead crane system is modeled using the Euler-Lagrange formulation, there is still difference between the model and the actual double pendulum types overheat crane system. Even when applying the technique to the Real Gain Swing-Up Inverted Pendulum system, the result might not be the same with the actual system because the parameter is not same.

5.2 Future work Recommendation

For future work, this technique can be considered to be applied to the real application at the industry. This way it can improve this technique and enhancing the industrial application.

REFERENCES

[1] Yusop, M., A., (2006)., Input shaping for vibration-free positioning of flexible systems, Master Thesis, Universiti Teknologi Malaysia.

[2] Zainal, Z., (2005), *Modelling and Vibration Control of a Gantry Crane*, Master Thesis, Universiti Teknologi Malaysia.

[3] William Singhose, Jason Lawrence, Khalid Sorensen, Dooroo Kim, *Applications And Educational Users of Crane Oscillation Control*. Georgia Institute of Technology Woodruff School of Mechanical Engineering.

[4] M.A.Ahmad, R.M.T Raja Ismail, M.S. Ramli, A.N.K. Nasir, N.M. Abd Ghani , N.H.Noordin., (2009).,*Comparison of Input Shaping Techniques for Sway Suppression in a Double- Pendulum-Type Overhead Crane*. Faculty of Electrical and Electronics Engineering Universiti Malaysia Pahang, Lebuhraya Tun Razak, 26300, Kuantan, Pahang, Malaysia.

[5] N.C. Singer and W.P. Seering, *Preshaping Command Inputs to Reduce System Vibration*, Journal of Dynamic Systems, Measurement and Control, 112, 1990, pp.76- 82.

[6] W. Singhose and N. Singer, *Effects of Input Shaping on Two-Dimensional Trajectory* Following, IEEE Trans. on Robotics and Automation, Vol. 12, No. 6, 1996, pp.881-887

[7] Micheal Kenison, William Singhose , (1999). *Input Shaper Design For Double-Pendulum Planar Gantry Crane*. Department of Mechanical Engineering Georgia Institute of Technology Atlanta, GA 30332 USA.

[8] E. Kriikku, N. Singer, W.Singhose. *An Input Shaping Controller Enabling Crane Move Without Sway*. American Nuclear Society 7th Topical Meeting on Robotics and Remote Systems

[9] Sirri Sunay Gurleyuk, Ozgur Bahadir, Yunus Turkkan and Hakan Usenti, *Improved Three-Step Input Shaping Control of Crane System*. Issue 6, Vol.7, June 2008.

[10] William E. Singhose, Samuel T. Towell,(1998*). Double-Pendulum GantrCrane Dynamics and Control*. Proceedings of the 1998 IEEE International Conference on Control Applications Trieste, Italy 1-4 September 1998.

[11] M. J. Robertson and W. E. Singhose, Closed-Form Deflection-Limiting Commands, American Control Conference, Portland, USA, 2005, pp.2104-2109

[12] M.A.Ahmad, F.R. Misran, M.S. Ramli and R.M.T. Raja Ismail., (2010).,*Experimental Investigations of Low pass Filter Techniques for Sway Control of a Gantry Crane System.* Faculty of Electrical and Electronics Engineering Universiti Malaysia Pahang, Pekan, 26600, Pahang, Malaysia

[13] M.A.Ahmad, R.M.T. Raja Ismail, A.N.K. Nasir and M.S. Ramli.,(2009).,*Anti-sway Control of a Gantry Cane System based on Feedback Loop Approaches.* Control and Instrumentation Research Group (COINS) Faculty of Electrical and Electronics Engineering, Universiti Malaysia Pahang (UMP), Lebuhraya Tun Razak, 26300, Kuantan, Pahang, Malaysia.

[14] M.A. Ahmad, R.M.T. Raja Ismail, M.S. Ramli, N.M. Abd Ghani and N. Hambali.,(2009).,*Investigations of Feed-forwad Techniques for Anti-Sway Control of 3-D Gantry Crane System.* Faculty of Electrical and Electronics Engineering Universiti Malaysia Pahang, Lebuhraya Tun Razak, 26300, Kuantan, Pahang, Malaysia

APPENDIX

Program Listing

Positive Zero Sway (PZS)

```
starting_time=0;
simulation_time=30;
sampling_time=0.001;
t=starting_time:sampling_time:simulation_time;

%Bang-bang torque uncontroller

for i=(0/sampling_time)+1:(1/sampling_time)+1
   u(i,1)=1;
end
for i=(1/sampling_time)+1:(2/sampling_time)+1
   u(i,1)=-1;
end
for i=(2/sampling_time)+1:(30/sampling_time)+1
   u(i,1)=0;
end


% Positive ZS shaper (2-impulse)
% mode 1

pi=22/7;
z1=0.01;
k1=exp((-z1*pi)/((1-z1^2)^0.5));
wn1=0.4883*2*pi;
wd1=wn1*(sqrt(1-z1^2));
```

```
%Determine the amplitudes and time location of the input shaper

ip=2;

   tt1a(1)=0;
   tt1a(2)=pi/wd1;
   A1a(1)=1/(1+k1);
   A1a(2)=A1a(1)*k1;

tt1a=tt1a./0.001;
tt1a=round(tt1a);
tt1a=tt1a.*0.001;

for i=1
   v1a(i,1)=A1a(1);
end

ni=1;
while ni<=ip-1
   for i=((tt1a(ni)/sampling_time)+2):((tt1a(ni+1)/sampling_time)+1)
      v1a(i,1)=0;
   end
   for i=(tt1a(ni+1)/sampling_time)+1
      v1a(i,1)=A1a(ni+1);
   end
   ni=ni+1;
end

for i=((tt1a(ni)/sampling_time)+2):((30/sampling_time)+1)
   v1a(i,1)=0;
end
```

```
 %mode 2

pi=22/7;
z2=0.02;
k2=exp((-z2*pi)/((1-z2^2)^0.5));
wn2=1.099*2*pi;
wd2=wn2*(sqrt(1-z2^2));

%Determine the amplitudes and time location of the input shaper

ip=2;

   tt2a(1)=0;
   tt2a(2)=pi/wd2;
   A2a(1)=1/(1+k2);
   A2a(2)=A2a(1)*k2;

tt2a=tt2a./0.001;
tt2a=round(tt2a);
tt2a=tt2a.*0.001;

for i=1
   v2a(i,1)=A2a(1);
end

ni=1;
while ni<=ip-1
   for i=((tt2a(ni)/sampling_time)+2):((tt2a(ni+1)/sampling_time)+1)
      v2a(i,1)=0;
   end
```

```
for i=(tt2a(ni+1)/sampling_time)+1
        v2a(i,1)=A2a(ni+1);
    end
    ni=ni+1;
end

for i=((tt2a(ni)/sampling_time)+2):((30/sampling_time)+1)
    v2a(i,1)=0;
end

%mode 3

pi=22/7;
z3=0.03;
k3=exp((-z3*pi)/((1-z3^2)^0.5));
wn3=1.587*2*pi; %
wd3=wn3*(sqrt(1-z3^2));

%Determine the amplitudes and time location of the input shaper

ip=2;

    tt3a(1)=0;
    tt3a(2)=pi/wd3;
    A3a(1)=1/(1+k3);
    A3a(2)=A3a(1)*k3;

tt3a=tt3a./0.001;
tt3a=round(tt3a);
tt3a=tt3a.*0.001;
```

```
for i=1
   v3a(i,1)=A3a(1);
end

ni=1;
while ni<=ip-1
   for i=((tt3a(ni)/sampling_time)+2):((tt3a(ni+1)/sampling_time)+1)
      v3a(i,1)=0;
   end
   for i=(tt3a(ni+1)/sampling_time)+1
      v3a(i,1)=A3a(ni+1);
   end
   ni=ni+1;
end

for i=((tt3a(ni)/sampling_time)+2):((30/sampling_time)+1)
   v3a(i,1)=0;
end


imp1a=conv(v1a,v2a);
imp2a=conv(imp1a,v3a);
impa=imp2a(1:(30/sampling_time)+1);

shp1a=conv(impa,u);
PZS=shp1a(1:(30/sampling_time)+1);
```

Positive Zero Sway Derivative (PZSD)

```
starting_time=0;
simulation_time=30;
sampling_time=0.001;
t=starting_time:sampling_time:simulation_time;

%Bang-bang torque uncontroller

for i=(0/sampling_time)+1:(1/sampling_time)+1
u(i,1)=1;
end
for i=(1/sampling_time)+1:(2/sampling_time)+1
u(i,1)=-1;
end
for i=(2/sampling_time)+1:(30/sampling_time)+1
u(i,1)=0;
end

% Positive ZSD shaper (3-impulse)
% mode 1

pi=22/7;
z1=0.01;
k1=exp((-z1*pi)/((1-z1^2)^0.5));
wn1=0.4883*2*pi;
wd1=wn1*(sqrt(1-z1^2));
```

```
%Determine the amplitudes and time location of the input shaper

ip=3;

tt1b(1)=0;
tt1b(2)=pi/wd1;
tt1b(3)=2.*tt1b(2);
A1b(1)=1/(1+2.*k1+k1.^2);
A1b(2)=A1b(1)*2*k1;
A1b(3)=A1b(1)*k1^2;

tt1b=tt1b./0.001;
tt1b=round(tt1b);
tt1b=tt1b.*0.001;

for i=1
v1b(i,1)=A1b(1);
end

ni=1;
while ni<=ip-1
for i=((tt1b(ni)/sampling_time)+2):((tt1b(ni+1)/sampling_time)+1)
v1b(i,1)=0;
end
for i=(tt1b(ni+1)/sampling_time)+1
v1b(i,1)=A1b(ni+1);
end
ni=ni+1;
end
```

```
for i=((tt1b(ni)/sampling_time)+2):((30/sampling_time)+1)
v1b(i,1)=0;
end

%mode 2

pi=22/7;
z2=0.02;
k2=exp((-z2*pi)/((1-z2^2)^0.5));
wn2=1.099*2*pi;
wd2=wn2*(sqrt(1-z2^2));

%Determine the amplitudes and time location of the input shaper

ip=3;

tt2b(1)=0;
tt2b(2)=pi/wd2;
tt2b(3)=2.*tt2b(2);
A2b(1)=1/(1+2.*k2+k2.^2);
A2b(2)=A2b(1)*2*k2;
A2b(3)=A2b(1)*k2^2;

tt2b=tt2b./0.001;
tt2b=round(tt2b);
tt2b=tt2b.*0.001;

for i=1
v2b(i,1)=A2b(1);
end
```

```
ni=1;
while ni<=ip-1
for i=((tt2b(ni)/sampling_time)+2):((tt2b(ni+1)/sampling_time)+1)
v2b(i,1)=0;
end
for i=(tt2b(ni+1)/sampling_time)+1
v2b(i,1)=A2b(ni+1);
end
ni=ni+1;
end

for i=((tt2b(ni)/sampling_time)+2):((30/sampling_time)+1)
v2b(i,1)=0;
end

%mode 3

pi=22/7;
z3=0.03;
k3=exp((-z3*pi)/((1-z3^2)^0.5));
wn3=1.587*2*pi;
wd3=wn3*(sqrt(1-z3^2));
```

```
%Determine the amplitudes and time location of the input shaper

ip=3;

tt3b(1)=0;
tt3b(2)=pi/wd3;
tt3b(3)=2.*tt3b(2);
A3b(1)=1/(1+2.*k3+k3.^2);
A3b(2)=A3b(1)*2*k3;
A3b(3)=A3b(1)*k3^2;

tt3b=tt3b./0.001;
tt3b=round(tt3b);
tt3b=tt3b.*0.001;

for i=1
v3b(i,1)=A3b(1);
end

ni=1;
while ni<=ip-1
for i=((tt3b(ni)/sampling_time)+2):((tt3b(ni+1)/sampling_time)+1)
v3b(i,1)=0;
end
for i=(tt3b(ni+1)/sampling_time)+1
v3b(i,1)=A3b(ni+1);
end
ni=ni+1;
end
```

```
for i=((tt3b(ni)/sampling_time)+2):((30/sampling_time)+1)
v3b(i,1)=0;
end


imp1b=conv(v1b,v2b);
imp2b=conv(imp1b,v3b);
impb=imp2b(1:(30/sampling_time)+1);

shp1b=conv(impb,u);
PZSD=shp1b(1:(30/sampling_time)+1);
```

Positive Zero Sway Derivative-Derivative (PZSDD)

```
starting_time=0;
simulation_time=30;
sampling_time=0.001;
t=starting_time:sampling_time:simulation_time;

%Bang-bang torque uncontroller

for i=(0/sampling_time)+1:(1/sampling_time)+1
   u(i,1)=1;
end
for i=(1/sampling_time)+1:(2/sampling_time)+1
   u(i,1)=-1;
end
for i=(2/sampling_time)+1:(30/sampling_time)+1
   u(i,1)=0;
end

% Positive ZVDD shaper (4-impulse)
% mode 1

pi=22/7;
z1=0.01;
k1=exp((-z1*pi)/((1-z1^2)^0.5));
wn1=0.4883*2*pi;
wd1=wn1*(sqrt(1-z1^2));
```

```
%Determine the amplitudes and time location of the input shaper

ip=4;

   tt1c(1)=0;
   tt1c(2)=pi/wd1;
   tt1c(3)=2.*tt1c(2);
   tt1c(4)=3*tt1c(2);
   A1c(1)=1/(1+3.*k1+3*k1.^2+k1^3);
   A1c(2)=A1c(1)*3*k1;
   A1c(3)=A1c(2)*k1;
   A1c(4)=A1c(1)*k1^3;

tt1c=tt1c./0.001;
tt1c=round(tt1c);
tt1c=tt1c.*0.001;

for i=1
   v1c(i,1)=A1c(1);
end

ni=1;
while ni<=ip-1
   for i=((tt1c(ni)/sampling_time)+2):((tt1c(ni+1)/sampling_time)+1)
      v1c(i,1)=0;
   end
   for i=(tt1c(ni+1)/sampling_time)+1
      v1c(i,1)=A1c(ni+1);
   end
   ni=ni+1;
end
```

```
for i=((tt1c(ni)/sampling_time)+2):((30/sampling_time)+1)
   v1c(i,1)=0;
end

%mode 2

pi=22/7;
z2=0.02;
k2=exp((-z2*pi)/((1-z2^2)^0.5));
wn2=1.099*2*pi;
wd2=wn2*(sqrt(1-z2^2));

%Determine the amplitudes and time location of the input shaper

ip=4;

   tt2c(1)=0;
   tt2c(2)=pi/wd2;
   tt2c(3)=2*tt2c(2);
   tt2c(4)=3*tt2c(2);
   A2c(1)=1/(1+3*k2+3*k2^2+k2^3);
   A2c(2)=A2c(1)*3*k2;
   A2c(3)=A2c(2)*k2;
   A2c(4)=A2c(1)*k2^3;

tt2c=tt2c./0.001;
tt2c=round(tt2c);
tt2c=tt2c.*0.001;
```

```
for i=1
   v2c(i,1)=A2c(1);
end

ni=1;
while ni<=ip-1
   for i=((tt2c(ni)/sampling_time)+2):((tt2c(ni+1)/sampling_time)+1)
      v2c(i,1)=0;
   end
   for i=(tt2c(ni+1)/sampling_time)+1
      v2c(i,1)=A2c(ni+1);
   end
   ni=ni+1;
end

for i=((tt2c(ni)/sampling_time)+2):((30/sampling_time)+1)
   v2c(i,1)=0;
end

%mode 3

pi=22/7;
z3=0.03;
k3=exp((-z3*pi)/((1-z3^2)^0.5));
wn3=1.587*2*pi; %
wd3=wn3*(sqrt(1-z3^2));
```

```
%Determine the amplitudes and time location of the input shaper

ip=4;

   tt3c(1)=0;
   tt3c(2)=pi/wd3;
   tt3c(3)=2*tt3c(2);
   tt3c(4)=3*tt3c(2);
   A3c(1)=1/(1+3*k3+3*k3^2+k3^3);
   A3c(2)=A3c(1)*3*k3;
   A3c(3)=A3c(2)*k3;
   A3c(4)=A3c(1)*k3^3;

tt3c=tt3c./0.001;
tt3c=round(tt3c);
tt3c=tt3c.*0.001;

for i=1
   v3c(i,1)=A3c(1);
end

ni=1;
while ni<=ip-1
   for i=((tt3c(ni)/sampling_time)+2):((tt3c(ni+1)/sampling_time)+1)
      v3c(i,1)=0;
   end
   for i=(tt3c(ni+1)/sampling_time)+1
      v3c(i,1)=A3c(ni+1);
   end
   ni=ni+1;
end
```

```
for i=((tt3c(ni)/sampling_time)+2):((30/sampling_time)+1)
   v3c(i,1)=0;
end


imp1c=conv(v1c,v2c);
imp2c=conv(imp1c,v3c);
impc=imp2c(1:(30/sampling_time)+1);

shp1c=conv(impc,u);
PZSDD=shp1c(1:(30/sampling_time)+1);
```

Plot Graf Coding

```
Fs=1000;
n_fft=8192;

figure(1);
[Pn,f]=psd(tha,n_fft,Fs);
plot(f,10*log10(Pn),'-k','linewidth',2);grid on;
xlabel('Frequency (Hz)','fontsize',12);
ylabel('Power Spectral Density Hook Swing Angle (dB) ','fontsize',12);
axis([0 5 -160 20 ]);

figure(2);
[Pn,f]=psd(thb,n_fft,Fs);
plot(f,10*log10(Pn),'-k','linewidth',2);grid on;
xlabel('Frequency (Hz)','fontsize',12);
ylabel('Power Spectral Density Load Swing Angle (dB) ','fontsize',12);
axis([0 5 -160 20 ]);

figure(3);
plot(tha,'-k','linewidth',2);
axis([0 30000 -0.01 0.01]);
grid;
xlabel('Time (s)');
ylabel('Hook Swing Angle (rad)');
```

```
figure(4);
plot(thb,'-k','linewidth',2);
axis([0 30000 -0.01 0.01]);
grid;
xlabel('Time (s)');
ylabel('Load Swing Angle (rad)');

figure(5);
plot(x,'-k','linewidth',2);
axis([0 30000 0 0.1]);
grid;
xlabel('Time (s)');
ylabel('Trolley Position (cm)');

figure(6);
plot(PZS,'-k','linewidth',1)
axis([0 30000 -0.6 0.6]);
grid;
Title('Bang-bang input of PZS')
xlabel('Time (s)');
ylabel('Bang-bang torque');
```